A MECHANISM FOR EXOSITE-MEDIATED FACTOR IX ACTIVATION BY FACTOR XIa

By

Yipeng Geng

Dissertation

Submitted to the Faculty of the

Graduate School of Vanderbilt University

in partial fulfillment of the requirements

for the degree of

DOCTOR OF PHILOSOPHY

in

Pathology

May, 2014

Nashville, Tennessee

Approved:

Paul E. Bock

Olivier G. Boutaud

Michael Laposata

Samuel A. Santoro

Jonathan G. Schoenecker

Ingrid M. Verhamme

ACKNOWLEDGEMENT

Studying abroad is the biggest decision that I ever made. The journey has been fraught with challenge and moments of frustration, but also filled with moments of achievement and true joy. There are a number of people without whom this thesis might not have been written, and to whom I am greatly indebted.

First, I would like to express my sincere gratitude to my mentor, Dr Dave Gailani, for his continuous support of my ph.D study. He has been on my side for the past few years as a patient teacher, an enthusiastic guider and a sincere friend. I cannot imagine having a better mentor for my Ph.D study.

I would like to thank my dissertation committee members: Dr Bock, Dr Boutaud, Dr Laposata, Dr Santoro and Dr Schoenecker for their guidance, patience and support as I completed my dissertation. I want to thank Dr Verhamme for assisting me to interpret the enzyme kinetics, as well as serving in my dissertation committee. My sincere thanks also go to Dr Bajaj and his colleague at UCLA, who offer me the resources and guidance to understand the mechanism of factor IX activation.

I am greatly indebted to the past and current members of Gailani lab, especially Maofu Sun, Qiufang Cheng, Anton Matafonov and Steve Smith. I'm thankful for their patience to teach me experimental techniques, and their helpful suggestions. Without them, my long journey would be lonely and difficult.

Finally, I would like to thank my mother Xiaole Geng and my father Wei Li, as well as my husband Shiwei Guo. Thank you for your unconditional trust and support, standing by me through all the emotional highs and lows. I love you!

PUBLICATIONS

Geng, Y., Verhamme, I.M., Messer, A., Sun, M.F., Smith, S.B., Bajaj, S.P., Gailani, D. (2012) A Sequential Mechanism for Exosite-mediated Factor IX Activation by Factor XIa. J Biol Chem *287*, 38200–38209.

Geng, Y., Verhamme, I.M., Smith, S.B., Sun, M.F., Matafonov, A., Cheng, Q., Smith, S.A., Morrissey, J.H., Gailani, D. (2013) The dimeric structure of factor XI and zymogen activation. Blood *121*, 3962-3969.

Geng, Y., Verhamme, I.M., Sun, M.F., Bajaj, S.P., Emsley, J., Gailani, D. (2013) Analysis of the Factor XI Variant Arg184Gly Suggests a Structural Basis for Factor IX Binding to Factor XIa. J Thromb Haemost *11*, 1374–84.

Geng, Y., Verhamme, I.M., Smith, S.A., Cheng, Q., Sun, M.F., Sheehan, J.P., Morrissey, J.H., Gailani, D. (2014) Factor XI Anion-Binding Sites are required for Productive Interactions with Polyphosphate. J Thromb Haemost *11*, 2020-8.

Matafonov, A., Cheng, Q., **Geng, Y**., Verhamme, I.M., Umunakwe, O., Tucker, E.I., Sun, M.F., Serebrov, V., Gruber, A., Gailani, D. (2013) Evidence for factor IX-independent roles for factor XIa in blood coagulation. J Thromb Haemost *11,* 2118-27.

Gailani, D., **Geng, Y**., Verhamme, I.M., Sun, M.F., Bajaj, S.P., Messer, A., Emsley, J. (2014) The mechanism underlying activation of factor IX by factor XIa. (in press - Thrombosis Research).

TABLE OF CONTENTS

LIST OF TABLES

LIST OF FIGURES

LIST OF ABBREVIATIONS

Factor XI – FXI

Factor IX – FIX

Factor X – FX

Factor VII – FVII

Tissue factor – TF

Tissue factor pathway inhibitor – TFPI

Factor XII – FXII

von Willebrand factor – vWF

Prekallikrein – PK

High-molecular-weight-kininogen – HK

Activated partial thromboplastin time – aPTT

Polyphosphate – polyP

Glycoprotein 1bα – GP1bα

Anion binding exosite – ABE

C1-inhibitor – C1-INH

Antithrombin – AT

Vitamin K-dependent – VKD

Epidermal growth factor – EGF

Activation peptide – AP

γ-carboxyglutamic acid – Gla

Surface plasmon resonance – SPR

Phosphatidylserine – PS

Enzyme-to-substrate – E:S

Dextran sulfate – DS

Corn trypsin inhibitor – CTI

Hydrodynamic tail-vein injection – HTI

Anion binding site – ABS

Apolipoprotein E receptor 2 – ApoER2

Neutrophil extracellular trap – NET

CHAPTER I

OVERVIEW OF COAGULATION

Hemostasis

The ability of the body to restore vascular integrity following injury is paramount to survival. The rapid formation of a fibrin and platelet rich clot over the site of vascular damage, and the subsequent dissolution of the clot at the appropriate time is termed "hemostasis". During the initial phase of hemostasis three processes occur: vasoconstriction, platelet plug formation, and fibrin clot formation (Troy *et al.* 1988). In response to vessel injury, vascular smooth muscle cells contract, constricting the damaged vessels rapidly to diminish blood loss. Circulating platelets then adhere to exposed subendothelial collagen in a reaction involving von Willebrand factor (vWF), and bind to each other (aggregation) to form a platelet plug. This process is often referred to as primary hemostasis. Simultaneously, plasma proteins called coagulation factors contribute to a series of enzymatic reactions to generate the serine protease thrombin. Among its many activities, thrombin converts fibrinogen into fibrin strands (previously referred to as secondary hemostasis) that act as "molecular glue" to strengthen the platelet plug. One of the plasma proteins involved in thrombin generation is the protease factor XIa (FXIa). In this dissertation thesis, I will present results of structural and functional studies on FXIa, and discuss the biological and therapeutic implications of how this protease contributes to thrombin generation.

Hemostasis is a highly regulated process. Disorders of hemostasis can lead to a risk of

bleeding (hemorrhage). Bleeding diatheses can be caused by hypocoagulability due to genetic deficiency of certain coagulation factors (for example hemophilia A, factor VIII deficiency), to acquired disorders caused by disease states (liver disease, malignancies, infections…) or to the use of anticoagulant medications.

At the other end of the clinical spectrum are thrombotic disorders, which are characterized by formation of clot within the lumen of a blood vessel. The thrombus can obstruct the circulation at its site of formation, or can break free from its site of origin and migrate through the circulation. The latter process is called embolization. Thrombo-embolism results in reduced blood flow to tissue leading to ischemia and infarction, and ultimately organ malfunction and failure. Collectively, arterial and venous thrombosis, and most importantly myocardial infarction, stroke, and deep vein thrombosis and its complication pulmonary embolism, constitute major causes of morbidity and mortality worldwide.

Most current antithrombotic therapies fall into two main categories: anticoagulants that reduce thrombin generation, and antiplatelet agents that inhibit platelet activation or aggregation. Conventional anticoagulants include heparin and the vitamin K-antagonist warfarin (Fuster *et al.*, 2012). These anticoagulants have effects on a variety of coagulation proteases including thrombin and the protease directly responsible for thrombin production, factor Xa (FXa). The consequence of inhibiting these important components of hemostasis is that use of these drugs is associated with a significant risk of life-threatening bleeding. Drug level monitoring can reduce, but not eliminate the bleeding risk. Anticoagulants that specifically inhibit thrombin or FXa have been introduced recently into clinical practice (Müller *et al.*, 2011). While these drugs produce a more predictable

effect and are, therefore, safer than warfarin, bleeding remains a major problem because they inhibit proteins that are critical for hemostasis (to be discussed in the following section). A major goal of coagulation research is to develop novel strategies to treat or prevent thrombotic disorders with fewer bleeding complications. Therapeutic inhibition of FXIa may be such a strategy.

Coagulation Pathways

Thrombin generation, and subsequent fibrin formation, is mediated by a group of plasma proteins (coagulation factors), many of which are zymogens of serine proteases. Coagulation factors are components of a proteolytic amplifying process that leads to thrombin generation at a wound site (Figure 1-1) (Furie and Furie, 1988). Coagulation factors are assigned Roman numerals, with a lowercase "a" appended to the numeral to indicate the active form. Initiation of thrombin generation occurs at a site of vessel injury when factor VIIa (FVIIa), which accounts for about 1% of factor VII (FVII) in blood, binds to the cofactor tissue factor (TF) (Brummel-Ziedins *et al.*, 2012). TF is a *trans*-membrane glycoprotein expressed constitutively on many cells that underlie vascular endothelium. TF expression can also be induced on the surface of monocytes and platelets, and it can be found on circulating microparticles of monocyte or platelet origin upon vessel injury or in a variety of pathological conditions (Mackman *et al.*, 2007). The FVIIa/TF complex activates factor X (FX) and factor IX (FIX) in the presence of calcium and phospholipid, leading to thrombin and fibrin formation. Activation of FX by FVIIa/TF is quickly inhibited by tissue factor pathway inhibitor (TFPI), which provides a negative feedback mechanism that is essential for the regulation of hemostasis (Broze *et al.*, 1990). Sustained

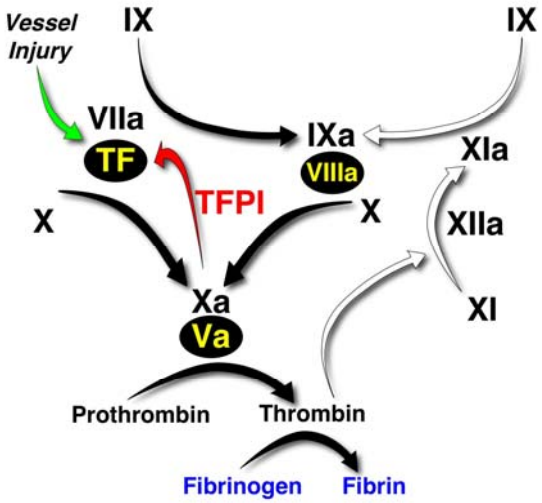

Figure 1-1 Model of fibrin formation. Fibrin generation is initiated by a series of proteolyic reactions involving plasma proteases (Roman numeral in black). Black and white arrows indicate protease-mediated reactions, with white arrows indicating reactions involved in FXI activation and FXIa activity. The red arrow indicates feedback inhibition of FVIIa/TF by TFPI. Cofactors are shown as yellow lettering within black ovals. Lower case "a" indicates the actived form of the factor.

thrombin generation requires FVIIa/TF activation of FIX. It appears that in most cases FIX activation is largely the role of the FVIIa/TF complex. However, in some situations FIX activation by the protease factor XIa (FXIa) is also required (Davie *et al.*, 1991). In the model shown in Figure 1-1, FXIa contributes to the reinforcement of a clot, after the initiation of coagulation.

FXIa is traditionally thought of as a component of the process of contact activation. Contact activation was first identified as a series of reactions that allow blood to clot rapidly when it comes into contact with non-biologic charged surfaces such as glass or celite, or polyanions such as dextran sulfate. The plasma proteins Factor XII (FXII), prekallikrein (PK) and high-molecular-weight-kininogen (HK) are the other components necessary for contact activation (Figure 1-2). The process is thought to be initiated by autoactivation of FXII on anionic polymers or surfaces. Activated FXII (FXIIa) converts PK to α-kallikrein, which in turn activates additional FXII to amplify the process (Kaplan *et al.*, 1987). Concurrently, FXIIa activates FXI to FXIa, which then converts FIX to FIXaβ in the presence of calcium ions. FIXaβ forms a FX-activating complex with FVIIIa

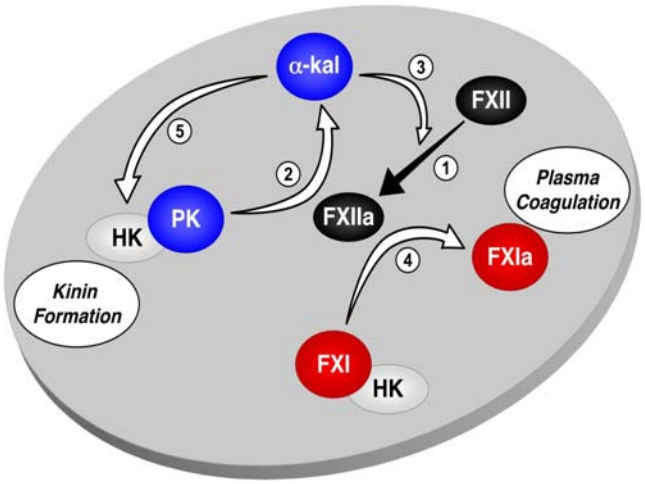

Figure 1-2. Contact Activation. Contact activation is initiated by the conversion of FXII to FXIIa when plasma is exposed to a negatively charged surface (gray disk). Reciprocal activation of PK to α-kallikrein (α-kal) by FXIIa (reaction 2), and FXII by α-kal (reaction 3) enhances FXII activation. FXIIa promotes coagulation through activation of FXI (reaction 4). α-Kallikrein also cleaves high molecular weight kininogen (HK) to liberate bradykinin (reaction 5).

on the surface of activated platelets, thereby contributing to thrombin generation.

While clinical laboratories widely use assays based on contact activation-initiated coagulation to study blood clotting in patients, contact activation is thought to be dispensable for hemostasis *in vivo*. Deficiencies of FXII, PK and HK are not associated with hemostatic abnormalities (Gailani *et al.*, 2010). Actually, these proteins appear to play more important roles in inflammation and in innate immune responses to infection than to coagulation. Currently, the tissue factor-initiated pathways shown in Figure 1-1 are thought to be the major initiators of thrombin generation *in vivo*, while the contact activation system plays little, or no, role in hemostasis.

Factor XI in Hemostasis and Thrombosis

In current models of coagulation, FIX may be activated by either FVIIa/TF or FXIa. While severe FIX deficiency is associated with spontaneous hemorrhage into soft tissues and joints that can be life threatening (Ragni *et al.*, 2009), FXI deficiency in humans is associated with a relatively mild clinical bleeding abnormality (Asakai *et al.*, 1991;

Seligsohn, 2007). FXI-deficient mice do not have a demonstrable bleeding disorder. These clinical observations indicate that FXI is unlikely to be required for initiating hemostasis, and it is currently thought that the primary function of FXIa is to enhance thrombin generation in certain situations to prevent premature clot breakdown by fibrinolysis (Gailani and Broze, 1991; von dem Borne *et al.*, 1995). Consistent with this, tissues with high intrinsic levels of fibrinolytic activity, including the oropharynx, nasopharynx and the urinary tract, are most often sites of excessive bleeding in FXI-deficient patients.

The relatively modest contribution of FXI to hemostasis intuitively suggests that the protein would have a limited impact on pathologic coagulation, particularly thrombosis. However, epidemiologic data indicate a clear role for FXI in thrombotic events. In multiple studies, elevated FXI levels have been identified as a risk factor for myocardial infarction (Doggen *et al.*, 2006), cerebrovascular disease (Yang *et al.*, 2006), and venous thrombosis (Meijers *et al.*, 2000); while FXI deficiency reduces risk for these diseases (Salomon *et al.*, 2008; 2009). Recent work with vascular injury models in mice, rabbits, and primates supports the impression that FXI has a disproportionately greater role in thrombosis than in hemostasis. FXI-deficient mice are protected from arterial thrombus formation induced by $FeCl_3$ to an extent comparable to supratherapeutic doses of heparin (Wang *et al.*, 2005; Gailani *et al.*, 2010). FXII deficiency, selectively blocking FXI activation by FXIIa, or inhibiting the activation of FIX by FXIa has similar protective effects (Renné *et al.*, 2005; Cheng *et al.*, 2010; Tucker *et al.*, 2009). Cumulatively, these data indicate that contact activation-driven activation of FXI may contribute to thrombosis, despite being unimportant for hemostasis.

A Potential Cofactor for Factor XI Activation During Coagulation

Reactions involving FXI and FXII activation occur very slowly in solution. The importance of a negatively charged surface (usually purified clay) for initiation of contact activation and for FXI activation in *in vitro* assays in plasma is well-established, however, the identity of endogenous substances that would serve a similar function *in vivo* has been long debated. Some studies have shown that basement membrane-collagen exposed by vascular damage can facilitate FXII activation (van der Meijden *et al.*, 2009), while others identified extracellular RNA from damaged or necrotic cells as promoters of contact activation (Kannemeier *et al.*, 2007). Recently, several groups have provided evidence that polymers of inorganic phosphate (polyphosphate [polyP]) secreted during platelet activation are activators of the contact system *in vivo* (Smith *et al.*, 2006).

PolyP is a linear polymer of orthophosphate groups linked through high-energy phosphoanhydride bonds. It is ubiquitous, being found in almost all organisms ranging from bacteria to mammals (Kornberg *et al.*, 1999). Each internal phosphate group carries a negative charge at physiologic pH, making polyP a highly anionic molecule. PolyP has been extensively studied in prokaryotes, where it acts as a calcium chelator in the electron-dense acidic organelles called acidocalcisomes (Docampo, 2006). In addition, the high energy phosphoanhydride bond serves as an ATP source in times of starvation or environmental stress. The dense granules of mammalian platelets are thought to be homologous to acidocalcisomes, indicating these organelles were conserved during evolution from prokaryotes to eukaryotes (Ruiz *et al.*, 2004). PolyP is present at high concentrations in dense granules, and is efficiently secreted upon platelet activation (Smith *et al.*, 2006). Upon full platelet activation, human blood is calculated to contain 1 to 3 μM

polyP (concentration given in terms of phosphate monomers), and the concentration may be much higher in platelet-rich thrombi (Morrissey *et al.*, 2012). After secretion, polyP has a half-life of about 1.5 to 2 hours in human blood, and presumably undergoes depolymerization by polyphosphatases (Smith *et al.*, 2006).

A group of recent studies identified polyP as a potent regulator of hemostasis. In addition to triggering contact activation, polyP accelerates FV activation, and enhances fibrin formation (Morrissey *et al.*, 2012) (Figure 1-3). Recently, polyP was reported to serve as a cofactor that accelerates FXI activation by thrombin and FXIa (to be discussed in detail in the next chapter) (Choi *et al.*, 2012). The polymer length of polyP varies from only a few to several thousand phosphate units, depending on the type of organism or cell type it is isolated from. Interestingly, different length polymers exert different effects on coagulation (Smith *et al.*, 2010). The very long polymers (hundreds to thousands of phosphate units) found in microorganisms are fairly potent triggers of FXII autoactivation and the contact pathway. In contrast, the relatively short polymers (~60-100 phosphate units) released by activated platelets are less potent activators of contact activation, but retain full capacity to promote FV and FXI activation. These findings support the hypothesis that platelet polyP functions primarily to enhance clot formation, while the longer microbial polyP can trigger contact activation, possibly as part of the host response to a pathogen (part of the innate immune response).

The Purpose of Studies Described in this Thesis

FXI is part of the traditional contact activation pathway, which historically received relatively little attention as a significant target to treat thrombosis, based on its minor role

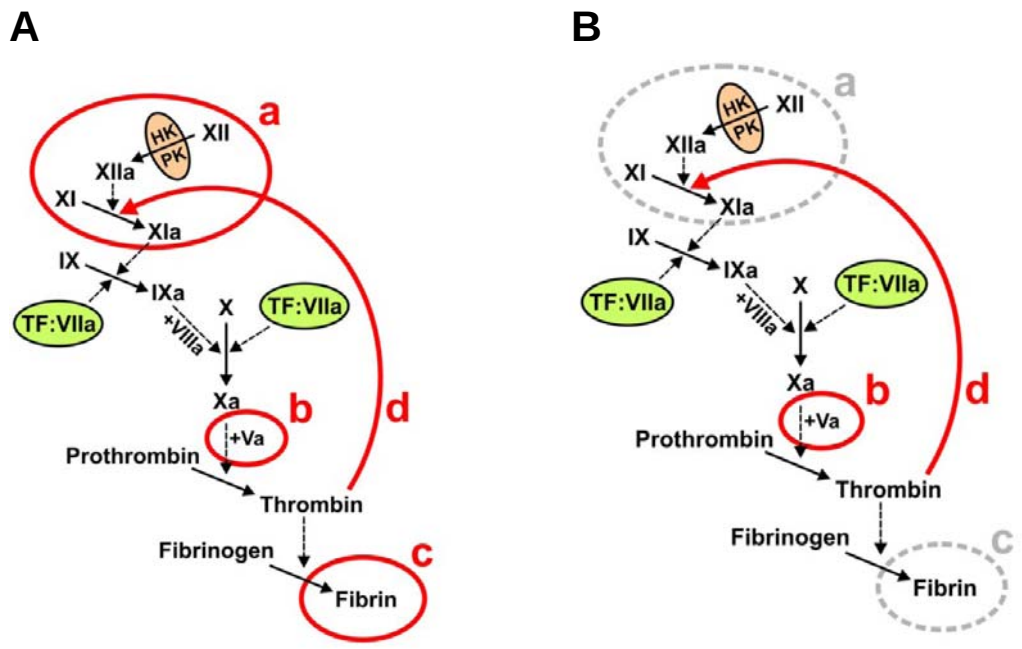

Figure 1-3. The role of polyphosphate in blood coagulation (Image adapted from Choi *et al.*, 2011). (A) Long-chain polyP (over 500 phosphate units long) acts at 4 points in the clotting cascade, indicated in red: 1, initiates the contact pathway of blood clotting; 2, accelerates FV activation; 3, enhances fibrin polymerization; and 4, accelerates FXI activation by thrombin. **(B)** Platelet-size polyP (60-100 phosphate units) acts primarily at points 2 and 4 in clotting cascade, with moderate effect on point 3.

in hemostasis. Abundant recent epidemiologic and animal data demonstrating that FXI plays a critical role in thrombosis, challenging the previous intuitive assumption that thrombosis is merely dysregulated hemostasis. Therapeutically targeting proteases such as FXIa or FXIIa could produce an anticoagulant effect with little effect on hemostasis. This would allow clinicians to broaden the current clinical indications for antithrombotic therapy, and decrease the cost for monitoring bleeding risk for patients under treatment.

The work discussed in this thesis was designed to provide insight into the mechanisms by which FXI is converted to an active protease, and by which FXIa interacts with its substrate. The initial set of the experiments focuses on mechanisms involved in FXI activation by the proteases FXIIa, thrombin and FXIa, and the effects of polyP and other

polyanions on the activation reaction. The second group of experiments analyzes the novel mechanism by which FXIa converts FIX to FIXaβ, and describes a possible FIX binding site on FXIa. We expect this work will facilitate development of novel therapeutic agents to treat thromboembolic disease, as well as improve our understanding of the role of FXI and contact activation in blood coagulation.

References

Asakai, R., Chung, D.W., Davie, E.W., Seligsohn, U. (1991) Factor XI deficiency in Ashkenazi Jews in Israel. N Engl J Med *325*, 153-158.

Broze, G., Girard, T., Novotny, W. (1990) Regulation of coagulation by a multivalent Kunitz-type inhibitor. Biochemistry *29*, 7539-7546.

Brummel-Ziedins, K., and Mann, K.G. (2012) Molecular basis of blood coagulation, In: Hematology: basic principles and practice, 6th Ed., Churchill Livingstone-Elsevier, Philadelphia, pp 1821-41

Cheng, Q., Tucker, E.I., Pine, M.S., Sisler, I., Matafonov, A., Sun, M.F. White-Adams, T.C., Smith, S.A., Hanson, S.R., McCarty, O.J., Renné, T., Gruber, A., Gailani, D. (2010) A role for factor XIIa-mediated factor XI activation in thrombus formation *in vivo*. Blood *116*, 3981-3989.

Choi, S.H., Smith, S.A., Morrissey, J.H. (2011) Polyphosphate is a cofactor for the activation of factor XI by thrombin. Blood *118*, 6963-70.

Davie, E.W., Fujikawa, K., Kisiel, W. (1991) The coagulation cascade: initiation, maintenance, and regulation. Biochemistry *30*, 10363-10370.

Docampo, R. (2006) Acidocalcisomes and polyphosphate granules. In: Shively JM, editor. Microbiol Monograph: Inclusion in Prokaryotes. Berlin-Heidelburg: Springer-Verlag. pp. 53–70.

Doggen, C.J., Rosendaal, F.R., Meijers, J.C. (2006) Levels of intrinsic coagulation factors and the risk of myocardial infarction among men: Opposite and synergistic effects of factors XI and XII. Blood *108*, 4045-4051.

Furie, B., and Furie, B. C. (1988) The molecular basis of blood coagulation. Cell *53*, 505-518.

Fuster, V., Bhatt, D.L., Califf, R.M., Michelson, A.D., Sabatine, M.S., Angiolillo, D.J., Bates, E.R., Cohen, D.J., Coller, B.S., Furie, B., Hulot, J.S., Mann, K.G., Mega, J.L., Musunuru, K., O'Donnell, C.J., Price, M.J., Schneider, D.J., Simon, D.I., Weitz, J.I., Williams, M.S., Hoots, W.K., Rosenberg, Y.D., Hasan, A.A. (2012) Guided antithrombotic therapy: current status and future research direction: report on a National Heart, Lung and Blood Institute working group. Circulation *126*, 1645-1662.

Gailani, D., and Broze, G.J. (1991) Factor XI activation in a revised model of blood coagulation. Science *253*, 909-912.

Gailani, D., Renné, T., Emsley, J., (2010) Factor XI and the contact system, in: Valle D, Beaudet AL, Vogelstein B, et al, eds. The Online Metabolic and Molecular Basis of Inherited Disease. Philadelphia.

Kannemeier, C., Shibamiya, A., Nakazawa, F., Trusheim, H., Ruppert, C., Markart, P., Song, Y., Tzima, E., Kennerknecht, E., Niepmann, M., von Bruehl, M.L., Sedding, D., Massberg, S., Günther, A., Engelmann, B., Preissner, K.T. (2007) Extracellular RNA constitutes a natural procoagulant cofactor in blood coagulation. Proc Natl Acad Sci USA *104*, 6388-6393.

Kaplan, A., and Silberberg, M., (1987) The coagulation-kinin pathway of human plasma. Blood *70*, 1-15.

Kornberg, A., Rao, N.N., Ault-Riche, D. (1999) Inorganic polyphosphate: a molecule of many functions. Annu Rev Biochem. *68*, 89-125.

Mackman, N., Tilley, R.E., Key, N.S. (2007) Role of the extrinsic pathway of blood coagulation in hemostasis and thrombosis. Arterioscler Thromb Vasc Biol *27*, 1687-1693.

Meijers, J.C., Tekelenburg, W.L., Bouma, B.N., Bertina, R.M., Rosendaal, F.R. (2000) High levels of coagulation factor XI as a risk factor for venous thrombosis. N Engl J Med *342*, 696-701.

Morrissey, J.H., Choi, S.H., Smith, S.A. (2012) Polyphosphate: an ancient molecule that links platelets, coagulation and inflammation. Blood *119*, 5972-5979.

Müller, F., Gailani, D., Renné, T. (2011) Factor XI and XII as antithrombotic agents. Curr Opin Hematol. *18*, 349-55.

Ragni, N.V., Kessler, C.M., Lozier, J.N. (2009) Clinical aspects and therapy of hemophilia, in: Hoffman R, Benz E, Shattil S, Furie B,, Silberstein L, McGlave P, Heslop H (eds): Hematology: Basic Principles and Practice, 5th ed. New York: Churchill Livingstone - Elsevier, pp 1911-1930.

Renné, T., Pozgajová, M., Grüner, S., Schuh, K., Pauer, H.U., Burfeind, P., Gailani, D., Nieswandt, B. (2005) Defective thrombus formation in mice lacking coagulation factor

XII. J Exp Med *202*, 271-281.

Ruiz, F.A., Lea, C.R., Oldfield, E., Docampo, R. (2004) Human platelet dense granules contain polyphosphate and are similar to acidocalcisomes of bacteria and unicellular eukaryotes. J Biol Chem *279*, 44250-44257.

Salomon, O., Steinberg, D.M., Koren-Morag, N., Tanne, D., Seligsohn, U. (2008) Reduced incidence of ischemic stroke in patients with severe factor XI deficiency. Blood *111*, 4113-4117.

Salomon, O., Zivelin, A., Tamarin, I., Steinberg, D.M., Varon, D., Seligsohn, U. (2009) Patients with severe factor XI deficiency have a reduced incidence of venous thromboembolism. Blood *114*, 3491a.

Seligsohn, U. (2007) Factor XI in haemostasis and thrombosis: past, present and future. Thromb Haemost *98*, 84-89.

Smith, S.A., Choi, S.H., Davis-Harrison, R., Huyck, J., Boettcher, J., Rienstra, C.M., Morrissey, J.H. (2010) Polyphosphate exerts differential effects on blood clotting, depending on polymer size. Blood *116*, 4353-4359.

Smith, S.A., Mutch, N.J., Baskar, D., Rohloff, P., Docampo, R., Morrissey, J.H. (2006) Polyphosphate modulates blood coagulation and fibrinolysis. Proc Natl Acad Sci USA *103*, 903-908.

Troy, G.C. (1988) An overview of hemostasis. Vet Clin North Am Small Anim Pract *18*, 5-20.

Tucker, E.I., Marzec, U.M., White-Adams, T.C., Hurst, S., Rugonyi, S., McCarty, O.J., Gailani, D., Gruber, A., Hanson, S.R. (2009) Prevention of vascular graft occlusion and thrombus-associated thrombin generation by inhibition of factor XI. Blood *113*, 936-944.

van der Meijden, P.E., Munnix, I.C., Auger, J.M., Govers-Riemslag, J.W., Cosemans, J.M., Kuijpers, M.J., Spronk, H.M., Watson, S.P., Renné, T., Heemskerk, J.W. (2009) Dual role of collagen in factor XII-dependent thrombus formation. Blood *114*, 881-890.

von dem Borne, P.A., Meijers, J.C., Bouma, B.N. (1995) Feedback activation of factor XI by thrombin in plasma results in additional formation of thrombin that protects fibrin clots from fibrinolysis. Blood *86*, 3035-3042.

Wang, X., Cheng, Q., Xu, L., Feuerstein, G.Z., Hsu, M.Y., Smith, P.L., Seiffert, D.A., Schumacher, W.A., Ogletree, M.L., Gailani, D. (2005) Effects of factor IX or factor XI deficiency on ferric chloride-induced carotid artery occlusion in mice. J Thromb Haemost *3*, 695-702.

Yang, D.T., Flanders, M.M., Kim, H., Rodgers, G.M. (2006) Elevated factor XI activity

levels are associated with an increased odds ratio for cerebrovascular events. Am J Clin Pathol *126*, 411-415.

CHAPTER II

STRUCTURE AND FUNCTION OF FACTOR XI AND FACTOR XIa

Factor XI Structure

FXI is a 160 kDa dimeric glycoprotein consisting of two identical subunits connected by a disulfide bond (Fujikawa *et al.*, 1986; McMullen *et al.* 1991). It is synthesized in hepatocytes, and circulates in blood plasma at a concentration of 25 to 40 nM (4 to 6 μg/mL) in a noncovalent complex with HK (Bouma and Griffin, 1977; Thompson *et al.* 1977). The primary sequence and disulfide bond structure of a FXI polypeptide chain is shown in Figure 2-1. Each FXI subunit contains four apple domains designated A1 through A4, and a protease domain (Fujikawa *et al.*, 1986). Apple domains are members of the PAN (Plasminogen, Apple, Nematode) family of domains. Crystal structures have been reported for full-length zymogen FXI (Papagrigoriou *et al.*, 2006), and the isolated active protease domain of FXIa in complex with inhibitors (Jin *et al.*, 2005; Navaneetham *et al.*, 2005). The catalytic domain of FXIa is a typical chymotrypsin-like serine protease. The catalytic domain active site contains a standard catalytic triad consisting of His^{413}, Asp^{462}, and Ser^{557}. The four apple domains of each FXI subunit pack into a flat disk-like structure. The polypeptide takes a 180° turn between A2 and A3 so that A3 and A4 run anti-parallel to A1 and A2 (Figure 2-2). A remarkable feature of the FXI structure is the intimate linkage of the apple domains to form a disk-like platform around the base of the catalytic domain, resulting in a structure that is compact. This differs significantly from the more open linear structures of vitamin K–dependent coagulation proteases. In the FXI dimer the

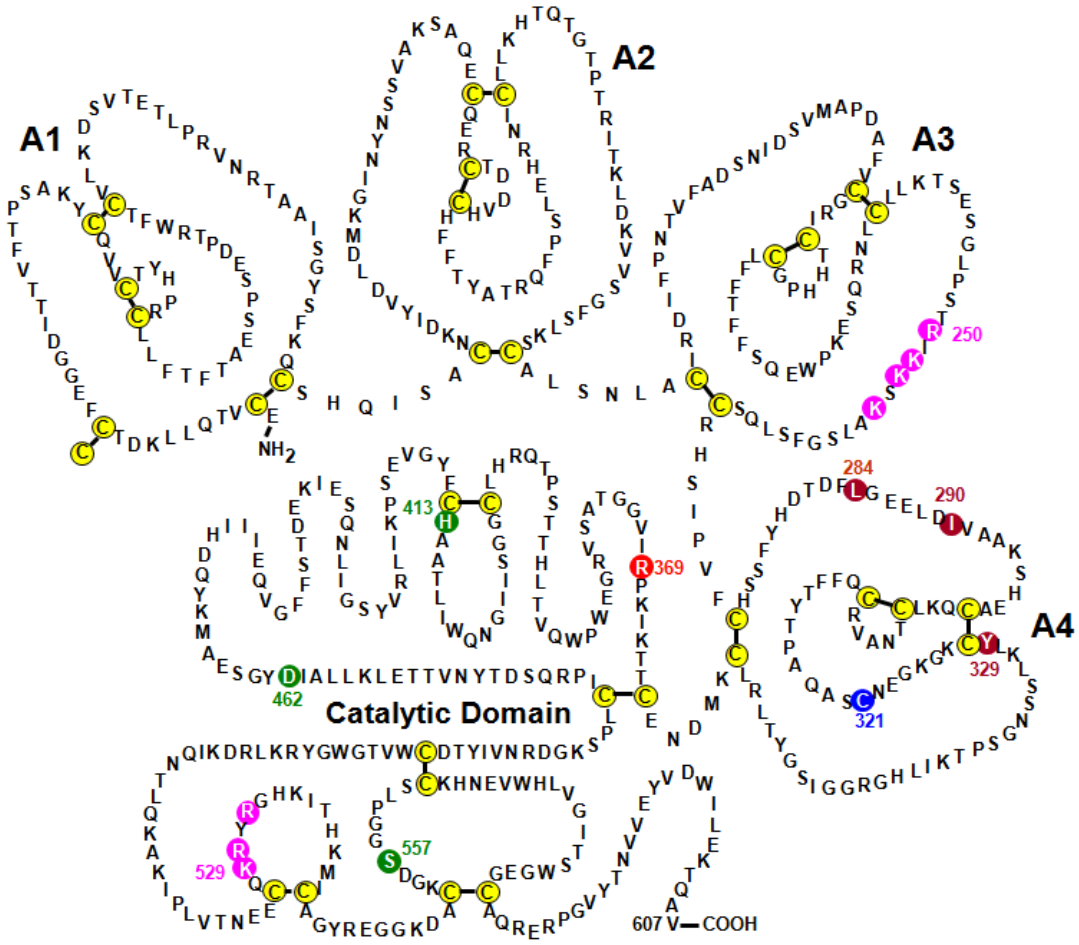

Figure 2-1. The amino acid sequence and disulfide bond locations of human FXI. Schematic diagram of the primary structure of FXI as reported by Fujikawa *et al.* The apple domains are designated A1-A4. Cysteine residues that form disulfide bonds within a FXI subunit are shown in yellow. Cys^{321} in A4 forms the disulfide bond between the dimer subunits. FXI is cleaved after Arg^{369} to form FXIa. The residues of the protease domain catalytic triad are shown in green. Amino acids that are involved in the hydrophobic core of the dimer interface are shown in maroon. The two anion binding sites are in magenta.

planes of the apple domain disks of the two subunits are inclined at a 70° angle relative to each other (Figure 2-2). The FXI subunit shares a high degree of homology in both amino acid sequence and domain structures with the monomeric plasma protein PK, which is the zymogen of the protease α-kallikrein (Fujikawa *et al.*, 1986; McMullen *et al.* 1991). Comparisons of the amino acid sequences of FXI with PK have greatly facilitated identification of residues of functional relevance.

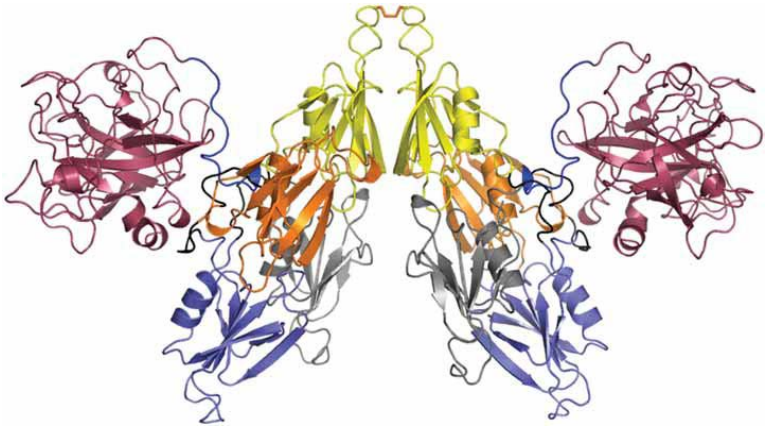

Figure 2-2 The structure of FXI. Topology diagram showing the structure of FXI zymogen. A1-A4 domains and protease domains are shown in gray, blue, orange, yellow and maroon, respectively.

While the FXI protease domain shares common structural and functional features with other trypsin-like coagulation proteases, the apple domains distinguish FXI from other proteases required for hemostasis. Apple domains contribute to the majority of binding interactions between FXI/FXIa and macromolecular ligands and substrates involved in protease function and regulation (Figure 2-3). Studies with FXI/PK chimeras in which individual FXI apple domains are replaced by the corresponding domain from PK indicate that the A2 domain is required for binding to HK (Renné *et al.*, 2002), with contributions from A1 and A4 (Baglia *et al.*, 1990; 1992). Thrombin binds to the A1 domain of FXI, with

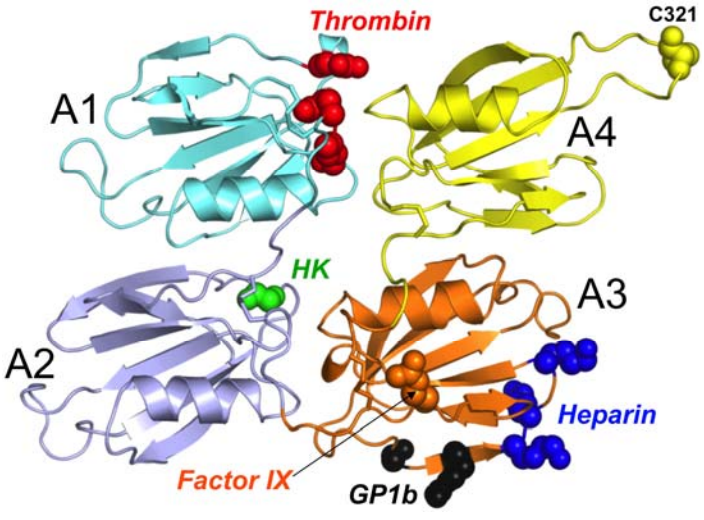

Figure 2-3. FXI apple domain disk. Shown is the disk structure formed by the apple domains (A1, A2, A3, and A4) of human FXI, which are shown in light blue, gray, orange, and yellow, respectively. Locations of amino acids implicated in putative ligand binding sites are shown as space filling images in red for thrombin, green for HK, black for glycoprotein Ib (Gp Ib), blue for heparin and orange for FIX.

residues Glu66, Lys83, and Gln84 forming part of the binding site (Baglia *et al.*, 1996; Papagrigoriou *et al.*, 2006). The residues involved in binding to FXIIa have not been clearly established. While studies using peptide mimicry point to a FXIIa binding site on the A4 domain (Ala317-Gly350) (Baglia *et al.*, 1993), a monoclonal antibody binding to A2 interferes with FXI activation by FXIIa (Cheng *et al.*, 2010). The A3 domain contains a binding site for FIX that is only exposed on the activated protease FXIa (Sun *et al.*, 1996; Sun *et al.*, 1999). A3 also supports interactions with polyanions and the platelet receptor Glycoprotein 1bα (GP 1bα) (Baglia *et al.*, 1995; 2004). The importance of the A3 domain to interactions with FIX will be elaborated on in detail in the next chapter.

The Dimeric Structure of Factor XI

The most unusual feature of FXI is its homodimeric structure. The dimer interface involves residues within the A4 domain on each subunit (Figure 2-4) (Papagrigoriou *et al.*, 2006). A loop containing Cys321 projects away from the body of the domain, and Cys321 forms an interchain disulfide bond with Cys321 from the opposite subunit. The FXI homolog PK is a monomer with Cys321 paired with Cys326, a residue not present in FXI (McMullen *et al.*, 1991). Human FXI in which Cys321 is replaced with another amino acid still forms non-covalently associated dimers (Meijers *et al.*, 1992; Cheng *et al.*, 2003). Furthermore, substituting Cys326 in PK with Gly, which prevents intradomain disulfide bond formation, does not induce PK dimerization (Cheng *et al.*, 2003). This indicates that non-covalent interactions are primarily responsible for maintaining the dimeric structure. The FXI crystal structure reveals a mixture of electrostatic and hydrophobic interactions in dimer interface (Samuel *et al.*, 2007). Leu284, Ile290, and Tyr329 form the hydrophobic

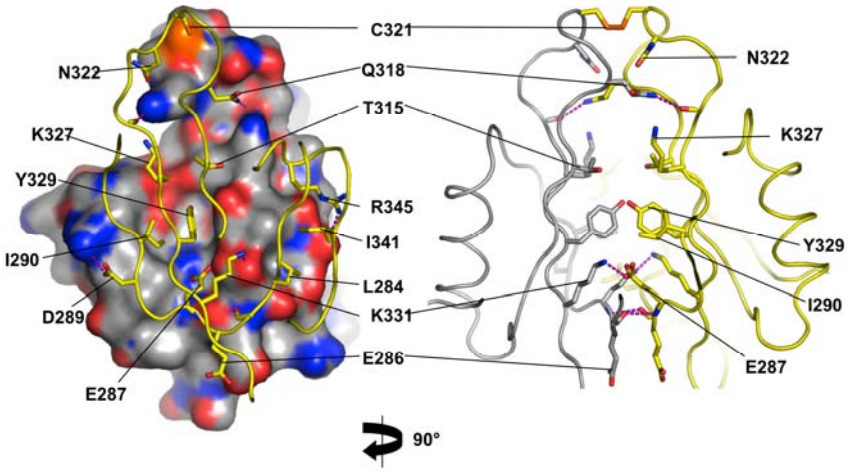

Figure 2-4. Two perspectives of the FXI A4 domain dimer interface. Left: one A4 domain as a charge-surface representation, and the other A4 domain as a ribbon diagram showing the side chains of residues that interact with the opposite A4 domain. Right: ribbon diagram of two A4 domains with the hydrogen bonds and electrostatic interface in magenta. (After Papagrigoriou *et al.*, 2006)

the core of the interface, and salt bridges form between Lys^{331} from one subunit and Glu^{287} from the other subunit. In Chapter VII, a monomeric FXI species will be generated by replacing some of the residues that are critical for dimer formation.

The dimeric structure of FXI is unique among trypsin-like coagulation proteases, and is conserved across mammalian species (Ponczek *et al.*, 2008), indicating functional importance. Over the past 35 years a significant amount of effort has been put into understanding the physiologic significance of the FXI dimer. Previous speculation on the function of the dimeric structure includes proper protein secretion (Meijers *et al.*, 1992) or FIX activation (Wolberg *et al.*, 1997). However, subsequent work refuted these possibilities (Wu *et al.*, 2008; Smith *et al.*, 2008). Recent studies by Papagrigoriou *et al.* and Wu *et al.* suggest FXI may be activated by a *trans*-activating mechanism, where the activating protease binds one FXI subunit while activating the opposite subunit through proteolytic cleavage. Work discussed in Chapter VII addresses the importance of the

dimeric structure to zymogen activation in detail. Previous studies of FXI activation were performed primarily in systems with purified proteins, and used non-physiologic polyanions to enhance the activation rates. We will assess the importance of FXI dimeric structure in more physiologically relevant systems, including studies with polyP as a cofactor.

Activation of Factor XI

Conversion of a FXI subunit to FXIa involves cleavage of the Arg^{369}-Ile^{370} bond, resulting in a 45 kDa heavy chain (comprised of the 4 apple domains), and a 35 kDa light chain (the catalytic domain). The heavy and light chains remain connected by a disulfide bonds between Cys^{362} in the A4 domain and Cys^{482} in the catalytic domain (McMullen *et al.*, 1991). Cleavage after Arg^{371} activates PK in a similar manner (Hooley *et al.*, 2007). After activation, FXIa Ile^{370} (the new free N-terminus of the catalytic domain) moves approximately 20 Å to insert into the activation pocket of FXIa (Figure 2-5), and contributes to the proper conformation of the newly formed active site by forming a salt bridge with Asp^{556} (Navaneetham *et al.*, 2005).

While crystal structures are not available for full-length dimeric or monomeric FXIa, small-angle X-ray scattering and electron microscopy studies indicate that a large conformational change occurs with activation, from an elongated (dumbbell-shaped) structure to a more compact (box-like) arrangement (Samuel *et al.*, 2007). Consistent with this, a comparison of the NMR structure of the isolated FXI A4 domain and the crystal structure of A4 in full-length FXI suggests that cleavage of the covalent linkage between A4 and the catalytic domain in FXI zymogen causes a major conformational change

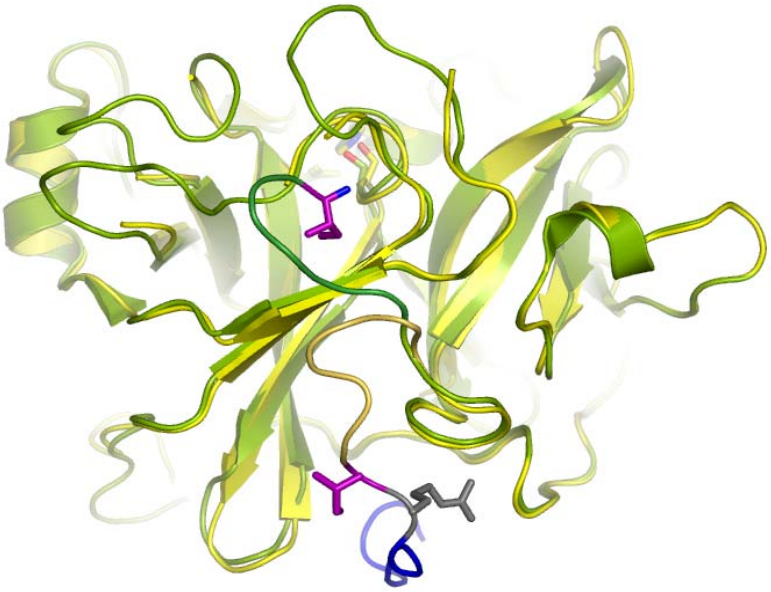

Figure 2-5. FXI catalytic domain. Shown is a ribbon diagram superimposing the protease domain structure of FXI zymogen (yellow) and FXIa (green). Ile^{370} (purple) positions into the protease core after cleavage of the Arg^{369}-Ile^{370} bond. (After Papagrigoriou *et al.*, 2006)

that brings the two catalytic domains of the dimer into closer proximity (Samuel *et al.*, 2007). While the structure of full-length FXIa remains speculative, it is clear from structures of the isolated FXIa catalytic domain that significant structural changes accompany zymogen activation.

In the original waterfall-cascade model of coagulation, FXI is activated by FXIIa (Davie *et al.*, 1991). However, people with FXII deficiency do not have a bleeding disorder (Walsh and Gailani 2006), while FXI deficient patients can experience abnormal bleeding (Salomon *et al.*, 2006). This suggests that FXIIa is not the only activator of FXI *in vivo*. In 1991, two groups reported that thrombin can activate FXI and that FXI can undergo autoactivation in the presence of polyanions (Naito and Fujikawa, 1991; Gailani and Broze, 1991). There have been different opinions on the importance of thrombin-mediated FXI activation. Pedicord *et al.* did not find evidence for FXIIa-independent activation of FXI in plasma, and concluded that previous results demonstrating FXIIa-independent FXI

activation may have been compromised by an artifact of plasma preparation (Pedicord *et al,* 2007). Subsequently, Kravtsov *et al.* showed that FXI can be activated in plasma in the absence of FXII under conditions that controlled for FXIa contamination (Kravtsov *et al.,* 2009). In contrast to the controversy surrounding the role of FXI activation by FXIIa during normal hemostasis, multiple recent studies have suggested an important role for this reaction in thrombosis. FXI- or FXII-deficient mice have a significant defect in experimentally induced arterial thrombus formation (Wang *et al.*, 2005; Renné *et al.*, 2005), and an antibody blocking FXI activation by FXIIa prevented thrombus formation in wild type mice to a similar degree as total FXI deficiency (Cheng *et al.*, 2010).

It is now thought that thrombin generated as a consequence of FVIIa/TF activity can feed back to activate FXI (Figure 1-1), FXIa can then sustain thrombin generation through activation of FIX. This seems compatible with proposed role of FXI in maintaining fibrin clot integrity during normal hemostasis. FXI can be activated by several products of prothrombin activation (von dem Borne *et al.*, 1997; Matafonov *et al.*, 2011). The main product, α-thrombin, has two anion binding exosites (ABE I and ABE II) that are required for interactions with substrates, receptors, and inhibitors (Krishnaswamy *et al.*, 2005). ABE I mediates binding to fibrinogen and fibrin, while ABE II mediates binding to polyanions including heparin and polyphosphate. During coagulation, prothrombin is converted initially by FXa to the protease meizothrombin, which expresses ABE I (Anderson *et al.*, 2003). Meizothrombin is rapidly converted to α-thrombin, which can undergo additional cleavage to form β-thrombin and γ-thrombin (Bovill *et al.*, 1995; Jenny *et al.*, 2006). The latter two proteases have intact ABE II, but reduced activity for ABE I-dependent reactions. There are controversial results concerning the importance of the

anion binding sites on thrombin for FXI. Yun *et al*. suggested that ABE I is required for binding and activation of FXI (Yun *et al*., 2003). However, Matafonov *et al*. recently presented evidence that β-thrombin and γ-thrombin are capable of activating FXI in plasma (Matafonov *et al*., 2011), which argues against the importance of ABE I.

Although thrombin has received increasing attention as an activator of FXI, the physiologic significance of FXI activation by thrombin was questioned because of the extremely slow reaction rate *in vitro*. It had been established that non-physiologic polyanions, such as dextran sulfate, heparin, or high levels of sulfatides accelerate FXI activation by thrombin (Gailani and Broze, 1991; 1993). In fact, polyanions can support FXI activation in the absence of FXIIa or thrombin. This process has been termed "autoactivation", and is likely triggered by traces of FXIa in FXI preparations, although the possibility that zymogen FXI has protease activity after binding to polyanions cannot be completely ruled out. Recently, polyP from platelet dense granules has been shown to promote FXI activation by thrombin or autoactivation (Choi *et al.*, 2011). Synthetic polyP of the size secreted by platelets, or boiled platelet releasates (which degrade all associated proteins) markedly accelerated the rate of FXI activation by thrombin, suggesting that polyP released from platelets is a natural cofactor for FXI activation *in vivo*. Furthermore, FXI binding to polyP appears to be required for cofactor activity. In Chapter IX we will examine this interaction using FXI mutants that are defective in binding to polyanions, and assess the physiologic consequence of this interaction *in vivo*.

As FXI is a homodimer, it must be cleaved at two spatially separated Arg^{369}-Ile^{370} bonds for activation of both subunits. Traditionally, this process has been treated as a one-step process, in which a protease with both subunits (FXIa) is produced directly from

FXI. However, recent work demonstrates that FXI activation by FXIIa or α-thrombin proceeds through an intermediate with one activated subunit (1/2-FXIa) (Smith *et al.*, 2008), which may actually be a major species of activated FXI in plasma. Work examining the importance of the dimeric structure of FXI to activation, and the relative activation rate of the two FXI subunits is presented in Chapter VI.

Inhibition of Factor XIa

Activated FXIa is regulated by plasma serine protease inhibitors (serpins), including C1-inhibitor (C1-INH) (Forbes *et al.*, 1970), antithrombin (AT) (Damus *et al.*, 1973), α1-antitrypsin (Heck and Kaplan, 1974), α2-antiplasmin (Saito *et al.*, 1979), protease nexin 1 (Knauer *et al.*, 2000) and protein Z-dependent protease inhibitor (Han *et al.*, 2000). The specificity of the inhibition is determined to a large extent by basic amino acids in the FXIa autolysis loop (Arg^{504}, Lys^{505}, Arg^{507} and Lys^{509}) (Rezaie *et al.*, 2000). In addition to serpins, FXIa is inhibited by protease nexin 2, a Kunitz-type protease inhibitor secreted by activated platelets (Smith *et al.*, 1990). The inhibition is reported to be a reversible process that requires interactions between the Kunitz protease inhibitor domain of PN2 and the catalytic domain of FXIa (Badellino and Walsh, 2000; Navaneetham *et al.*, 2005).

In plasma, C1-inhibtor (C1-INH) appears to be the predominant regulator of FXIa (Wuillemin *et al.*, 1996). While antithrombin (AT) normally inhibits FXIa at lower rates than C1-INH, the presence of the glycosaminoglycan heparin, enhances inhibition of FXIa by AT up to 500-fold (Zhao *et al.*, 1998; Olson *et al.*, 2004). Two anion binding sites on FXIa are involved in the interaction with heparin (Figure 2-6). A binding site on the A3 domain (Lys^{252}, Lys^{253} and Lys^{255}) is unique to FXI and FXIa, and facilitates

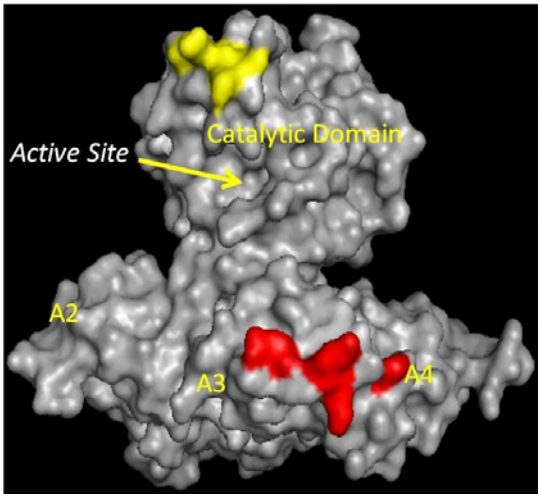

Figure 2-6. Topology of a FXI subunit in surface representation. Residues composing the A3 domain and the protease domain anion binding sites (ABS-1 and ABS-2, respectively) are in black.

AT-mediated inhibition through a mechanism that involves FXIa and AT binding in proximity on the heparin (a template mechanism, Zhao *et al.*, 1998). A second binding site on the catalytic domain (Lys^{529}, Arg^{530}, Arg^{532}, Lys^{536} and Lys^{540}) is similar to heparin binding sites found on other coagulation proteases. Its role in FXIa inhibition is complex and may include charge neutralization or an allosteric effect that overcomes repulsive interactions between AT and basic residues on the catalytic domain (Yang *et al.*, 2009). Like heparin, polyP is a negatively charged polymer that needs to bind to FXI for its effects on the protein to become apparent. In Chapter IX we will assess the importance of the known anion binding sites on FXI to the FXI interaction with polyP.

References

Anderson, P.A. and Bock, P.E. (2003) Role of prothrombin fragment I in the pathway of regulatory exosite I formation during conversion of human prothrombin to thrombin. J Biol Chem *278*, 44489-44495.

Badellino, K.O., and Walsh, P.N. (2000) Protease nexin II interactions with coagulation

factor XIa are contained within the Kunitz protease inhibitor domain of protease nexin II and the factor XIa catalytic domain. Biochemistry *39*, 4769-4777.

Baglia, F., Jameson, B., Walsh, P. (1995) Identification and characterization of a binding site for platelets in the apple 3 domain of coagulation factor XI. J Biol Chem *270*, 6734-6740.

Baglia, F.A. and Walsh, P.N. (1996) A binding site for thrombin in the apple 1 domain of factor XI. J Biol Chem *271*, 3652-3658.

Baglia, F.A., Gailani, D., López, J.A., Walsh, P.N. (2004) Identification of a binding site for glycoprotein Ibα in the Apple 3 domain of factor XI. J Biol Chem *279*, 45470-45476.

Baglia, F.A., Jameson, B.A., Walsh, P.N. (1990) Localization of the high molecular weight kininogen binding site in the heavy chain of human factor XI to amino acids phenylalanine 56 through serine 86. J Biol Chem *265*, 4149-4154.

Baglia, F.A., Jameson, B.A., Walsh, P.N. (1992) Fine mapping of the high molecular weight kininogen binding site on blood coagulation factor XI through the use of rationally designed synthetic analogs. J Biol Chem *267*, 4247-4252.

Baglia, F.A., Jameson, B.A., Walsh, P.N. (1993) Identification and characterization of a binding site for factor XIIa in the Apple 4 domain of coagulation factor XI. J Biol Chem *268*, 3838-3844.

Bouma, B., and Griffin, J. (1977) Human blood coagulation factor XI, purification, properties, and mechanism of activation by activated factor XII. J Biol Chem *252*, 6432-6437.

Bovill, E.G., Tracy, R.P., Hayes, T.E., Jenny, R.J., Bhushan, F.H., Mann, K.G. (1995) Evidence that meizothrombin is an intermediate product in the clotting of whole blood. Arterioscler Thromb Vasc Biol *15*, 754-758.

Cheng, Q., Sun, M.F., Kravtsov, D.V., Aktimur, A., Gailani, D. (2003) Factor XI apple domains and protein dimerization. J Thromb Haemost *1*, 2340-2347.

Cheng, Q., Tucker, E.I., Pine, M.S., Sisler, I., Matafonov, A., Sun, M.F. White-Adams, T.C., Smith, S.A., Hanson, S.R., McCarty, O.J., Renné, T., Gruber, A., Gailani, D. (2010) A role for factor XIIa-mediated factor XI activation in thrombus formation *in vivo*. Blood *116*, 3981-3989.

Choi, S.H., Smith, S.A., Morrissey, J.H. (2011) Polyphosphate is a cofactor for the activation of factor XI by thrombin. Blood *118*, 6963-70.

Damus, P.S., Hicks, M., Rosenberg, R.D. (1973) Anticoagulant action of heparin. Nature *246*, 355-357.

Davie, E.W., Fujikawa, K., Kisiel, W. (1991) The coagulation cascade: initiation, maintenance, and regulation. Biochemistry *30*, 10363-10370.

Forbes, C.D., Pensky, J., Ratnoff, O.D. (1970) Inhibition of activated Hageman factor and activated plasma thromboplastin antecedent by purified serum C1 inactivator. J Lab Clin Med *76*, 809-815.

Fujikawa, K., Chung, D.W., Hendrickson, L.E., Davie, E.W. (1986) Amino acid sequence of human factor XI, a blood coagulation factor with four tandem repeats that are highly homologous with plasma prekallikrein. Biochemistry *25*, 2417-24.

Gailani, D. and Broze, G. (1993) Factor XII-independent activation of factor XI in plasma: Effects of sulfatides on tissue factor-induced coagulation. Blood *82*, 813-819.
Gailani, D., and Broze, G.J. (1991) Factor XI activation in a revised model of blood coagulation. Science *253*, 909-912.

Han, X., Fiehler, R., Broze, G. J., Jr. (2000) Characterization of the protein Z-dependent protease inhibitor. Blood *96*, 3049-3055.

Heck, L.W., and Kaplan, A.P. (1974) Substrates of Hageman factor. I. Isolation and characterization of human factor XI (PTA) and inhibition of the activated enzyme by α 1-antitrypsin. J Exp Med *140*, 1615-1630.

Hooley, E., McEwan, P.A., and Emsley, J. (2007) Molecular modeling of the prekallikrein structure provides insights into high-molecular-weight kininogen binding and zymogen activation. J Thromb Haemost *5*, 2461-2466.

Jenny, N.S., Lundblad, R.L., Mann, K.G. (2006) Thrombin. In: Colman RW, Marder VJ, Clowes AW, George JN, Goldhaber SZ, eds. Hemostasis and Thrombosis: Basic Principles and Practice, 5th ed. Philadelphia,PA: Lippincott Williams & Wilkins; pp193-213.

Jin, L., Pandey, P., Babine, R.E., Gorga, J.C., Seidl, K.J., Gelfand, E., Weaver, D.T., Abdel-Meguid, S.S., Strickler, J.E. (2005) Crystal structures of the FXIa catalytic domain in complex with ecotin mutants reveal substrate-like interactions. J Biol Chem *280*, 4704-4712.

Jin, L., Pandey, P., Babine, R.E., Weaver, D.T., Abdel-Meguid, S.S., Strickler, J.E. (2005) Mutation of surface residues to promote crystallization of activated factor XI as a complex with benzamidine: an essential step for the iterative structure-based design of factor XI inhibitors. Acta Crystallogr D Biol Crystallogr *61*, 1418-1425.

Knauer, D.J., Majumdar, D., Fong, P.C., Knauer, M.F. (2000) SERPIN regulation of factor XIa. The novel observation that protease nexin 1 in the presence of heparin is a more potent inhibitor of factor XIa than C1 inhibitor. J Biol Chem *275*, 37340-37346.

Kravtsov, D.V., Matafonov, A., Tucker, E.I., Sun, M.F., Walsh, P.N., Gruber, A., Gailani,

D. (2009) Factor XI contributes to thrombin generation in the absence of factor XII. Blood *114*, 452-458.

Krishnaswamy, S. (2005) Exosite-driven substrate specificity and function in coagulation. J Thromb Haemost *3* 54–67.

Mandle, R.J., Colman, R.W., Kaplan, A.P. (1976) Identification of prekallikrein and high-molecular-weight kininogen as a complex in human plasma. Proc Natl Acad Sci USA *73*, 4179-4183.

Matafonov, A., Sarilla, S., Sun, M.F., Sheehan, J.P., Serebrov, V., Verhamme, I.M., Gailani D. (2011) Activation of factor XI by products of prothrombin activation. Blood *118*, 437-445.

McMullen, B.A., Fujikawa, K., Davie, E.W. (1991) Location of the disulfide bonds in human coagulation factor XI: the presence of tandem apple domains. Biochemistry *30*, 2056-2060.

McMullen, B.A., Fujikawa, K., Davie, E.W. (1991) Location of the disulfide bonds in human plasma prekallikrein: the presence of four novel apple domains in the amino-terminal portion of the molecule. Biochemistry *30*, 2050-2056.

Meijers, J. C., Davie, E. W., Chung, D. W. (1992) Expression of human blood coagulation factor XI: Characterization of the defect in factor XI type III deficiency, Blood *79*, 1435-1440.

Meijers, J., Mulvihill, E., Davie, E., Chung, D. (1992) Apple 4 in human blood coagulation factor XI mediates dimer formation. Biochemistry *31*, 4680-4684

Naito, K., and Fujikawa, K. (1991) Activation of human blood coagulation factor XI independent of factor XII. Factor XI is activated by thrombin and factor XIa in the presence of negatively charged surfaces. J Biol Chem *266*, 7353-7358.

Navaneetham, D., Jin, L., Pandey, P., Strickler, J.E., Babine, R.E., Abdel-Meguid, S.S., Walsh, P.N. (2005) Structural and mutational analyses of the molecular interactions between the catalytic domain of factor XIa and the Kunitz protease inhibitor domain of protease nexin 2. J Biol Chem *280*, 36165-36175.

Olson, S. T., Swanson, R., Raub-Segall, E., Bedsted, T., Sadri, M., Petitou, M., Herault, J. P., Herbert, J. M., Bjork, I. (2004) Accelerating ability of synthetic oligosaccharides on antithrombin inhibition of proteinases of the clotting and fibrinolytic systems. Comparison with heparin and low-molecular-weight heparin. Thromb Haemost *92*, 929-939.

Papagrigoriou, E., McEwan, P.A., Walsh, P.N., and Emsley, J. (2006) Crystal structure of the factor XI zymogen reveals a pathway for transactivation. Nat Struct Mol Biol *13*, 557-558.

Pedicord, D.L., Seiffert, D., Blat, Y. (2007) Feedback activation of factor XI by thrombin does not occur in plasma. Proc Natl Acad Sci USA *104*, 12855-12860.

Ponczek, M.B., Gailani, D., Doolittle, R.F. (2008) Evolution of the contact phase of vertebrate blood coagulation. J Thromb Haemost *6*, 1876-1883.

Renné, T., Gailani, D., Meijers, J.C., Müller-Esterl, W. (2002) Characterization of the H-kininogen-binding site on factor XI: a comparison of factor XI and plasma prekallikrein. J Biol Chem *277*, 4892-4899.

Renné, T., Pozgajová, M., Grüner, S., Schuh, K., Pauer, H.U., Burfeind, P., Gailani, D., Nieswandt, B. (2005) Defective thrombus formation in mice lacking coagulation factor XII. J Exp Med *202*, 271-281.

Rezaie, A.R., Sun, M.F., Gailani, D. (2006) Contributions of basic amino acids in the autolysis loop of factor XIa to serpin specificity. Biochemistry *45*, 9427-9433.

Saito, H., Goldsmith, G. H., Moroi, M., Aoki, N. (1979) Inhibitory spectrum of α 2-plasmin inhibitor, Proc Natl Acad Sci USA *76*, 2013-2017.

Salomon, O., Steinberg, D.M., Seligshon, U. (2006) Variable bleeding manifestations characterize different types of surgery in patients with severe factor XI deficiency enabling parsimonious use of replacement therapy. Haemophilia *12*, 490-493.

Samuel, D., Cheng, H., Riley, P.W., Canutescu, A.A., Nagaswami, C., Weisel, J.W., Bu, Z., Walsh, P.N., and Roder, H. (2007) Solution structure of the A4 domain of factor XI sheds light on the mechanism of zymogen activation. Proc Natl Acad Sci USA *104*,15693-15698.

Smith, R., Higuchi, D., Broze, G. (1990) Platelet coagulation factor XIa-inhibitor, a form of Alzheimer Amyloid Precursor Protein. Science *248*, 1126-1128.

Smith, S.B., Verhamme, I.M., Sun, M.F., Bock, P.E., Gailani, D. (2008) Characterization of novel forms of coagulation factor XIa: independence of factor XIa subunits in factor IX activation. J Biol Chem *283* 6696-6705.

Sun, M.F., Zhao, M., Gailani, D. (1999) Identification of amino acids in the factor XI apple 3 domain required for activation of factor IX. J Biol Chem *274*, 36373-8.

Sun, Y., and Gailani, D. (1996) Identification of a factor IX binding site on the third apple domain of activated factor XI. J Biol Chem *271*, 29023-8.

Thompson, R.E., Mandle, R., Kaplan, A.P. (1977) Association of factor XI and high molecular weight kininogen in human plasma. J Clin Invest *60*, 1376-1380.

von dem Borne, P.A., Mosnier, L.O., Tans, G., Meijers, J.C., Bouma, B.N. (1997) Factor

XI activation by meizothrombin: stimulation by phospholipid vesicles containing both phosphatidylserine and phosphatidylethanolamine. Thromb Haemost *78*, 834-839.

Walsh, P.N. and Gailani, D. (2006) Factor XI. In: Colman RW, Marder VJ, Clowes AJ, George JN, Goldhaber SZ, eds. Hemostasis and Thrombosis: Basic Principles and Clinical Practice. Vol 5. Philadelphia, PA: Lippincott Williams & Wilkins; pp221-233.

Wang, X., Cheng, Q., Xu, L., Feuerstein, G.Z., Hsu, M.Y., Smith, P.L., Seiffert, D.A., Schumacher, W.A., Ogletree, M.L., Gailani, D. (2005) Effects of factor IX or factor XI deficiency on ferric chloride-induced carotid artery occlusion in mice. J Thromb Haemost *3*, 695-702.

Wolberg, A. S., Morris, D. P., Stafford, D. W. (1997) Factor IX activation by factor XIa proceeds without release of a free intermediate. Biochemistry *36*, 4074–4079.

Wu, W., Sinha, D., Shikov, S., Yip, C.K., Walz, T., Billings, P.C., Lear, J.D., Walsh, P.N. (2008) Factor XI homodimer structure is essential for normal proteolytic activation by factor XIIa, thrombin, and factor XIa. J Biol Chem *283*, 18655-18664.

Wuillemin, W.A., Hack, C.E., Bleeker, W.K., Biemond, B.J., Levi, M., Cate, H. (1996) Inactivation of factor XIa *in vivo*: Studies in chimpanzees and in humans. Thromb Haemost *76*, 549.

Yang, L., Sun, M.F., Gailani, D., Rezaie, A.R. (2009) Characterization of a heparin-binding site on the catalytic domain of factor XIa: Mechanism of heparin acceleration of factor XIa inhibition by the serpins antithrombin and C1-inhibitor. Biochemistry *48*, 1517–24.

Yun, T.H., Baglia, F.A., Myles, T., Navaneetham, D., López, J.A., Walsh, P.N., Leung, L.L. (2003) Thrombin activation of factor XI on activated platelets requires the interaction of factor XI and platelet glycoprotein Ib α with thrombin anion-binding exosites I and II, respectively. J Biol Chem *278*, 48112-48119.

Zhao, M., Abdel-Razek, T., Sun, M.F., Gailani, D. (1998) Characterization of a heparin binding site on the heavy chain of factor XI. J Biol Chem *273*, 31153–9.

CHAPTER III

STRUCTURE AND ACTIVATION OF FACTOR IX

Structure of Factor IX

Factor IX (FIX) is the zymogen of a key enzyme in blood coagulation, factor IXaβ (FIXaβ). Deficiency of its activity in plasma results in an X-linked bleeding disorder, Hemophilia B, which occurs once in every 25,000-30,000 male births (Ragni *et al.*, 2009). The disease is characterized by prolonged or recurrent bleeding after mild trauma, or in severe cases, spontaneous joint or deep-muscle bleeding. Zymogen FIX is a single polypeptide of 57 kDa (415 amino acids). It is synthesized in hepatocytes and secreted into the plasma where it circulates at a concentration of ~80-100 nM (Schmidt and Bajaj, 2003). A fraction of secreted FIX forms a non-circulating pool bound to collagen in the subendothelial basement membranes of blood vessels (Gui *et al.*, 2009). As discussed in Chapter I, both FVIIa/TF and FXIa convert FIX to the active enzyme FIXaβ. FIXaβ, with its cofactor VIIIa, forms the "intrinsic Xase" complex on phospholipid membranes.

FIX is a member of the family of Vitamin K-dependent (VKD) coagulation proteins. Starting from the N-terminus, FIX is composed of an N-terminal Gla domain, a hydrophobic stack region, two epidermal growth factor domains (EGF1 and EGF2) connected by a short linker, an activation peptide (AP), and a C-terminal trypsin-like catalytic serine protease domain (Figure 3-1). There are no published crystal structures for full length human FIX or FIXaβ (there are crystal structures for porcine FIXaβ [Brandstetter *et al.*, 1995], the EGF2 and protease domain of human FIXaβ [Hopfner *et al.*,

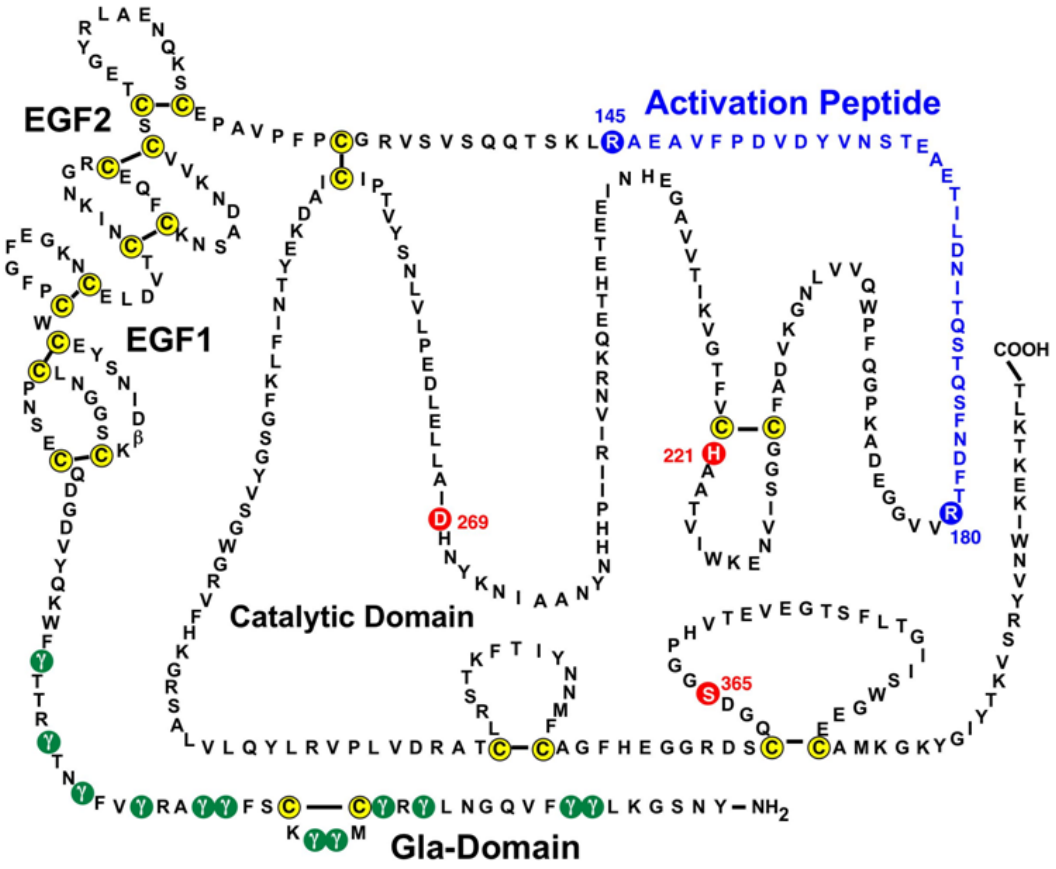

Figure 3-1. Amino acid sequence and disulfide bond locations of FIX. Cysteine residues are in yellow. γ-carboxylated glutamic acid are shown in green, and the activation peptide in blue. Residues Arg^{145} and Arg^{180} are the cleavage sites for protease activation. The protease domain catalytic triad is shown in red.

1999]; as well as several crystal and NMR structures of individual Gla [Shikamoto *et al.*, 2003; Huang *et al.*, 2004] and EGF1 domains [Baron *et al.*, 1992]). Figure 3-2 shows a space-filling structure for FIX and FIXaβ based on available information (image courtesy of Dr S. Paul Bajaj, UCLA). FIX has the typical elongated profile of a VKD coagulation protease, with Gla domain and catalytic domains at opposite ends of the molecule. Structure-function studies indicate that the Gla, EGF1, EGF2, and catalytic domains of FIX are involved in specific interactions with substrates, phospholipid surfaces and cofactors. The Gla and EGF1 domains and the AP contain recognition sites for the

FVIIa/TF complex, while the protease and EGF2 domains of FIXaβ contain recognition sites for FVIIIa (Schmidt and Bajaj, 2003).

The Factor IX Gla Domain

A structural element common to all VKD proteins is an N-terminal γ-carboxyglutamic acid-rich "Gla" domain. The FIX Gla domain contains 12 glutamic acid residues (Figure 3-1) that undergo post-translational modification by addition of a carboxyl group to the γ-carbon (Bandyopadhyay, 2008). This process is mediated by the enzyme γ-glutamyl carboxylase, and requires reduced vitamin K as a cofactor. The widely used anticoagulant

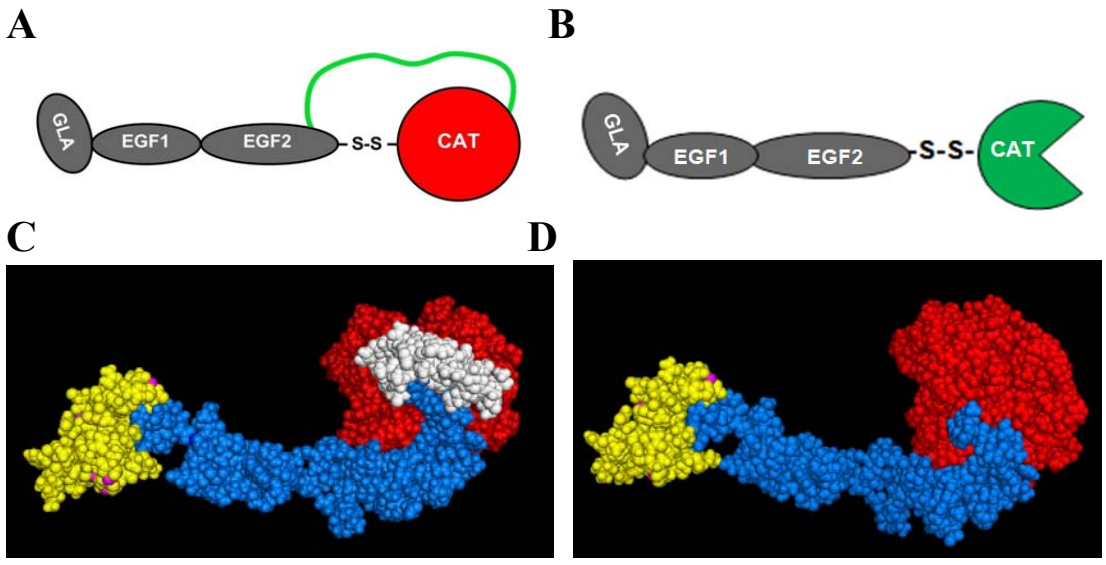

Figure 3-2. Structure of FIX and FIXa. A and B: The schematic diagram of human FIX **(A)** and FIXaβ **(B)** with the domains labeled. Abbreviations for domains are: Gla - γ-carboxyglutamic acid domain, and EGF - epidermal growth factor domain. The catalytic domains (CAT) is shown in red and green, and the activation peptide is shown in green. C and D: A space filling model of human FIX **(C)** and FIXaβ **(D)** based on published structure of parts of the molecule. Gla domain is shown in yellow, EGF1 and 2 are in blue, the activation peptide in white and the catalytic domain in red. Divalent cations in the Gla domain are shown as magenta spheres. Model courtesy of Dr. S. Paul Bajaj (University of California, Los Angeles).

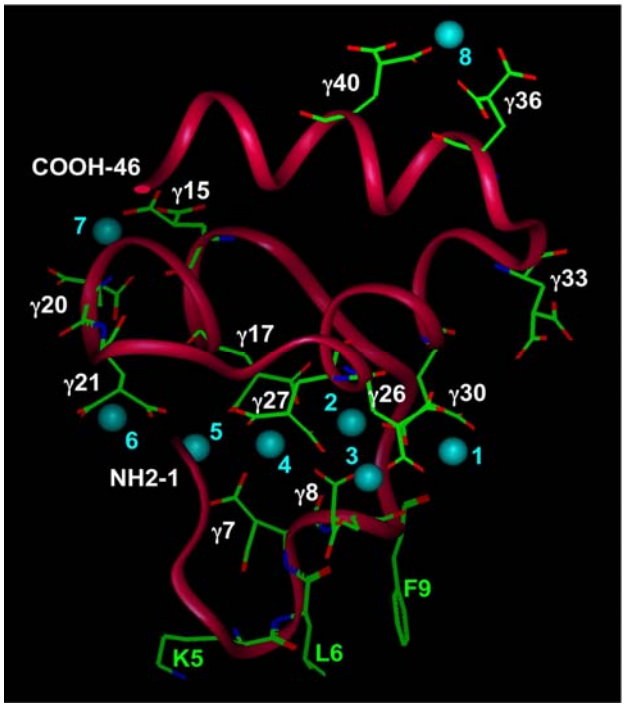

Figure 3-3. A ribbon diagram of the Gla domain of FIX. Shown are the N-terminus residue to residue 46. Side chains of γ-carboxyglutamic acid residues (γ), and Lys 5, Leu6 and Phe9 in the omega loop are in green. Divalent cations are shown as cyan spheres (numbered). (Adapted from Agah and Bajaj, 2009)

warfarin inhibits γ-carboxylation by interfering with regeneration of reduced vitamin K (Holbrook *et al.*, 2005). The malonate-like side chains of γ-carboxylated glutamic acid residues in FIX bind 8 divalent metal ions, five of which are internal and three of which are on the surface of the Gla domain (Figure 3-3) (Schmidt and Bajaj, 2003). At physiologic plasma Ca^{2+} and Mg^{2+} concentrations, sites 2, 3, 5 and 6 are occupied by Ca^{2+}, while sites 1, 4, 7 and 8 are occupied by Mg^{2+} (Shikamoto *et al.*, 2003; Agah and Bajaj, 2009). Binding of these divalent cations induces a structural transition in the Gla domain from an unfolded nonfunctional form to one that is tightly folded (Vadivel *et al.*, 2012). This allows the entire domain to adopt a "functional" conformation that facilitates binding to phospholipids and protein ligands. The Gla domain binds to phospholipid membranes through a solvent-exposed hydrophobic patch termed the "ω-loop" (omega loop). In FIX,

the ω-loop is composed of residues 4-11 at the N-terminus of the Gla domain (Huang *et al.*, 2003). Residues Lys^5, Leu^6 and Phe^9 of the ω-loop interact with the head-group and glycerol backbone of phosphotidylserine, while the divalent cations bound to the Gla domain form bridges with the negatively charged head-groups (Huang *et al.*, 2003; Grant *et al.*, 2004). Residue Lys^5 on FIX is also required for binding to type IV collagen, a ubiquitous component of endothelial cell basement membrane (Cheung *et al.*, 1992; Gui *et al.*, 2002). This interaction is likely to influence distribution of FIX, as described above (Gui *et al.*, 2009).

Although distant from the activation cleavage sites on FIX, the Gla domain plays a critical role in FIX activation by FVIIa/TF and FXIa. FVIIa and FIX have similar elongated structures. The Gla domains of each protein contribute to assembly of an enzyme-substrate complex on a phospholipid membrane. These binding reactions are largely responsible for determining the Michaelis constant (K_m) for the reaction. In a modeled structure of the FVIIa-TF-FIX ternary complex, the FIX Gla and EGF1 domains interact with tissue factor near the phospholipid surface (Chen *et al.*, 2002).

In contrast to FVIIa, FXIa lacks a Gla domain. Probably as a consequence, phospholipid does not affect FIX activation by FXIa. However, studies suggest that the FIX Gla domain is essential for direct binding to FXIa. A recombinant chimera consisting of FIX with the FVII Gla domain (FIX/VII-Gla), as well as recombinant wild type FIX (FIX-WT) expressed in the presence of warfarin (to inhibit γ-carboxylation) do not bind to FXIa and, therefore, are activated poorly by FXIa (Aktimur *et al.*, 2003). For comparison, replacing the FIX Gla domain with the Gla domain of either FVII or protein C does not affect its activation by FVIIa/TF (Aktimur *et al.*, 2003; Ndonwi *et al.*, 2007). These

findings suggest that the FIX Gla domain contains a specific epitope(s) that interacts with FXIa that is distinct from the regions that bind to FVIIa/TF. In Chapter VI, studies investigating the residues on the FIX Gla domain that are required for the interaction with FXIa will be presented.

Activation of Factor IX

Activation of human FIX requires proteolytic cleavage of the Arg^{145}-Ala^{146} and Arg^{180}-Val^{181} peptide bonds, resulting in release of the 35-amino acid activation peptide. The activated protease, FIXaβ, contains a light chain (Gla, EGF1 and EGF2 domains) and a heavy chain (protease domain) connected by a single disulfide bond (Figure 3-4). Cleavage

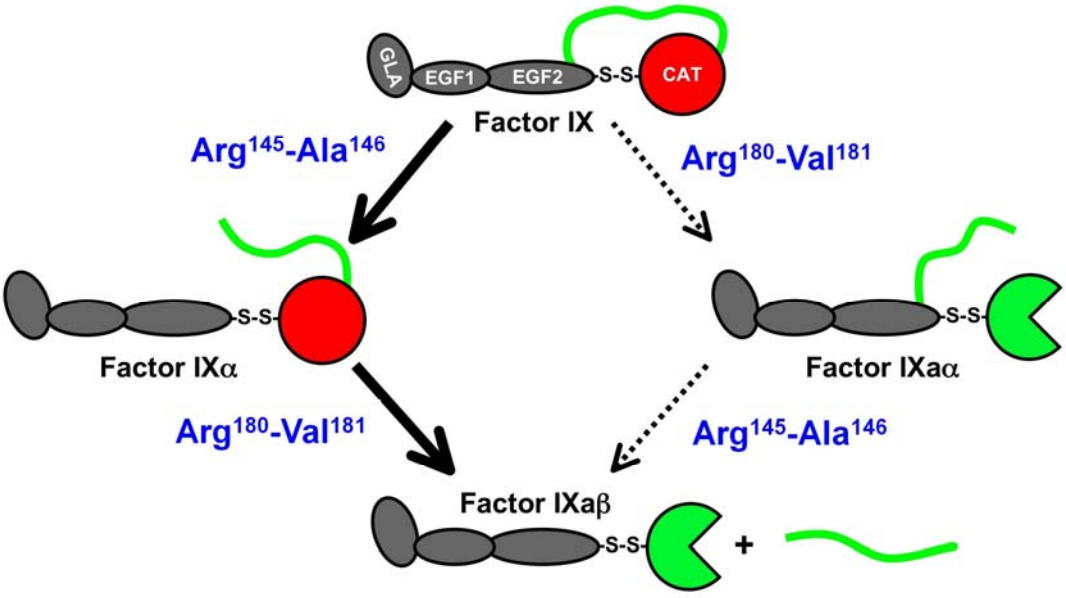

Figure 3-4. FIX activation. FIX is converted to FIXaβ by sequential cleavage at the Arg^{145}-Ala^{146} and Arg^{180}-Val^{181} bonds, releasing the activation peptide (green ribbon), and converting the inactive catalytic domain (red) to active protease (green). Initial cleavage at Arg^{180}-Val^{181}(forming the alternative intermediate factor IXaα) is a minor reaction (dashed arrow) during plasma coagulation.

of the Arg^{180}-Val^{181} bond results in formation of a new N-terminus for the heavy chain (Val^{181}) that forms a salt bridge with Asp^{364}. This critical event induces the active site of the protease domain to assume an active conformation (Thompson, 1991).

The two proteolytic cleavages that activate FIX appear to be sequential and ordered, as only one of the two possible intermediates normally is formed. The FIX activation intermediate cleaved after Arg^{145} (FIXα) is observed during reaction time courses, and a recombinant FIX mutant containing Arg^{145}Ala substitution is cleaved poorly by FXIa (Smith *et al.*, 2008). These observations indicate that the Arg^{180}-Val^{181} bond is either not readily available or is not preferred for initial cleavage by either FXIa or FVIIa/TF. Cleavage after Arg^{145} may change the conformation of the substrate, facilitating subsequent cleavage after Arg^{180}. Interestingly, a protease in the venom from Russell's Viper (RVV) preferentially cleaves FIX at Arg^{180}-Val^{181}, resulting in a FIX intermediate with the activation peptide remaining attached to the light chain (FIXaα) (Griffith *et al.*, 1985). Although the protease domain of FIXaα is in an active conformation, the enzyme has only ~20% of the activity of FIXaβ towards activating FX (Griffith *et al.*, 1985), suggesting that complete removal of the activation peptide is essential for normal function of activated FIX in coagulation.

After cleavage of the Arg^{145}-Ala^{146} bond, FIXα is released from FVIIa/TF and must rebind for the Arg^{180}-Val^{181} bond to be cleaved. As the second cleavage is rate-limiting, FIXα accumulates during activation. In contrast, FIX activation by FXIa does not require phospholipid or a cofactor, and there is little, if any, FIXα accumulation. Therefore, it is reasonable to hypothesize that different mechanisms are involved in FIX activation by the two proteases. As discussed in Chapter II, FXIa has a homodimeric structure that is very

different from that of FVIIa and the other vitamin K-dependent coagulation proteases. A possible explanation for the lack of intermediate accumulation during FIX activation by FXIa is that the two catalytic domains of FXIa cleave both scissile bonds of FIX simultaneously. However, subsequent work demonstrated that each subunit of FXIa behaves as an independent enzyme toward FIX (Smith *et al.*, 2008), with little FIXα accumulation detected using FXIa species with only one active subunit. A major goal of the work discussed in this thesis is to investigate the mechanism by which FXIa activates FIX, and to understand the reasons for the absence of FIXα accumulation during the reaction.

Like most trypsin-like serine proteases, the FXIa active site contains a catalytic triad consisting of histidine (His^{413}), aspartic acid (Asp^{462}) and serine (Ser^{557}) residues. These residues correspond to His^{57}, Asp^{102} and Ser^{195} in chymotrypsin. The chymotrypsin numbering system is often used to compare trypsin-like serine proteases. Catalysis mediated by a trypsin-like protease requires a nucleophilic attack on the carbonyl carbon of the properly positioned substrate by Ser^{195}, with His^{57} and Asp^{102} involved in positioning of Ser^{195} and in stabilizing the substrate-enzyme intermediate (Stryer, 1995). While the catalytic triad is responsible for substrate cleavage, residues flanking the cleavage site on the substrate (which are designated P), and their complementary residues on the enzyme (designated S) are important for docking interactions between substrate and enzyme (Krishnaswamy, 2005). Residues extending from the scissile bond towards the N-terminus are designated P1, P2…Pn, and the residues that interact with them on the enzyme are designated S1, S2…Sn (Schechter and Berger, 1967). The S1 to S3 sites on FXIa are Asp^{551}, Ser^{576} and Gly^{578} (Asp^{189}, Ser^{214} and Gly^{216} in chymotrypsin numbering). They

are located in close proximity to the catalytic triad on the FXIa catalytic domain and contribute to the correct conformation of the cleft-shaped active site.

While specificity of coagulation proteases for small substrates and inhibitors is determined largely by sites in proximity to the active site, such as the S1 to S3 sites, specificity for macromolecular substrates is often dictated by binding interactions at sites remote from the active site (Krishnaswamy *et al.*, 2005). These remote binding sites are referred to as exosites. There is compelling evidence that one or more exosites on FXIa are required for normal FIX activation (Sun *et al.*, 1999; Ogawa *et al.*, 2005), but there is a lack of agreement on their locations. It is established that FIX activation requires the FXIa heavy chain (Sinha *et al.*, 1987; Baglia *et al.*, 1989). In 1991 it was reported that a FIX-binding exosite resides on A2 domain of FXIa, based on work with inhibitory peptides (Baglia *et al.*, 1991). However, studies using FXI proteins in which individual apple domains were replaced by the corresponding domains of PK (a poor activator of FIX) indicated that FIX interacts with an exosite on the FXIa A3 domain (Sun *et al.*, 1996). Subsequent work identified a relatively restricted region within the A3 domain (Ile^{183}-Ile^{197}, Phe^{260}-Ser^{265}) that is required for the normal FIX activation by FXIa (Sun *et al.*, 1999). More recently, evidence has been presented for a distinct FIX-binding exosite on the FXIa catalytic domain (Sinha *et al.*, 2007). The authors reported similar K_ms for FIX activation by the isolated FXIa catalytic domain (a species lacking the entire heavy chain) and full-length FXIa, implying the catalytic domain was largely responsible for recognition and specificity of FIX binding. These data are not compatible with those showing that FXIa A3 domain substitution results in a marked increase in K_m for FIX activation (Sun *et al.*, 1999; Ogawa *et al.*, 2005). In Chapter IV, we will present a kinetic

analysis of conversion of FIX to the intermediate FIXα and the final product FIXaβ by FXIa and FXIa variants that addresses these conflicting results, and will propose a mechanism for FIX activation by FXIa.

References

Agah, S., and Bajaj, SP. (2009) Role of magnesium in factor XIa catalyzed activation of factor IX: calcium binding to factor IX under physiologic magnesium. J Thromb Haemost *7*, 1426–1428.

Aktimur, A., Gabriel, M. A., Gailani, D., and Toomey, J. R. (2003) The factor IX γ-carboxyglutamic acid (Gla) domain is involved in interactions between factor IX and factor XIa. J Biol Chem *278*, 7981–7987.

Baglia, F.A., Jameson, B.A., Walsh, P.N. (1991) Identification and chemical synthesis of a substrate-binding site for factor IX on coagulation factor XIa. J Biol Chem *266*, 24190–24197.

Baglia, F.A., Sinha, D., Walsh, P.N. (1989) Functional domains in the heavy-chain region of factor XI. A high molecular weight kininogen-binding site and a substrate-binding site for factor IX. Blood *74*, 244–251.

Bandyopadhyay, P.K. (2008) Vitamin K-dependent gamma-glutamylcarboxylation: an ancient posttranslational modification. Vitam Horm *78*, 157-184.

Baron, M., Norman, D.G., Harvey, T.S., Handford, P.A., Mayhew, M., Tse, A.G., Brownlee, G.G., Campbell, I.D. (1992) The three-dimensional structure of the first EGF-like module of human factor IX: comparison with EGF and TGF-α., Protein Sci *1*, 81-90.

Brandstetter, H., Bauer, M., Huber, R., Lollar, P., Bode, W. (1995) X-ray structure of clotting factor IXa: active site and module structure related to Xase activity and hemophilia B. Proc Natl Acad Sci USA *92*, 9796–800.

Chen, S.W., Pellequer, J.L., Schved, J.F., and Giansily-Blaizot, M. (2002) Model of a ternary complex between activated factor VII, tissue factor and factor IX. Thromb Haemost *88*, 74-82.

Cheung, W.F., Hamaguchi, N., Smith, K.J., Stafford, D.W. (1992) The binding of human factor IX to endothelial cells is mediated by residues 3–11. J Biol Chem *267*, 20529–31.

Ragni, M.V., Kessler, C.M., Lozier,J.N.(2009) Clinical aspects and therapy of hemophilia,

Hoffman, R., Benz, E., Shattil, S., Furie, B., Silberstein, L., McGlave, P, and Heslop, H. (editors). Hematology: Basic Principles and Practice, 5th edition. New York:Churchill Livingstone - Elsevier pp 1911-1930.

Schmidt, A.E., and Bajaj, S.P. (2003) Structure-function relationships in factor IX and factor IXa. Trends Cardiovasc Med *13*, 39-45.

Grant, M.A., Baikeev, R.F., Gilbert, G.E., Rigby, A.C. (2004) Lysine 5 and phenylalanine 9 of the factor IX omega-loop interact with phosphatidylserine in a membrane-mimetic environment. Biochemistry *43*, 15367-78.

Griffith, M.J., Breitkreutz, L., Trapp, H., Briet, E., Noyes, C.M., Lundblad, R.L., Roberts, H.R. (1985) Characterization of the clotting activities of structurally different forms of activated factor IX. Enzymatic properties of normal human factor IXaα, factor IXaβ, and activated factor IX Chapel Hill. J Clin Invest *75*, 4-10.

Gui, T., Lin, H.F., Jin, D.Y., Hoffman, M., Straight, D.L., Roberts, H.R., Stafford, D.W. (2002) Circulating and binding characteristics of wild-type factor IX and certain Gla domain mutants *in vivo*. Blood *100*, 153–8.

Gui, T., Reheman, A., Ni, H., Gross, P.L., Yin, F., Monroe, D., Monahan, P.E., Stafford, D.W. (2009) Abnormal hemostasis in a knock-in mouse carrying a variant of factor IX with impaired binding to collagen type IV. J Thromb Haemost *7*, 1843-51.

Holbrook, A.M., Pereira, J.A., Labiris, R., McDonald, H., Douketis. J.D., Crowther, M., Wells, P.S. (2005) Systematic overview of warfarin and its drug and food interactions. Arch. Intern. Med *165*, 1095–106.

Hopfner, K.P., Lang, A., Karcher, A., Sichler, K., Kopetzki, E., Brandstetter, H., Huber, R., Bode, W., Engh, R.A. (1999) Coagulation factor IXa: the relaxed conformation of Tyr99 blocks substrate binding. Structure *7*, 989-96.

Huang, M., Furie, B.C., Furie, B. (2004) Crystal structure of the calcium-stabilized human factor IX Gla domain bound to a conformation-specific anti-factor IX antibody. J Biol Chem *279*, 14338-46.

Huang, M., Rigby, A.C., Morelli, X., Grant, M.A., Huang, G.Q., Furie, B., Seaton, B., Furie, B.C. (2003) Structural basis of membrane binding by Gla domains of vitamin K-dependent proteins. Nat Struct Biol *10*, 751–6.

Krishnaswamy, S. (2005) Exosite-driven substrate specificity and function in coagulation. J Thromb Haemost *3* 54–67.

Ndonwi, M., Broze, G.J., Agah, S., Schmidt, A.E., Bajaj, S.P. (2007) Substitution of the Gla domain in factor X with that of protein C impairs its interaction with factor VIIa/tissue

factor: lack of comparable effect by similar substitution in factor IX. J Biol Chem *282*, 15632-44.

Ogawa, T., Verhamme, I.M., Sun, M.F., Bock, P.E., and Gailani, D. (2005) Exosite-mediated substrate recognition of factor IX by factor XIa. The factor XIa heavy chain is required for initial recognition of factor IX. J Biol Chem *280*, 23523–23530.

Schechter, I., and Berger, A. (1967) On the size of the active site in proteases. I. Papain.Biochem Biophys Res Commun *27*, 157-62.

Sinha, D., Marcinkiewicz, M., Navaneetham, D., Walsh, P.N. (2007) Macromolecular substrate-binding exosites on both the heavy and light chains of factor XIa mediate the formation of the Michaelis complex required for factor IX activation. Biochemistry *46*, 9830–9839.

Sinha, D., Seaman, F. S., and Walsh, P. N. (1987) Role of calcium ions and the heavy chain of factor XIa in the activation of human coagulation factor IX. Biochemistry *26*, 3768–3775.

Shikamoto, Y., Morita, T., Fujimoto, Z., Mizuno, H. (2003) Crystal structure of Mg2+- and Ca^{2+}-bound Gla domain of factor IX complexed with binding protein. J Biol Chem *278*, 24090-4.

Smith, S.B., Verhamme, I.M., Sun, M.F., Bock, P.E., Gailani, D. (2008) Characterization of novel forms of coagulation factor XIa: independence of factor XIa subunits in factor IX activation. J Biol Chem *283* 6696-6705.

Stryer, L. (1995) Enzymes: basic concepts and kinetics, in Biochemistry, 4th edition, New York: W.H. Freeman pp181-206.

Sun, Y., and Gailani, D. (1996) Identification of a factor IX binding site on the third apple domain of activated factor XI. J Biol Chem *271*, 29023-8.

Sun, M.F., Zhao, M., Gailani, D. (1999) Identification of amino acids in the factor XI apple 3 domain required for activation of factor IX. J Biol Chem *274*, 36373-8.

Thompson, A.R. (1991) Molecular biology of the hemophilias. Prog Hemost Thromb *10*, 175.

Vadivel, K., Schmidt, A.E., Marder, V.J., Krishnaswamy, S., Bajaj, S.P. (2012) Structure and function of vitamin K-dependent coagulation and anticoagulation proteins, In: Hemostasis and Thrombosis: basic principles and clinical practice, 6th Ed., Lippincott, Williams & Wilkins, Philadelphia, pp 208-32

CHAPTER IV

A MECHANISM FOR FACTOR IX ACTIVATION BY FACTOR XIa

Cleavage of Factor IX and Factor IXα by Factor XIa

During coagulation, FIX is activated by FVIIa/TF and FXIa. Although FIXα forms during activation by either FVIIa or FXIa, it does not accumulate during the latter reaction (Wolberg *et al.*, 1997; Smith *et al.*, 2008). This indicates that different activation mechanisms are involved, and initially raised the possibility that the dimeric FXIa structure may be required to catalyze FIX activation without intermediate accumulation. However, subsequent studies clearly demonstrated that an isolated FXIa subunit is able to convert FIX to FIXaβ without intermediate accumulation (Smith *et al.*, 2008; Wu *et al.*, 2008). This implies sequential cleavages of the two scissile bonds of FIX by a single FXIa subunit, and not the two FXIa subunits of one dimer cleaving the two FIX scissile bonds simultaneously.

The combination of sequential cleavage of FIX scissile bonds and the absence of intermediate FIXα accumulation could be explained by two distinct mechanisms. FIX could be processed to the final product FIXaβ without release of the intermediate FIXα. Such a mechanism has been termed "processive" in prior studies (Wolberg *et al.*, 1997). However, this mechanism is not consistent with the subsequent observation that active site-blocked FXIa is capable of capturing FIXα during FIX activation by FXIa (Smith *et al.*, 2008). This demonstrates that at least a portion of FIXα is released from the enzyme, and indicates a mechanism in which FIXα would be released from FXIa after cleavage of the

Arg^{145}-Ala^{146} bond, with the intermediate being recaptured prior to cleavage of Arg^{180}-Val^{181}. Here, cleavage after Arg^{145} would have to be rate-limiting to account for the lack of intermediate accumulation. To address the conflicting hypotheses regarding the mechanism of FIX activation by FXIa, we conducted kinetic analysis to measure the cleavage rates of each FIX scissile bond.

Two strategies have been used to follow FIX activation. FIXaβ can be measured by cleavage of a chromogenic substrate (Ogawa *et al.*, 2005). However, this method lacks sensitivity, making it difficult to measure initial activation rates. Sensitivity can be improved by using a coupled assay in which FIXaβ converts FX to FXa in the presence of factor VIIIa, and FXa is then detected with a chromogenic substrate (Sun *et al.*, 1996; Sinha *et al.*, 2007). Because of its complexity, reproducibility is the major problem with this assay. Chromogenic substrate-based techniques share a limitation, in that they are uninformative about FIXα generation, because this intermediate lacks enzymatic activity. To address this problem, we monitored FIX activation by densitometry of Coomassie Blue-stained SDS-PAGE gels imaged at infrared wavelengths. The low signal to noise ratio facilitates studying reactions with substrate concentrations down to 25 nM. Full progress curves are constructed from data for the disappearance of FIX, and the appearance of FIXα and FIXaβ. A disulfide bond connects the polypeptides that comprise FIXα, which has essentially the same molecular mass as FIX (Figure 4-1A). Interestingly, despite having similar molecular masses, we observed that FIXα migrates slightly faster than FIX on non-reducing SDS-PAGE, likely due to conformational changes that accompany cleavage. This allowed us to accurately measure the amount of FIX and FIXα at different points in reactions by SDS-PAGE.

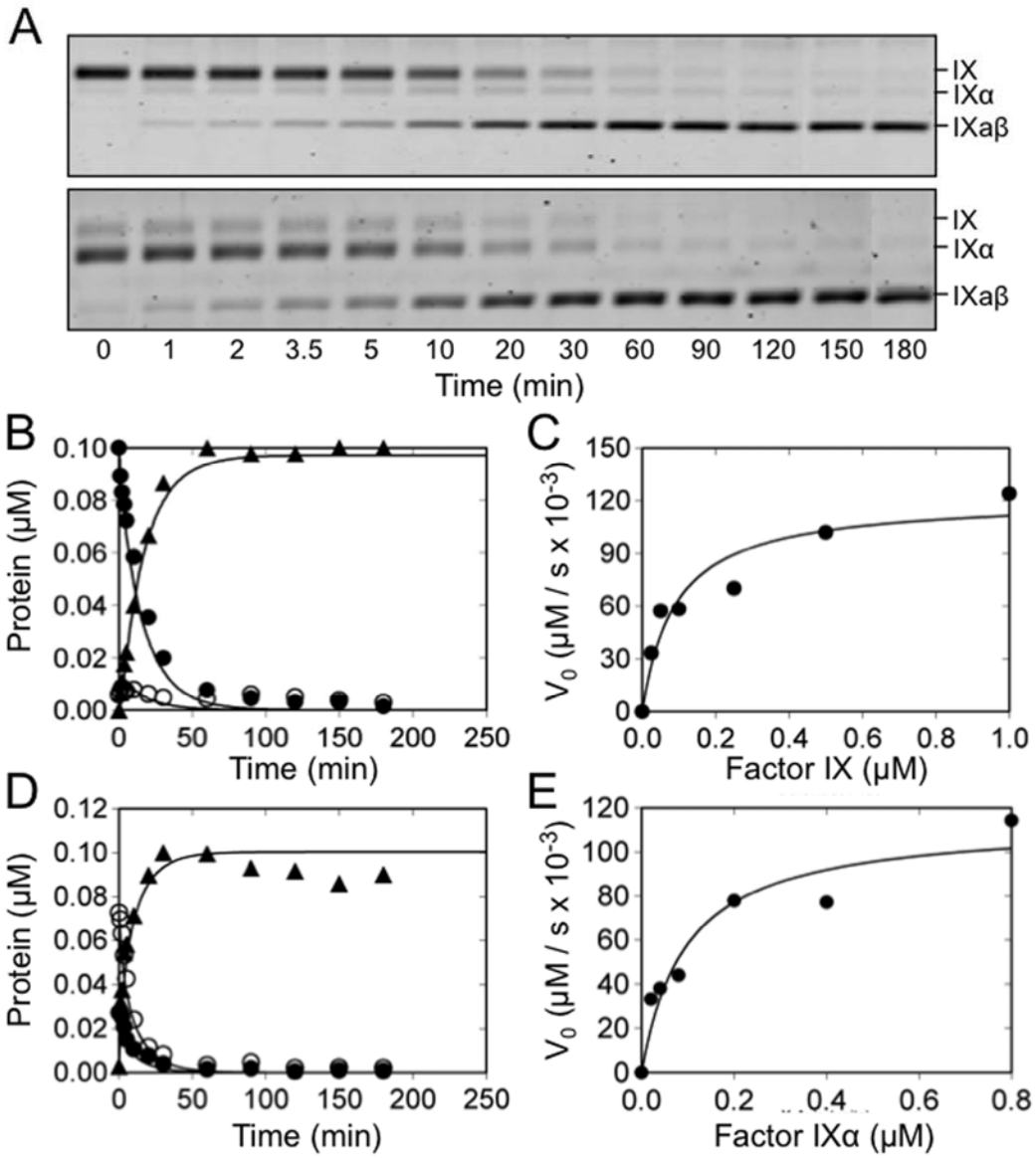

Figure 4-1 FIX and FIXα cleavage by FXIa-WT. (A) Nonreducing 17% polyacrylamide SDS gels of 100 nM FIX (top) or FIXα (bottom) in assay buffer (see "Methods") with Ca^{2+} incubated at room temperature with 3 nM (active sites) FXIa-WT. Positions of standards for FIX, FIXα, and FIXaβ are indicated at the right of each panel. **(B)** Progress curves of FIX disappearance (●), and FIXα (O), and FIXaβ (▲) generation from panel A (top). Lines represent the least-squares fits to the data. **(C)** Initial velocities of cleavage after Arg145 (conversion of FIX to FIXα) by 1 μM FXIa-WT active sites, as a function of FIX concentration. Initial rates were obtained from the slopes of the linear portions of progress curves documenting the disappearance of FIX with time. **(D)** Progress curves of FIXα cleavage by FXIa-WT determined from panel A (bottom). **(E)** Initial velocities of cleavage after Arg^{180} (conversion of FIXα to FIXaβ) by 1 μM FXIa-WT as a function of FIXα concentration.

We determined steady-state kinetic parameters for FIX cleavage by numerical integration and lease-squares fitting of full progress curves of FIX depletion, and FIXα and FIXaβ formation at FIX concentrations from 25 to 1000 nM. First, K_m, k_{cat}, K_d, K_i, and catalytic efficiency (k_{cat}/K_m) were determined for both cleavages during FIX activation simultaneously (Table 4-1). As a complementary method, a conventional Michaelis-Menten approach was also conducted, from which K_m and k_{cat} was calculated by analyzing the initial cleavage rate after Arg^{145} as a function of FIX concentration (Table 4-2). k_{cat}, the turnover number, is the maximum number of substrate molecules converted to product per enzyme molecule per minute. The Michaelis constant K_m is the substrate concentration at which the reaction rate is at half-maximum, and is a measure of the substrate affinity for the enzyme. Subsequently, the same method was used with FIXα as the initial substrate. As our FIXα preparations had up to 20% FIX contamination, analyses of conversion of FIXα to FIXaβ included the cleavage of the contaminating FIX.

Initially, we assessed FIX conversion to FIXaβ by recombinant FXIa (FXIa-WT) in the presence of Ca^{2+} ions (Figure 4-1 A-C). Ca^{2+} is essential for proper activation of FIX. As expected, little FIXα accumulation was observed. It should be noted that while FIXα is usually not detected when FIX is activated by plasma-derived FXIa, traces may be seen with recombinant FXIa. The analysis demonstrated that catalytic efficiency for the second cleavage after Arg^{180} is ~7-fold higher than for cleavage after Arg^{145} (400 ± 100 and 60 ± 6 μM^{-1} min^{-1}, respectively), with an estimated ~2.5-fold lower K_m and ~3-fold higher k_{cat} for cleavage after Arg^{180}. These results support a release-rebind mechanism, in which cleavage of the Arg^{145}–Ala^{146} bond increases the efficiency of cleavage of the Arg^{180}-Val^{181} bond, without FIXα accumulation.

In 1997, Wolberg *et al.* observed that the rate of cleavage of the Arg^{145}–Ala^{146} bond in the intermediate FIXaα (FIX cleaved after Arg^{180}) and the rate of cleavage of the Arg^{180}–Val^{181} bond in FIXα are comparable, and similar to the overall rate for conversion of FIX to FIXaβ. Based on this, they suggested that any intermediate formed may not be released prior to conversion to FIXaβ, explaining the lack of intermediate accumulation during activation by factor XIa. Our results do not agree with this model, and are more consistent with the observation that significant FIXα accumulates in competitive reactions in which FIX is activated by FXIa in the presence of active site-inhibited FXIa (Smith *et al.*, 2008).

We measured the cleavage rate of purified FIXα by FXIa-WT. To our surprise, the catalytic efficiency of cleavage after Arg^{180} in FIXα (130 ± 20 μM^{-1} min^{-1}) was ~3-fold lower than for FIXα formed *in situ* during FIX activation (Figure 4-1 A, D, and E, and Tables 4-1 and 4-2). This may reflect structural perturbations in FIXα acquired during its purification. Another possibility that could explain the difference is partial intermediate release, with a fraction of FIXα repositioned for cleavage after Arg^{180} while remaining bound to FXIa. This is taken into account in the reaction mechanism of kinetic analysis ("Methods"): FIXα* was used to indicate intermediate bound to FXIa in the correct orientation for cleavage after Arg^{180}, which is separate from FIXα in the aqueous phase (a transition from FIXα • XIa directly to FIXα* • FXIa). We simulated a model, using our data, that includes conformational repositioning of FIXα • FXIa to the productive complex FIXα* • FXIa without release, in parallel with release rebinding. Because the true ratio of FIXα • FXIa to FIXα* • XIa is unknown, we examined a range of values for the ratio (0.05–1), and found that the model fits data sets for cleavage after Arg^{180} for both nascent

and purified FIXα by FXIa-WT reasonably well at a ratio of 0.5, a K_d of ~100 nM for binding of FIXα to FXIa in a productive complex, and a k_{cat} of ~20 min^{-1}. The results suggest a possible upper limit of ~40% (the difference between k_{cat} of 35 min^{-1} and 20 min^{-1}) for FIXα proceeding to FIXaβ through repositioning without release-rebinding. If the mechanism only involved repositioning of FIXα without release, no transient intermediate should be observed in time courses with FXIa-WT, no FIXα would competitively bind to active site-blocked FXIa, and k_{cat} for the second cleavage would have to be exceedingly large (up to 60 - 150 min^{-1}). Our data indicate this scenario is not likely.

Cleavage of Factor IX by Factor XIa Loss-of-function Variants: the Importance of Apple Domains

As discussed in Chapter III, the FXIa heavy chain contains a substrate-binding exosite, with one study indicating it is located on the A2 domain (Baglia *et al.*, 1991), and earlier work from our laboratory pointing to the A3 domain (Sun *et al.*, 1996). A second FIX-binding exosite was postulated to reside on the catalytic domain (Sinha *et al.*, 2007). Because of the uncertainty that surrounded this issue, we conducted studies to identify the region on the FXIa heavy chain involved in high-affinity binding to FIX and FIXα, and investigated the possibility of a second exosite in FIX activation.

Fortuitously, the gene for FXI is the product of a duplication event involving the PK gene. The FXI subunit and PK (a monomeric protein) share identical domain structure, and are 58% identical in amino acid sequence in humans. Despite the similarities, the active form of PK (α-kallikrein) is a poor FIX activator, indicating that the FIX binding site is

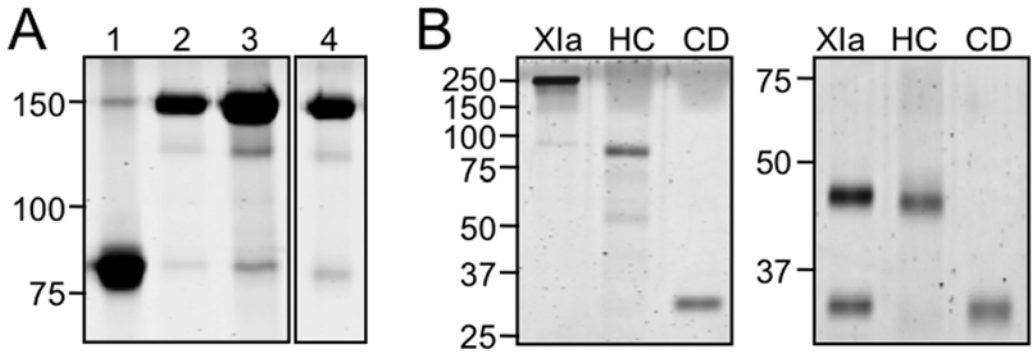

Figure 4-2. Purified FXI. (A) Nonreducing SDS-polyacrylamide gel stained with GelCode blue of recombinant 1. FXI-CD/PK-HC), 2. FXI-WT, 3. FXI/PKA3, and 4. FXI/PKA2-Ser^{140}. FXI-CD/PK-HC is an 80-kDa monomer, whereas other FXI species are 160-kDa dimers. **(B)** Purified FXIa heavy chain (HC) and catalytic domain (CD) isolated from FXI-Ser^{362}/Ser^{482} are compared with FXIa-WT (XIa) on nonreducing (left) and reducing (right) SDS-polyacrylamide gels. Positions of molecular mass standards are indicated on the left of each panel in kilodaltons.

unique on FXIa. FXIa in which the A3 domain is replaced with the PK A3 domain (Figure 4-2A) (FXIa/PKA3) was tested for its ability to cleave FIX and FIXα (Figure 4-3, Tables 4-1 and 4-2). The cleavage rates of the Arg^{145}–Ala^{146} and Arg^{180}–Val^{181} bonds were markedly reduced compared with FXIa-WT, with pronounced FIXα accumulation.

The A3 domain substitution in FXIa/PKA3 results in a K_m for FIX cleavage after Arg^{145} that is 25-fold higher compared with FXIa-WT, with a 60-fold reduction in catalytic efficiency. The catalytic efficiency of cleavage after Arg^{180} was impaired to an even greater degree. Only k_{cat}/K_m could be estimated accurately for the second cleavage because saturation could not be achieved for the reaction (Figure 4-3E). The values for K_m in Tables 1 and 2 should, therefore, be considered lower limits for the actual values. These data indicate that the A3 domain is important for binding both FIX and FIXα, and that loss of the A3 binding site has a deleterious effect on both cleavages in FIX. With FXIa/PKA3, FIXα accumulation is the result of an 11 to 14-fold higher catalytic efficiency for the cleavage of FIX Arg^{145}–Ala^{146} bond compared with the cleavage of Arg^{180}–Val^{181} bond.

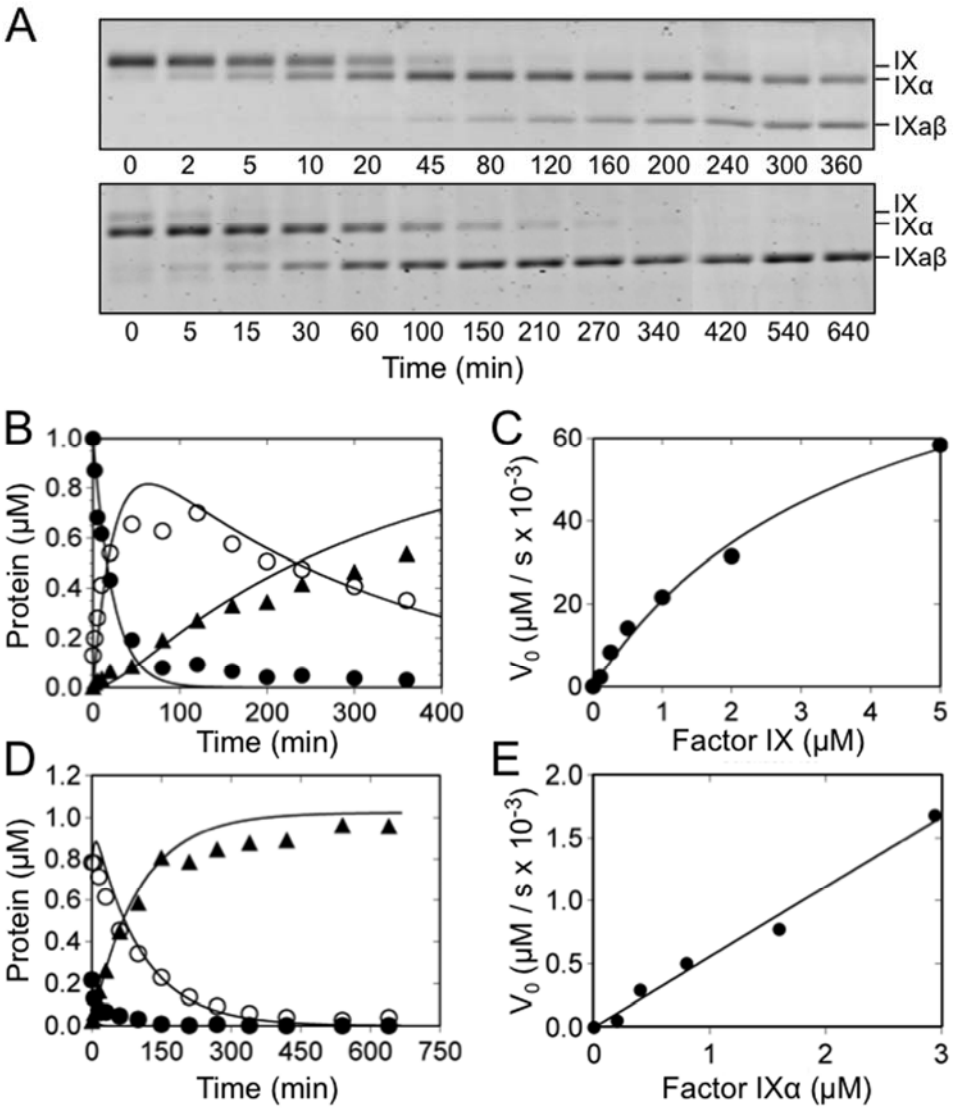

Figure 4-3. FIX and FIXα cleavage by FXIa/PKA3. (A) Non-reducing 17% polyacrylamide-SDS gels of 1000 nM FIX (top) or FIXα (bottom) in Assay Buffer with Ca^{2+} incubated at RT with FXIa/PKA3 (60 nM and 240 nM active sites for FIX and FIXα respectively). Positions of standards for FIX, FIXα and FIXaβ are indicated at the right of each panel. **B)** Progress curves of FIX disappearance (○), and FIXα (●) and FIXaβ (▲) generation from panel A (top). Lines represent least-squares fits to the data. **(C)** Initial velocities of cleavage after Arg^{145} (conversion of FIX to FIXα) by 1 nM FXIa/PKA3 active sites as a function of FIX concentration. The initial rates were obtained from the slopes of the linear portions of progress curves documenting disappearance of FIX with time. **(D)** Progress curves of FIXα cleavage by FXIa/PKA3 determined from panel A (bottom). **(E)** Initial velocities of cleavage after Arg^{180} (conversion of FIXα to FIXaβ) by 1 nM FXIa/PKA3 active sites as a function of FIXα concentration.

Table 4-1. Kinetic parameters for cleavage of FIX and FIXα by FXIa.

Fitting of full-progress experimental traces was performed with KinTek software (KinTek Explorer version 2.5) using the reaction equation shown under "Methods." K_m and k_{cat} for activation were calculated from individual rate constants for each step. K_i values were fixed to lower limits obtained by surface plasmon resonance. Values are the mean ± S.D. for each experiment.

Cleavage of FIX after Arg^{145}

Protease	Substrate	k_{cat} 1 (min^{-1})	K_d 1 (μM)	K_m 1 (μM)	Catalytic Efficiency 1 (μM^{-1} min^{-1})	K_i 1 (μM)
FXIa-WT	FIX	12 ± 1	0.10 ± 0.01	0.20 ± 0.01	60 ± 6	0.14
FXIa-CD	FIX	3.2 ± 0.1	4.9 ± 0.2	4.9 ± 0.2	0.7 ± 0.1	3
FXIa/PKA3	FIX	4.9 ± 0.1	4.9 ± 0.2	4.9 ± 0.2	1.0 ± 0.1	3
FXIa/PKA2-Ser^{140}	FIX	16 ± 1	0.03 ± 0.01	0.10 ± 0.01	160 ± 20	0.15
FXIa-CD/PK-HC	FIX	1.6 ± 0.1	2.4 ± 0.2	2.4 ± 0.2	0.7 ± 0.1	5
FXIa-Gly^{184}	FIX	13 ± 3	0.3 ± 0.1	0.7 ± 0.3	19 ± 10	0.4 ± 0.2
FXIa-Met^{575}	FIX	1.20 ± 0.06	0.20 ± 0.02	0.20 ± 0.02	5.0 ± 0.5	0.70 ± 0.05

Cleavage of FIX after Arg^{180}*

Protease	Substrate	k_{cat} 2 (min^{-1})	K_d 2 (μM)	K_m 2 (μM)	Catalytic Efficiency 2 (μM^{-1} min^{-1})	K_i 2 (μM)
FXIa-WT	FIX	35 ± 6	0.06 ± 0.01	0.08 ± 0.01	400 ± 100	0.06
FXIa-WT	FIXα	12 ± 1	0.08 ± 0.01	0.09 ± 0.01	130 ± 20	0.06
FXIa-CD	FIX	0.5 ± 0.1	11 ± 1	11 ± 1	0.05 ± 0.01	5
FXIa-CD	FIXα	0.5 ± 0.1	13 ± 2	13 ± 2	0.04 ± 0.01	5
FXIa/PKA3	FIX	0.6 ± 0.1	7 ± 1	7 ± 1	0.09 ± 0.02	3
FXIa/PKA3	FIXα	0.6 ± 0.1	7 ± 1	7 ± 1	0.09 ± 0.02	3
FXIa/PKA2-Ser^{140}	FIX	40 ± 10	0.04 ± 0.01	0.08 ± 0.02	500 ± 200	0.06
FXIa-CD/PK-HC	FIX	0.4 ± 0.1	10 ± 1	10 ± 1	0.04 ± 0.01	5
FXIa-CD/PK-HC	FIXα	0.4 ± 0.1	10 ± 1	10 ± 1	0.04 ± 0.01	5
FXIa-Gly^{184}	FIX	40 ± 10	0.2 ± 0.1	0.2 ± 0.1	200 ± 50	0.5 ± 0.2
FXIa-Met^{575}	FIX	5.50 ± 0.04	0.50 ± 0.04	0.50 ± 0.04	11.0 ± 0.9	0.040 ± 0.003

* Due to the low affinity between the enzyme and substrate in reactions using FXIa variants, we were not able to reach saturation for reactions with FXIa-CD, FXIa/PKA3, or FXIa-CD/PK-HC, or FXIa-WT in the absence of Ca^{2+}. Fits for k_{cat} and K_m are linked, with the listed K_ms representing lower estimates for the reaction. k_{cat}/K_m is the appropriate parameter for comparing these reactions.

Progress curve simulations for cleavage of isolated FIXα by FXIa/PKA3 suggests that Arg^{180}–Val^{181} is cleaved with similar, low catalytic efficiency when FIX or FIXα is the starting substrate, indicating that the exosite is important for efficient binding of both FIX and FIXα as substrates.

Previously, Baglia *et al.* reported that peptides derived from the FXIa A2 domain sequence were competitive inhibitors of FIX activation by FXIa, suggesting the presence of a FIX binding site on A2 (Baglia *et al.*, 1991). We studied cleavage of FIX by FXIa with a PK A2 substitution (Figure 4-2A). Lys^{140} in PK A2 was replaced with Ser to prevent auto-proteolysis (Hooley *et al.*, 2007). The resulting chimera, FXIa/PKA2-Ser^{140}, cleaved

Table 4-2. Kinetic parameters for cleavage of FIX and FIXα by FXIa determined from initial velocities.

The initial velocities (v_0) of cleavage after Arg^{145} in FIX, and cleavage after Arg^{180} in FIXα were plotted against initial substrate concentration, and analyzed using the Michaelis-Menten equation. K_m and k_{cat} were obtained from direct non-linear least squares analysis using Scientist Software.

Protease	Substrate	Bond cleaved	k_{cat} 1 (min^{-1})	K_m 1 (μM)	Catalytic Efficiency 1 (μM^{-1} min^{-1})
FXIa-WT	FIX	Arg^{145}	10 ± 1	0.27 ± 0.07	40 ± 10
FXIa-WT	FIXα	Arg^{180}	7.1 ± 0.3	0.09 ± 0.01	80 ± 10
FXIa-CD	FIX	Arg^{145}	2.4 ± 0.4	3 ± 1	0.8 ± 0.3
FXIa-CD	FIXα	Arg^{180}	ND*	> 4	0.018 ± 0.001
FXIa/PKA3	FIX	Arg^{145}	6 ± 1	3.9 ± 0.9	1.6 ± 0.4
FXIa/PKA3	FIXα	Arg^{180}	ND*	> 4	0.029 ± 0.003
FXIa-CD/PK-HC	FIX	Arg^{145}	5 ± 1	3 ± 1	2 ± 1
FXIa-CD/PK-HC	FIXα	Arg^{180}	ND*	> 4	0.02 ± 0.01
FXIa-Gly^{184}	FIX	Arg^{145}	11 ± 1	0.8 ± 0.2	12 ± 4
FXIa-Met^{575}	FIX	Arg^{145}	1.10 ± 0.06	0.05 ± 0.02	20 ± 10

Due to the low affinity between the enzyme and substrate in reactions using FXIa variants, we were not able to reach saturation for reactions with FXIa-CD, FXIa/PKA3, and FXIa-CD/PK-HC. Thus, values for K_m are approximate and values for k_{cat} were not determined (ND)

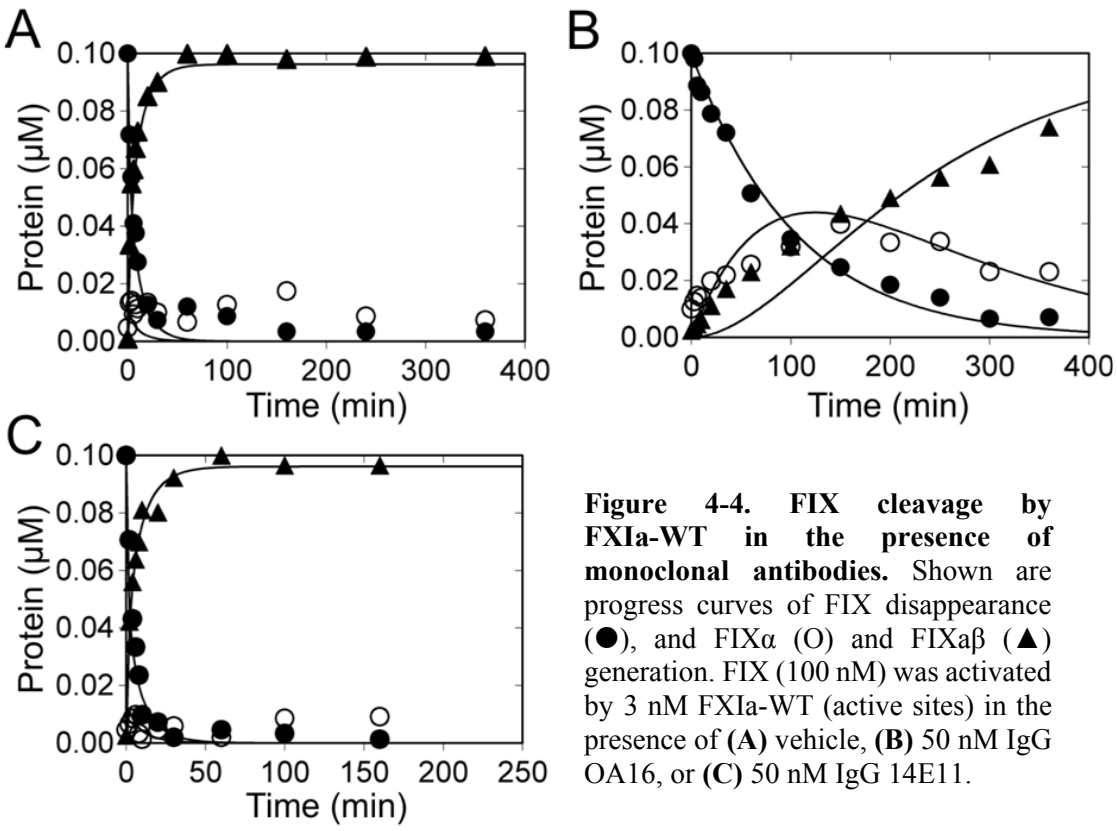

Figure 4-4. FIX cleavage by FXIa-WT in the presence of monoclonal antibodies. Shown are progress curves of FIX disappearance (●), and FIXα (O) and FIXaβ (▲) generation. FIX (100 nM) was activated by 3 nM FXIa-WT (active sites) in the presence of **(A)** vehicle, **(B)** 50 nM IgG OA16, or **(C)** 50 nM IgG 14E11.

both FIX scissile bonds similarly to FXIa-WT (Table 4-1), indicating that the FXI A2 domain does not contain a high affinity FIX or FIXα binding site.

The anti-human FXI monoclonal IgG O1A6 binds to the A3 domain at residues that overlap or are in close proximity to the FIX binding site (Sun *et al.*, 1999, Tucker *et al.*, 2009). In the presence of O1A6, FIX activation by FXIa-WT appears similar to activation by FXIa/PKA3, with decreased rates of cleavage for both bonds and FIXα accumulation (compare Figure 4-4 A and B, to 4-3B). In contrast, an IgG that binds to the A2 domain (14E11) had no effect on FIX activation by FXIa (Figure 4-4C), consistent with the interpretation that the A2 domain does not contain a FIX binding site, and that the inhibitory effect of O1A6 is not simply due to steric interference.

Investigation of a Factor IX Binding Exosite on the Factor XIa Catalytic Domain

Sinha *et al* suggested that a FIX binding exosite is located on the FXIa catalytic domain (Sinha *et al.*, 2007), and proposed a model that required FIX to first engage this exosite before conversion to FIXα. Conversion of FIXα to FIXaβ follows in a reaction that requires the heavy chain exosite. The proposed mechanism is based primarily on the observation that the isolated factor XIa catalytic domain converts FIX to FIXaβ with a K_m comparable to that of FXIa-WT, but a significantly reduced k_{cat}. It was concluded that FIX, but not FIXα, bound to an exosite on the catalytic domain. Their data and interpretations are incompatible with our observation that removing the A3 domain increases K_m for the overall reaction. Subsequently, the same group posited that catalytic domain amino acids Glu^{458} and Lys^{550} (Glu^{98} and Lys^{192} in chymotrypsin numbering) may be part of a FIX binding exosite (Su *et al.*, 2011). However, substitutions for these residues resulted in ~100-fold reductions in k_{cat} for FIX conversion to FIXaβ, more consistent with a catalytic defect. Cumulatively, these findings are not consistent with our results showing that the A3 domain contains the major binding site for proper activation of FIX and FIXα. To investigate this discrepancy further, we assessed cleavage of the Arg^{145}-Ala^{146} and Arg^{180}-Val^{181} bonds by FXIa isolated catalytic domain (FXIa-CD) (Figure 4-2B). Similar to results with FXIa/PKA3, we observed a ~90-fold decrease in catalytic efficiency for cleavage of FIX after Arg^{145}, and an even greater defect for cleavage of FIX and FIXα after Arg^{180} by FXIa-CD. Kinetic analysis indicated the poor cleavage rate was due to an increased K_m and to a lessert extent a decrease in k_{cat} (Table 4-1 and 4-2). Cleavage after Arg^{180} by FXIa-CD was also similar to FXIa/PKA3. The low affinity of the FXIa catalytic domain for FIX or FIXα demonstrated that it is not likely to harbor a binding site that is

required for initial substrate recognition. The reason for the differences between our results and those of Sinha *et al.* are not clear; however, their study used a chromogenic assay to examine FIX activation, which would not facilitate examination of the initial cleavage converting FIX to FIXα with the detail we were able to achieve with our densitometry-based approach.

The FXIa catalytic domain is attached to the heavy chain within a subunit by the Cys^{362}–Cys^{482} disulfide bond (McMullen *et al.*, 1991; Papagrigoriou *et al.*, 2006). In FXIa-CD, the heavy chain is absent and Cys^{482} is replaced with serine. These changes could have altered FXIa-CD sufficiently to reduce its ability to bind FIX, even if a FIX binding site is present on the catalytic domain. The chimera FXIa-CD/PK-HC consists of the FXIa catalytic domain attached to the heavy chain of PK (Figure 4-2A). Like the FXI heavy chain, the PK heavy chain contains four apple domains, and it is connected to the catalytic domain through a single disulfide bond involving Cys^{482}. Activation of FIX and FIXα by FXIa-CD/PK-HC (Tables 4-1 and 4-2) was similar to activation by FXIa/PKA3 and FXIa-CD. Taken as a whole, these data indicate that a major exosite for binding of FIX and FIXα is located on the FXIa A3 domain. Loss of this exosite, either in chimeras (FXIa/PKA3 or FXIa-CD/PK-HC) or through absence of the heavy chain (FXIa-CD), results in loss of the high affinity site and a marked increase in K_m for FIX activation. Although our data don't support the presence of a FIX binding exosite on the FXIa catalytic domain that is required for initial substrate recognition, they do not rule out the possibility that such a binding site is expressed as the result of initial binding of FIX to the A3 exosite (although such a process would not explain the differences between our results and published work). Previously, we noted that binding of FIX to FXIa results in a mixed-type

inhibition of cleavage of a tripeptide substrate by FXIa, consistent with FIX binding to A3 causing changes in the protease domain, in addition to competing with the tripeptide substrate at active site (Ogawa *et al., 2005*). In the future, resolving the crystal structure of FIX in complex with full-length FXIa (with alanine substitution for serine 557) will enhance our understanding of this interaction.

Binding of Factor XIa to Factor IX and Factor IXα

As a complementary method to kinetic analysis, we studied binding of active site-blocked FXIa to immobilized FIX, FIXα, and FIXaβ using surface plasmon resonance (SPR). The active site of FXIa was inhibited by a chloromethyl ketone (CMK), preventing FIX activation after FXIa binding. Zymogen FXI-WT did not bind to any FIX species in the presence of Ca^{2+}, nor did FXIa-WT in the presence of 10 mM EDTA (data not shown). In the presence of Ca^{2+}, FXIa-WT bound to FIX, FIXα, and FIXaβ. Binding at equilibrium was plotted as a function of the FXIa-WT concentration (Figure 4-5 A-C). K_d for binding to FIX (130 ± 20 nM), FIXα (140 ± 20 nM), and FIXaβ (60 ± 10 nM) are comparable (Table 4-3), and are consistent with published results (Aktimur *et al.*, 2003). Given the previous observation that FIXaβ is a competitive inhibitor of FIX activation by FXIa (Ogawa *et al.*, 2005), our data indicate that FIX, FIXα and FIXaβ are likely binding to the same position, or positions that are near each other, on FXIa.

Using SPR, we were not able to demonstrate binding of FXIa-CD, FXIa/PKA3, or FXIa-CD/PK-HC (Figure 4-5 D-G and Table 4-3) to FIX, FIXα, or FIXaβ at analyte concentrations up to 5 μM. In contrast, isolated FXIa heavy chain (FXIa-HC), and FXIa/PKA2 bound to FIX species with K_d values similar to those for FXIa-WT (Figure 4-5

H and I, Table 4-3). These results are consistent with our kinetic analysis, and indicate that high affinity binding between FIX or FIXα and FXIa is largely, if not completely, due to a Ca^{2+}-dependent binding to the A3 domain.

Recently, Marcinkiewicz *et al.* reported that cross-talk between the FXIa catalytic domain and heavy chain is required for expression of the FIX binding site on the heavy chain, based on observing that isolated FXIa heavy chain (FXIa-HC) does not bind to FIX (Marcinkiewicz *et al.*, 2012). This is not compatible with our SPR study showing that FXIa-HC and FXIa-WT bound to FIX and FIXα with similar affinity. To confirm that the FXIa heavy chain does not need the catalytic domain to bind to FIX, we tested the capacity of FXIa-HC to inhibit FIX conversion to FIXaβ by FXIa-WT, as shown in the western blots in Figure 4-5J. FXIa-HC slowed the activation rate of FIX by FXIa-WT, consistent with the heavy chain engaging FIX in the absence of the catalytic domain. Furthermore, accumulation of FIXα in the presence of FXIa-HC supports the premise that FIXα is released from FXIa and can bind to the isolated heavy chain.

Table 4-3. Affinity of FXIa binding to FIX, FIXα and FIXaβ.

Surface plasmon resonance studies were preformed as described in "methods". Data were corrected for non-specific binding by subtracting signals obtained with analytes infused through a flow cell without coupled protein. Binding was analyzed using a bivalent binding model for all species except FXIa-CD/PK-HC and FXIa-CD, which were evaluated with a 1:1 binding model. *Kd* values were calculated from the quotient of the derived dissociation (*kd*) and association (*ka*) rate constants, and were consistent with results calculated by steady state equilibrium analysis (not shown).

Analyte	K_d (nM) for binding of analyte to ligand		
	factor IX	factor IXα	factor IXaβ
FXIa-WT	130 ± 20	140 ± 30	60 ± 10
FXIa-HC	90 ± 20	70 ± 10	10 ± 10
FXIa-CD	> 5000	> 5000	> 5000
FXIa/PKA3	> 3000	> 3000	> 3000
FXIa-CD/PK-HC	> 5000	> 5000	> 5000
FXIa/PKA2-Ser^{140}	40 ± 10	40 ± 10	Not done

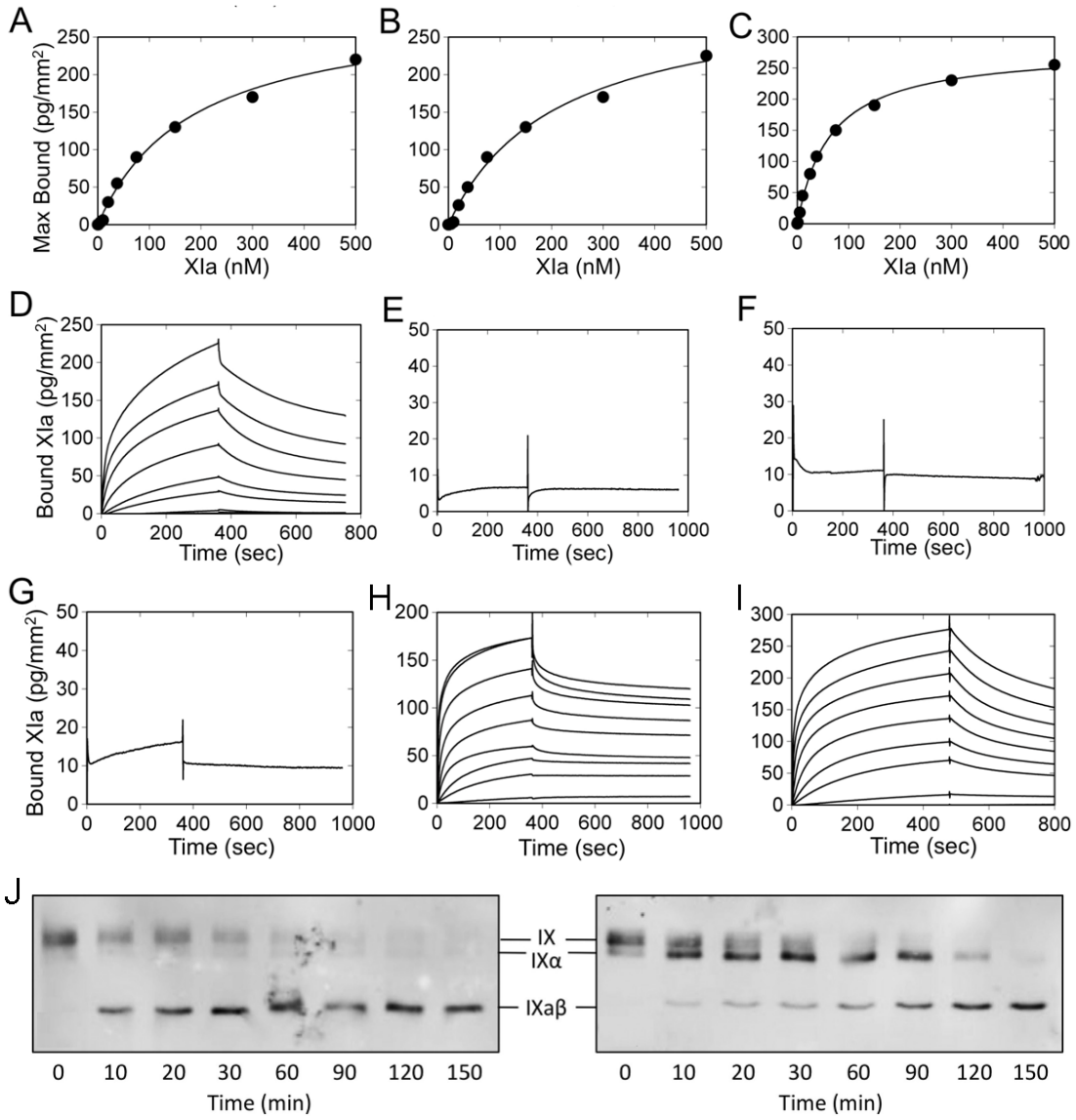

Figure 4-5. FXIa binding to FIX, FIXα, and FIXaβ. Surface Plasmon Resonance was used to assess binding of FXIa perfused over immobilized FIX, FIXα or FIXaβ in the presence of Ca^{2+} ions at 10 µl/min for 6 min. Dissociation was monitored for 10 min. **Panels A to C** – FXIa-WT binding. FXIa-WT concentrations tested were: 1, 5, 10 , 25, 37.5 , 75, 150, 300, and 500 nM. Affinity and kinetic parameters were determined after subtraction of non-specific binding from the control surface. Non-linear regression fitting of the steady state equilibrium binding of FXIa-WT to **(A)** FIX, **(B)** FIXα and **(C)** FIXaβ using a bivalent model**. Panels D, H and I**– SPR data for Ca^{2+} -dependent binding of **(D)** FXIa-WT, **(H)** FXIa-HC, and **(I)** FXIa/PKA2-Ser^{140} binding to FIX. **Panels E-G** –Binding curves for **(E)** FXIa-CD, **(F)** FXIa/PKA3, and **(G)** FXIa-CD/PK-HC at a single concentration (5000 nM). **(J)** FIX activation by FXIa-WT in the presence of FXIa-HC. Shown are western blots of time courses of FIX (100 nM) activated by FXIa-WT (1 nM) in the presence of vehicle control (left panel) or 1 µM FXIa-HC (right panel). Samples collected at various times (shown at bottom) into non-reducing SDS-sample buffer were size fractionated by SDS-PAGE. Detection was with a polyclonal anti-human FIX antibody and chemiluminescence. Positions of standards for FIX, FIXα, and FIXaβ are shown between the images.

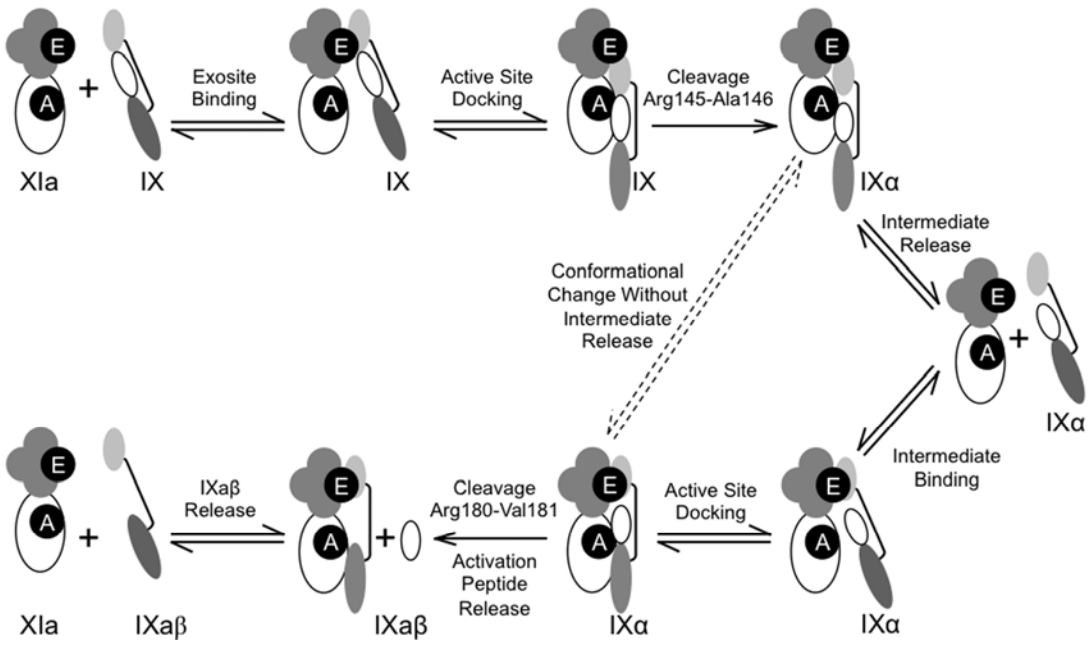

Figure 4-6. Model for FIX activation by FXIa. In the schematic diagram of FXIa, apple domains are shown as four clustered gray circles with the exosite on A3 indicated in black (E). The FXIa catalytic domain is a white ellipse with the active site indicated by a black circle (A). The FIX catalytic domain (dark gray ellipse) and light chain (light gray ellipse) are connected by a line representing a disulfide bond. The activation peptide is the white oval. Bi-directional arrows represent reversible binding, and uni-directional arrows represent proteolytic cleavage. FIX is activated by a FXIa subunit by sequential cleavage after Arg^{145} and Arg^{180}, with the intermediate FIXα released and then rebound to the FXIa A3 domain. Details of the model are described in the text.

Taken as a whole, the results reported above support an exosite-mediated release-rebind mechanism for FIX activation by FXIa (summarized in Figure 4-6), in which the efficiency of the second cleavage is enhanced by conformational changes resulting from the first cleavage. We propose that binding of FIX to the FXIa A3 domain is followed by docking with the active site and cleavage after Arg^{145} to form FIXα. FIXα is released from FXIa and then must rebind to FXI A3 prior to a second docking step with the active site, and cleavage after Arg^{180}. The ratio of the catalytic efficiencies of the two cleavages determines whether FIXα accumulates. If the A3 domain exosite is available,

catalytic efficiency for cleavage after Arg^{180} is 7-fold greater than for cleavage after Arg^{145}, and FIXα does not accumulate. In the absence of a functional exosite, the rates of both bond cleavages are markedly decreased, but the predominance of the catalytic efficiency of the second cleavage is lost, leading to FIXα accumulation.

Summary

In this chapter we describe a new mechanism for FIX activation by FXIa during blood coagulation. After cleavage of FIX at the Arg^{145}-Ala^{146} bond, the intermediate FIXα is released from FXIa, and must rebind for cleavage at Arg^{180}-Val^{181} to generate the protease FIXaβ. The catalytic efficiency of cleavage after Arg^{180} is 7-fold greater than for cleavage after Arg^{145}, limiting FIXα accumulation. Initial binding of FIX and FIXα requires the exosite on the FXIa A3 domain, but not the A2 or catalytic domain.

Methods

Recombinant FXIa. HEK293 fibroblasts (ATCC-CRL1573) were transfected with 40 μg of pJVCMV containing a FXI cDNA and 2 μg of pRSVneo encoding a neomycin resistance marker using an Electrocell Manipulator 600, (BTX, San Diego, CA) (Ogawa *et al.*, 2005). Cells were initially grown in Dulbecco's modified Eagle medium (DMEM) with 5% fetal bovine serum and 500 μg/mL G418, then switched to serum-free medium (Cellgro Complete, Mediatech, Herndon, VA). FXI was purified from conditioned media by affinity chromatography using anti-human FXI-IgG 1G5.12 (Ogawa *et al.*, 2005). Protein concentrations were determined by colorimetric assay (Bio-Rad,), and confirmed by densitometry on SDS-PAGE by comparison to standard plasma FXI or FIX preparations.

FXI chimeras in which apple domains are replaced with PK apple domains have been described (Sun *et al.*, 1996). We used FXI with the PK A2 or A3 domain (FXI/PKA2 or FXI/PKA3), and FXI in which the entire heavy chain is replaced with the PK heavy chain (FXI-CD/PK-HC) (Kravtsov *et al.*, 2009). In FXI/PKA2, Lys^{140} was changed to Ser to prevent auto-proteolysis (Hooley *et al.*, 2007).

FXI was converted to FXIa by incubation with FXIIa (100:1 substrate:enzyme) at 37 ˚C for 24 hrs in 50 mM Tris-HCl pH 7.4, 100 mM NaCl (TBS). Conversion of the 80-kDa zymogen FXI subunits to the 45-kDa heavy chain and 35-kDa catalytic domain of FXIa was confirmed by SDS-PAGE. In studies of FIX activation by FXIa and FXIa variants, removal of FXIIa, or inhibition of FXIIa, had no effect on FIX or FIXα cleavage.

To prepare isolated FXIa heavy chain (FXIa-HC) and isolated FXIa catalytic domain (FXIa-CD) (Fujikawa *et al.*, 1986), FXI with Cys^{362} and Cys^{482} changed to Ser (FXI-Ser^{362}/Ser^{482}) was activated and passed through a soybean-trypsin inhibitor (SBTI) agarose column. FXIa-CD binds to the column and is eluted with TBS containing 200 mM benzamidine, while FXIa-HC flows through the column.

Preparation of FIXα. FIX (14.3 μM) was incubated with 50 nM FXIa in TBS pH 7.4, 20 mM EDTA for 12 min at 37 ^{o}C to generate FIXα. Contaminating FIXaβ was inhibited by incubating 90 min at 37 ^{o}C with biotinylated EGR-chloromethylketones (CK) (10-fold molar excess over FIX). After dialysis against PBS, strepavidin immobilized on agarose was added, and incubated for 1 hour at room temperature (RT) with mixing. Agarose was removed by centrifugation, and the supernatant containing FIXα was dialyzed against 50 mM HEPES pH 7.4, 125 mM NaCl, 1 mg/mL polyethylene glycol 8000.

Hydrolysis of S-2366 by FXIa. FXIa (6 nM) was incubated with S-2366 (50-2000 μM) in

TBS at RT (reaction volume 40 µl). Generation of free *p*-nitroaniline (pNA) was followed by continuous monitoring of absorbance at 405 nm on a SpectraMax 340 plate reader (Molecular Devices, Sunnyvale, CA). Rates of *p*NA generation (nM/s) were determined using an extinction coefficient of 9920 M^{-1} cm^{-1} (405 nm). K_m and k_{cat} for S-2366 cleavage were determined by non-linear least squares fitting performed with Scientist Software (MicroMath Scientific Software).

Activation of FIX and FIXα by FXIa. FIX or FIXα (25 nM to 5 µM) in Assay Buffer (50 mM HEPES, pH 7.4, 125 mM NaCl, 5 mM $CaCl_2$, 1 mg/mL polyethylene glycol [PEG] 8000) was incubated at RT with FXIa species (1 to 240 nM active sites, depending on the protease and substrate tested) in tubes coated with PEG 20,000. At various times (0 to 640 min), aliquots were removed into non-reducing SDS-sample buffer, size fractionated on 17% polyacrylamide-SDS gels, and stained with GelCode Blue (Pierce). Gels were imaged under infrared wavelengths (excitation λ 685 nm, emission λ 720 nm) on an Odyssey Infrared Imaging System (LI-COR Biosciences, Lincoln, NE). The instrument converts infrared data into grayscale images. Conversion of FIX to FIXα and FIXaβ, and FIXα to FIXaβ was assessed by densitometry. To determine the amount of protein per band, standards were run on a separate gel, with one standard also run on the gel with the time course samples. Full progress curves were constructed from data for the disappearance of FIX, and the appearance of FIXα and FIXaβ. In some reactions, monoclonal antibodies to FXIa or FIX were included.

Kinetic Analyses. Steady-state kinetic parameters for FIX or FIXα cleavage were obtained by numerical integration fitting and least squares fitting of full progress curves of substrate depletion, and intermediate and product formation at substrate concentrations from 25 to

5000 nM; and by analysis of the initial rate dependence of substrate depletion as a function of substrate concentration. Rates of cleavage of the Arg^{145}–Ala^{146} and Arg^{180}–Val^{181} bonds were analyzed simultaneously with KinTek Explorer Version 2.5 software (Johnson *et al.*, 2009) using the reaction mechanism shown below. IXα* indicates the intermediate bound to FXIa in the correct orientation for cleavage after Arg^{180}.

$$IX + XIa \underset{k_{-1}}{\overset{k_1}{\rightleftharpoons}} IX{\bullet}XIa \xrightarrow{k_2} IX{\bullet}XIa \underset{k_{-3}}{\overset{k_3}{\rightleftharpoons}} IX\alpha + XIa$$

$$\underset{K_{-4}}{\overset{k_4}{\rightleftharpoons}} IX\alpha^{*}{\bullet}XIa \xrightarrow{k_5} IXa\beta{\bullet}XIa \underset{K_{-6}}{\overset{k_6}{\rightleftharpoons}} IXa\beta + XIa$$

$$K_{d1} = k_{-1}/k_1 \qquad K_{m1} = (k_{-1} + k_2)/k_1 \qquad k_{cat1} = k_2 \qquad K_{i1} = k_{-3} / k_3$$

$$K_{d2} = k_{-4}/k_4 \qquad K_{m2} = (k_{-4} + k_5)/k_4 \qquad k_{cat1} = k_5 \qquad K_{i2} = k_{-6} / k_6$$

We reported that the final product FIXaβ binds to FXIa and is a competitive inhibitor of FIX activation by FXIa (Ogawa *et al.*, 2005). A similar assumption was made for product inhibition by FIXα. K_d and K_i values were initially constrained to those obtained from surface plasmon resonance studies (below) and full progress curve analysis of FIXaβ formation, and no rapid equilibrium assumptions were imposed on association and dissociation rates. By fitting full progress curves for FIX disappearance, and FIXα and FIXaβ appearance, K_m, k_{cat}, K_d, K_i, and catalytic efficiency (k_{cat}/K_m) were determined for both cleavages in FIX. The same method was used with FIXα as substrate. As FIXα preparations have ~20% FIX contamination, analyses of conversion of FIXα to FIXaβ included the cleavage of the FIX.

Results of numerical analysis were compared with those obtained by conventional Michaelis-Menten analysis of both cleavages. With FIX as substrate, initial velocities (v_0)

of cleavage after Arg^{145} were determined from the initial slopes of progress curves for disappearance of FIX, normalized to 1 nM FXIa active sites. Values for v_0 were analyzed with the Michaelis-Menten equation, and values for K_m and k_{cat} were obtained from direct nonlinear least squares analysis using Scientist Software. With FIXα as substrate, K_m and k_{cat} for cleavage after Arg^{180} were determined in a similar manner. Competitive binding of FXIa to FIX in the FIXα preparation was calculated by a cubic equation, and was taken into account for determining the FXIa concentration available for the reaction with FIXα.

Surface Plasmon Resonance (SPR). Binding studies were performed on a Biacore T100 flow biosensor (Biacore, Uppsala, Sweden) at 25 °C. FIX, FIXα or FIXaβ were immobilized on carboxy-methyl dextran flow cells (CM5 sensor chips, GE Healthcare) using amine-coupling chemistry. To prevent cleavage of bound FIX or FIXα, FXIa active sites were blocked with FPR-CK. FIXaβ active sites were blocked with EGR-CK. Flow cell surfaces were activated with a mixture of 1-ethyl-3-(3-dimethylaminopropyl) carbodiimide and *N*-hydroxysulfosuccinimide for 5 min (flow rate 10 μL/min), after which protein (30 μg/mL in sodium acetate, pH 4.0) was injected onto the surface. Unreacted sites were blocked for 5 min with 1 M ethanolamine. Analytes (FXIa species, 1 to 5000 nM) were perfused through flow cells in HBS-P Buffer (10 mM HEPES pH 7.4, 150 mM NaCl, 2 mM $CaCl_2$, 1 mM benzamidine, 0.005% v/v P20) at 10 μL/min for 6 min. After changing to HBS-P Buffer without FXIa, analyte dissociation was monitored for 10 min. Flow cells were regenerated with HBS-P containing 30 mM EDTA. FXIa binding to FIX species was also tested in the absence of Ca^{2+} (10 mM EDTA). Data were corrected for non-specific binding by subtracting signals obtained with analytes infused through a flow cell without coupled protein.

Binding was analyzed with BIAevaluation software (Biacore) using a bivalent binding model for dimers (FXIa-WT, FXIa/PKA2, FXIa/PKA3) and a 1:1 binding model for monomers (FXIa-CD, FXIa-CD/PK-HC). K_d values were calculated from the quotient of the derived dissociation (k_d) and association (k_a) rate constants. In addition, a steady state affinity model was used in which K_d was derived from non-linear regression fitting of the response at equilibrium to FXIa concentration.

FIX Activation in the Presence of FXIa-HC. FIX (100 nM) was incubated with FXIa-WT (1 nM) with or without FXIa-HC (1 μM) in assay buffer at RT. At various times, aliquots were removed into nonreducing SDS sample buffer, size fractionated on 12% polyacrylamide-SDS gels, and transferred to a nitrocellulose membrane. Western blots were performed using an HRP-conjugated goat polyclonal anti-human FIX IgG and chemiluminescence for detection.

Reference

Aktimur, A., Gabriel, M. A., Gailani, D., and Toomey, J. R. (2003) The factor IX γ-carboxyglutamic acid (Gla) domain is involved in interactions between factor IX and factor XIa. J Biol Chem *278*, 7981–7987.

Baglia, F.A., Jameson, B.A., Walsh, P.N. (1991) Identification and chemical synthesis of a substrate-binding site for factor IX on coagulation factor XIa. J Biol Chem *266*, 24190–24197.

Hooley, E., McEwan, P.A., and Emsley, J. (2007) Molecular modeling of the prekallikrein structure provides insights into high-molecular-weight kininogen binding and zymogen activation. J Thromb Haemost *5*, 2461-2466.

Johnson, K.A., Simpson, Z.B., Blom, T.F. (2009) Global kinetic explorer. A new computer program for dynamic simulation and fitting of kinetic data. Anal Biochem *387*, 20–29.

Marcinkiewicz, M.M., Sinha, D., Walsh, P.N. (2012) Productive recognition of factor IX by factor XIa exosites requires disulfide linkage between the heavy and light chains of

factor XIa. J Biol Chem *287*, 6187–6195.

McMullen, B.A., Fujikawa, K., Davie, E.W. (1991) Location of the disulfide bonds in human coagulation factor XI: the presence of tandem apple domains.Biochemistry *30*, 2056-2060.

Ogawa, T., Verhamme, I.M., Sun, M.F., Bock, P.E., and Gailani, D. (2005) Exosite-mediated substrate recognition of factor IX by factor XIa. The factor XIa heavy chain is required for initial recognition of factor IX. J Biol Chem *280*, 23523–23530.

Papagrigoriou, E., McEwan, P.A., Walsh, P.N., and Emsley, J. (2006) Crystal structure of the factor XI zymogen reveals a pathway for transactivation. Nat Struct Mol Biol *13*, 557-558.

Sinha, D., Marcinkiewicz, M., Navaneetham, D., Walsh, P.N. (2007) Macromolecular substrate-binding exosites on both the heavy and light chains of factor XIa mediate the formation of the Michaelis complex required for factor IX activation. Biochemistry *46*, 9830–9839.

Smith, S.B., and Gailani, D. (2008) Update on the physiology and pathology of factor IX activation by factor XIa. Expert Rev Hematol *1*, 87–98.

Smith, S.B., Verhamme, I.M., Sun, M.F., Bock, P.E., Gailani, D. (2008) Characterization of novel forms of coagulation factor XIa: independence of factor XIa subunits in factor IX activation. J Biol Chem *283* 6696-6705.

Su, Y.C., Miller, T.N., Navaneetham, D., Schoonmaker, R.T., Sinha, D., Walsh, P.N. (2011) The role of factor XIa (FXIa) catalytic domain exosite residues in substrate catalysis and inhibition by the Kunitz protease inhibitor domain of protease nexin 2. J Biol Chem *286*, 31904–31914.

Sun, Y., and Gailani, D. (1996) Identification of a factor IX binding site on the third apple domain of activated factor XI. J Biol Chem *271*, 29023-8.

Sun, M.F., Zhao, M., Gailani, D. (1999) Identification of amino acids in the factor XI apple 3 domain required for activation of factor IX. J Biol Chem *274*, 36373-8.

Tucker, E.I., Marzec, U.M., White-Adams, T.C., Hurst, S., Rugonyi, S., McCarty, O.J., Gailani, D., Gruber, A., Hanson, S.R. (2009) Prevention of vascular graft occlusion and thrombus-associated thrombin generation by inhibition of factor XI. Blood *113*, 936-944.

Wolberg, A. S., Morris, D. P., Stafford, D. W. (1997) Factor IX activation by factor XIa proceeds without release of a free intermediate. Biochemistry *36*, 4074–4079.

Wu, W., Sinha, D., Shikov, S., Yip, C.K., Walz, T., Billings, P.C., Lear, J.D., Walsh, P.N. (2008) Factor XI homodimer structure is essential for normal proteolytic activation by factor XIIa, thrombin, and factor XIa. J Biol Chem *283*, 18655-18664.

CHAPTER V

ANALYSIS OF NATURALLY OCCURING FACTOR XIa MUTATIONS AND IMPLICATIONS FOR THE MECHANISM OF FACTOR IX ACTIVATION

Inherited deficiency of vitamin K-dependent coagulation proteases is often associated with circulating dysfunctional protein, and the mutations involved can provide information on structure-function relationships for these proteins. In contrast, FXI deficient patients typically have parallel reductions in FXI activity and antigen level (Saito *et al.*, 1985). This may be due to the compact structure of FXI, and particularly the apple domain disk, which may render it more susceptible to mutation-induced misfolding. Of the ~150 missense mutations identified in the FXI genes of FXI deficient patients, only twelve are, or may be, associated with circulating dysfunctional protein (Cross Reactive Material positive or CRM+ deficiency). Eight of the CRM+ mutations are associated with point mutation in the catalytic domain, and only four involve the heavy chain (www.factorxi.org).

In the following sections, data from two FXI CRM+ mutations will be discussed. Both mutations result in defective activation of FIX. One missense mutation results in a Gly substitution for Arg^{184} at the N-terminus of the FXI A3 domain, an area implicated in the exosite interaction with FIX (Sun *et al.*, 1999). The second missense mutation causes a Met to Thr substitution at residue 575 in the catalytic domain near the active site. Both mutant proteases were purified and tested for their capacity to activate FIX. Studies of these naturally occurring FXI variants provide additional information on the mechanism of FIX activation by FXIa.

Functional Analysis of FXIa-Gly^{184}

Guella *et al*. described a 24 year old woman with 10% of normal plasma FXI activity but ~50% of the normal antigen level (Guella *et al.*, 2008). This rare CRM+ patient is a compound heterozygote for point mutations in the FXI gene. One allele contained a mutation that disrupted an mRNA splice site, preventing FXI synthesis. The other contained a missence mutation resulting in a Gly substitution for Arg^{184}, a residue in the region of A3 implicated in FIX activation. To evaluate the functional activity of the Arg^{184}Gly mutation, the recombinant protein was expressed in HEK293 cells. The

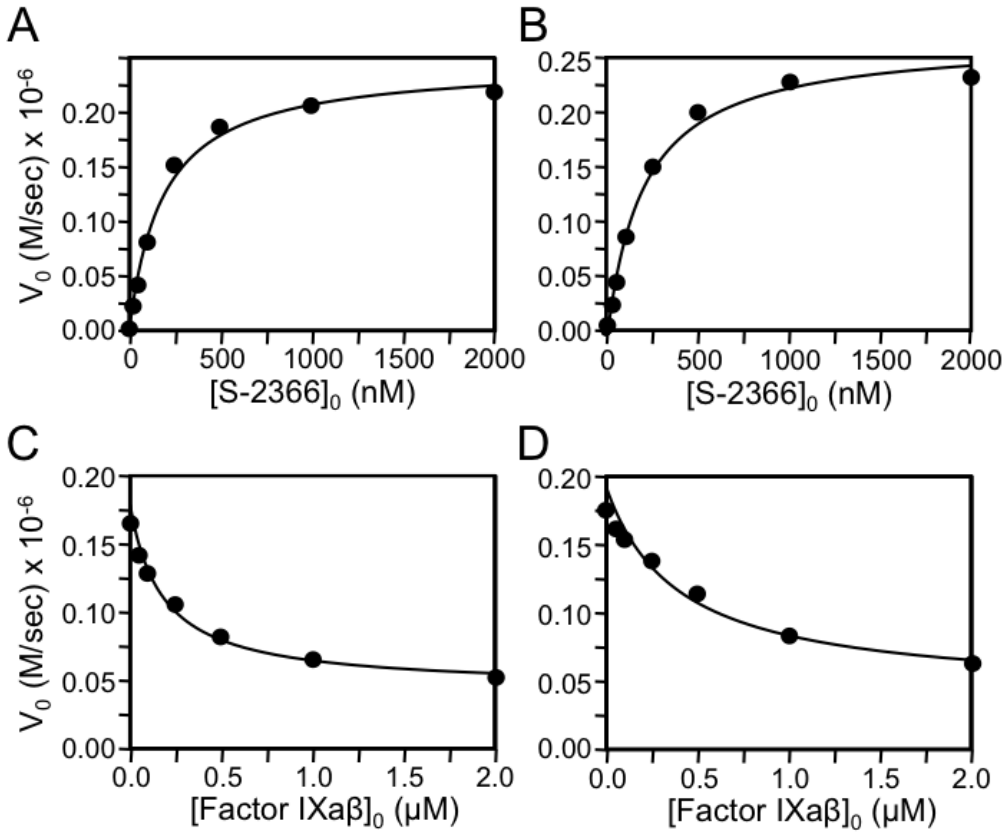

Figure 5-1. Cleavage of S-2366 by FXIa-WT and FXIa-Gly^{184}. (A, B) The rates of cleavage of the tripeptide substrate S-2366 by **(A)** 6 nM FXIa-WT or **(B)** FXI-Gly^{184}. **(C, D)** Cleavage of S-2366 (500 nM) by **(C)** 6 nM FXIa-WT or **(D)** FXI-Gly^{184} in the presence of varying concentrations of FIXaβ. For all panels, data points represent averages of duplicate runs.

expression level was comparable to FXI-WT. FXI-Gly^{184} and FXI-WT migrate at similar position on SDS-PAGE (Data not shown). The tripeptide S-2366 was cleaved similarly by FXIa-WT (Figure 5-1A, K_m 185 ± 40 μM, k_{cat} 41 ± 2 sec^{-1}) and FXIa-Gly^{184} (Figure 5-1B, K_m 200 ± 40 μM, k_{cat} 45 ± 2 sec^{-1}) indicating, as expected, that the Gly^{184} substitution does not alter the catalytic active site.

FXIa-WT and FXIa-Gly^{184} were tested in two types of plasma clotting assays. In the first, FXI was added to FXI-deficient plasma at various concentrations, and the clotting time of the supplemented plasma was measured in a standard activated partial thromboplastin time (aPTT) assay. Here, FXI must be activated by FXIIa, and FXIa then must activate FIX. FXI-Gly^{184} had ~25% of the activity of FXI-WT, consistent with results reported by Guella *et al*. In the second assay, FXIa was added directly to plasma, bypassing the requirement for activation of FXI by FXIIa. FXIa-Gly^{184} again demonstrated ~25% of the activity of FXIa-WT, indicating the reduced activity of FXI-Gly^{184} in the aPTT assay is due to a defect in FIX activation by FXIa.

The results from plasma clotting assays are supported by previous studies with site-directed mutagenesis, which showed that the region on A3 domain that contains Arg^{184} is required for binding to FIX (Sun *et al.*, 1999). Based on this, we assessed the affinity of FXIa-Gly^{184} for FIX. As discussed above, the interaction of FXIa with FIX involves both the A3 exosite and the active site. FIXaβ inhibits FXIa cleavage of the small peptide substrate S-2366 through a mixed mechanism, consistent with FIXaβ interacting with FXIa at the A3 domain and the active site (Ogawa *et al.*, 2005). K_i for these reactions is indicative of the affinity of FIXaβ for FXIa (see "Methods" for kinetic analysis). For FXIa-Gly^{184}, K_i for cleavage of S-2366 in the presence of FIXaβ (190 ± 30 nM, Figure

5-1D) was ~2-fold higher than FXIa-WT (90 ± 20 nM, Figure 5-1C), indicating binding of FIXaβ to FXIa-Gly^{184} is modestly weaker than to FXIa-WT.

Next, we compared the kinetic parameters of FIX activation by FXIa-Gly^{184} with FXIa-WT, using the densitometry based approach described previously. FXIa-Gly^{184} cleaves FIX more slowly than FXIa-WT, but significantly faster than FXIa/PKA3 (Figure 5-2 and Table 4-1). K_ms for cleavage of FIX after Arg^{145} and Arg^{180} by FXIa-Gly^{184} are 3- and 2-fold higher, respectively, than for cleavage by FXIa-WT (Table 4-1), while k_{cat}s are comparable. The result is a 3-fold and 2-fold reduced catalytic efficiency for the two FIX cleavages, respectively. Similar to FXIa-WT, and unlike FXIa/PKA3, relatively little FIXα accumulates during FIX activation by FXIa-Gly^{184} (Figure 5-2A), indicating a higher catalytic efficiency for the second cleavage at the Arg^{180}-Val^{181} bond. Michaelis-Menten analysis of conversion of FIX to FIXα was in agreement with the numerical integration analysis for cleavage after Arg^{145} (Table 4-2). These data indicate that the reduced capacity of FXIa-Gly^{184} to activate FIX is related to a modest decrease in affinity for both FIX and FIXα, resulting in a ~3-4 fold lower activity during blood coagulation due to a lower rate of FIXaβ generation.

The data suggest that Arg^{184} is part of a binding site for FIX and FIXα on the A3 domain. In the FXI zymogen crystal structure Arg^{184} is located on a loop connecting the A2 and A3 domains that is partially buried under the protease domain, and would not in the full-length zymogen. These data support the interpretation that Arg^{184} functions as a type of latch that keeps the catalytic domain in place over the A3 domain exosite in the be accessible to macromolecules such as FIX in aqueous phase (Papagrigoriou *et al.*, 2006)

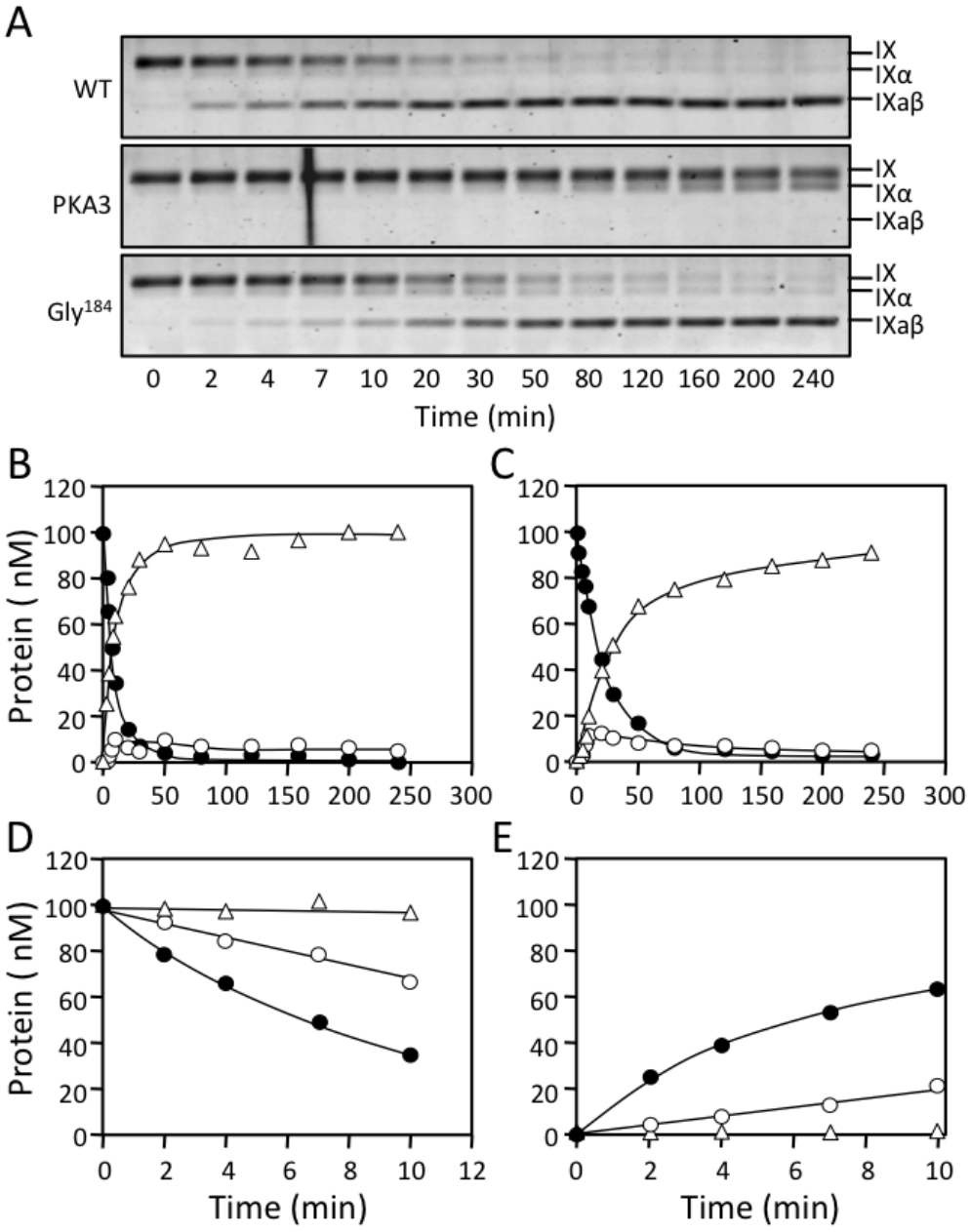

Figure 5-2. FIX cleavage by FXIa-Gly^{184}. (A) Non-reducing 17% polyacrylamide–SDS gels of 100 nM FIX in assay buffer with Ca2+ incubated at room temperature with 3 nM active sites of FXIa-WT (top), FXIa/PKA3 (middle), or FXIa-Gly^{184} (bottom). The positions of standards for FIX, FIXα and FIXaβ are indicated at the right of each panel. (B, C) Progress curves of FIX disappearance (●), and FIXα (○) and FIXaβ (Δ) generation, for **(B)** FXIa-WT or **(C)** FXIa-Gly^{184} from (A). Lines represent least-squares fits to the data. **(D)** Initial rates of FIX disappearance for FXIa-WT (●), FXIa-Gly^{184} (○), and FXIa/PKA3 (), determined over the first 10 min of activation form (A). (E) Initial rates of FIXaβ formation for FXIaWT (●), FXIa-Gly184 (○), and FXIa/PKA3 (Δ), determined over the first 10 min of activation from (A).

This is consistent with the observations that FIX and FIXα do not bind to zymogen FXI, and with the premise that conformational changes occur upon conversion of FXI to FXIa that exposes the substrate binding exosite. In the zymogen, Arg^{184} forms salt bridges with Asp^{488} and Asn^{566} in the catalytic domain (Figure 5-3), and it is likely that these bonds must be disrupted upon FXI activation. Crystal structures of isolated FXIa protease domain show that Asp^{488} and Arg^{566} form intra-catalytic domain interactions that are not present zymogen, and that must be released after cleavage of the FXI Arg^{369}-Ile^{370} bond to expose the exosite. The defect in FXIa-Gly^{184} in FIX activation is modest compared to the more severe defect seen with the chimeric protease FXIa/PKA3. This clearly indicates that the mutation does not completely disrupt the substrate binding exosite on A3, and that residues

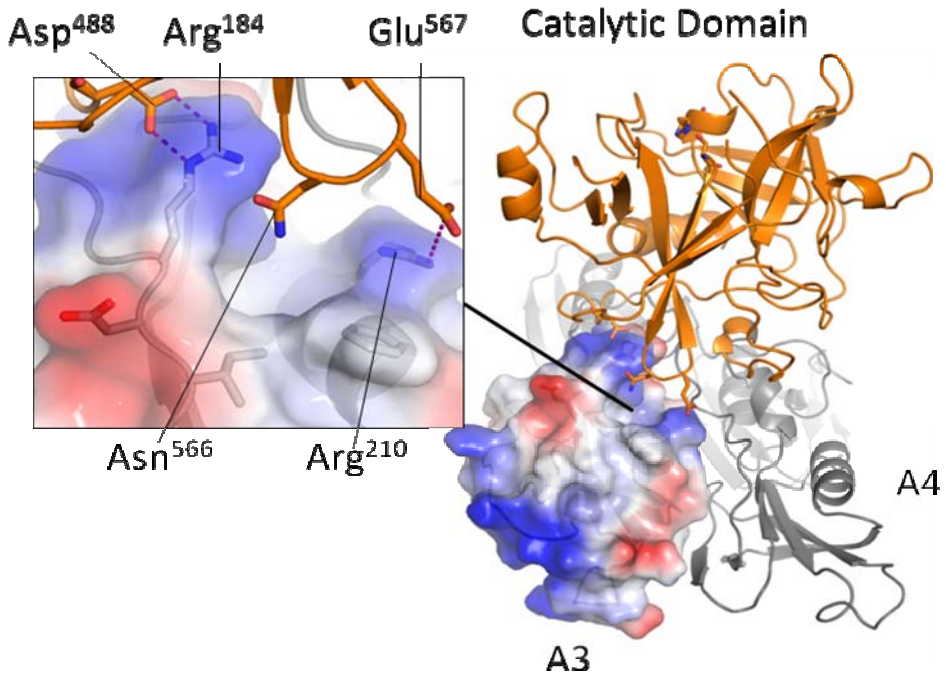

Figure 5-3. Position of Arg^{184} in FXI zymogen. Shown is a topology diagram of the zymogen FXI monomer with the A3 domain as a charged surface representation, and the A4 (gray) and catalytic domains (orange) as ribbon drawings. Note that Arg^{184} is covered by the catalytic domain. The inset shows specific interactions between side chains of the protease domain and the A3 domain. Arg^{184} forms salt bridges with Asp^{488} and Asn^{566} from the catalytic domain. (Image courtesy of Dr. Jonas Emsley.)

other than Arg^{184} are very likely involved in interaction with FIX. Data from studies investigating this possibility are presented in Chapter VI.

Functional Analysis of FXI-Met^{575}

The naturally occurring CRM+ FXI catalytic domain mutation Thr^{575}Met was first reported in 2004 (Quélin *et al.*, 2004). The propositus was heterozygous for this mutation, with a point mutation that results in a severly truncated FXI polypeptide on the other allele. Subsequently, homozygosity for Thr^{575}Met was reported in a 55 year-old Lebanese woman (Germanos-Haddad *et al.*, 2005). The substitution occurs in a highly conserved region of the catalytic domain, in proximity to the active site. Recombinant FXI-Met^{575} was expressed in HEK293 cells at levels comparable to FXI-WT, indicating that the mutation did not significantly disrupt protein folding. Conversion of FXI-WT and FXI-Met^{575} to FXIa-WT and FXIa-Met^{575}, respectively, by FXIIa proceeded at similar rates (data not shown).

Threonine is conserved at position 575 in FXI across species, indicating that the residue has functional importance. In the FXIa catalytic domain crystal structure, Thr^{575} (chymotrypsin number 213) is in close proximity to the active site serine residue (Ser^{557}, chymotrypsin Ser^{195}), and forms the back wall of the S1-specificity pocket of the active protease (Jin *et al.*, 2005) (Figure 5-4). This indicates that residue Thr^{575} either directly participates in substrate cleavage, or contributes to the correct conformation of the active site. The Thr^{575}Met substitution very likely causes significant perturbation in the active site conformation, because of the long side chain of methionine.

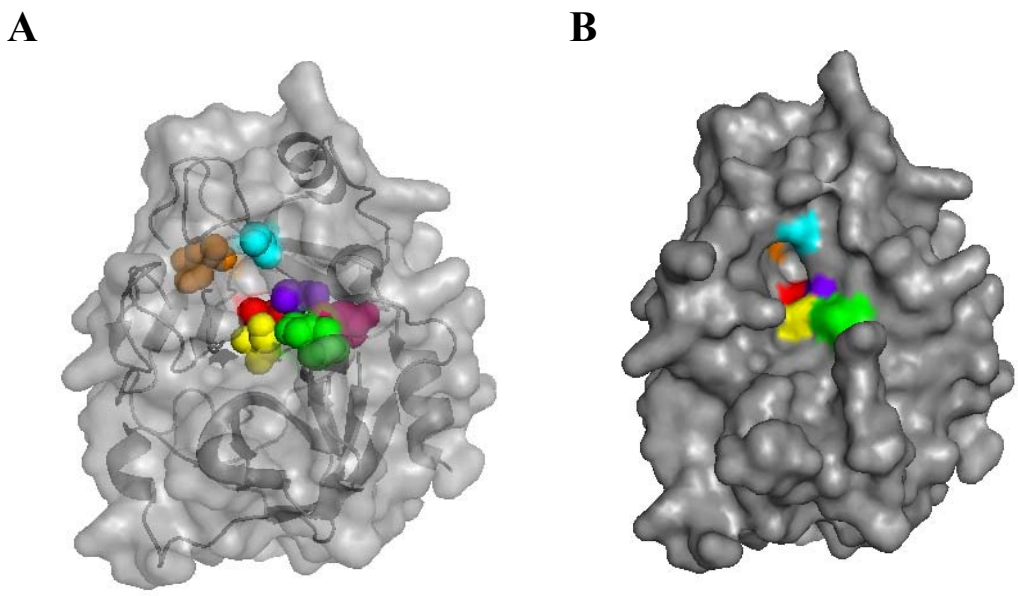

Figure 5-4. Surface representations of FXIa catalytic domain. Components of the catalytic triad within the active site of FXIa are labeled in green(His^{413}), magenta (D^{462}) and yellow (S^{557}). S1-S3 substrate binding sites are labeled as orange (Asp^{551}), purple (Ser^{576}) and Cyan (Gly^{578}). Thr^{575} (red) is in proximity to the catalytic triad and S1 site.

First, we tested the capacity of FXIa-Met^{575} to cleave the tripeptide substrate S-2366 (Glu-Pro-Arg-*p*-nitroaniline), which binds to FXIa through the S1 through S3 substrate binding sites. FXIa-Met^{575} cleaved S-2366 with ~30 fold reduced catalytic efficiency compared to FXIa-WT. Substrate saturation was not reached with S-2366 concentrations as high as 2000 μM, indicating a high K_m for FXIa-Met^{575} (compared to 970 ± 40 μM for FXIa-WT) (Figure 5-5 A and B). Because we could not reach saturation, k_{cat} could not be accurately determined. The decreased affinity for S-2366 suggests that the conformation of the S1-S3 sites in FXIa-Met^{575} are altered relative to FXIa-WT, consisted with predictions based on the crystal structure. The mutation may have altered the orientation of the catalytic triad of the active site, but this cannot be determined from the available data.

Studies with a second tripeptide substrate, S-2288 (Ile-Pro-Arg-*p*-nitroaniline), gave

similar results (Figure 5-5 C and D). We measured cleavage of S-2366 by FXIa-WT and FXIa-Met^{575} in the presence of a reversible inhibitor, aprotinin, which binds to the FXIa active site. As shown in Figure 5-5E, aprotinin competitively inhibited cleavage of S-2366 by FXIa-WT, indicating that aprotinin and S-2366 bind to the active site in a mutually exclusive manner. In contrast, aprotinin inhibition of S-2366 cleavage by FXIa-Met^{575} was significantly weaker, supporting the premise that the active site is altered in this protease. Based on the model in Figure 4-6, residues near the FXIa active site would likely be important for the docking interaction between the substrate FIX and the active site, but would not be as important for FIX affinity and specificity as they are for the small

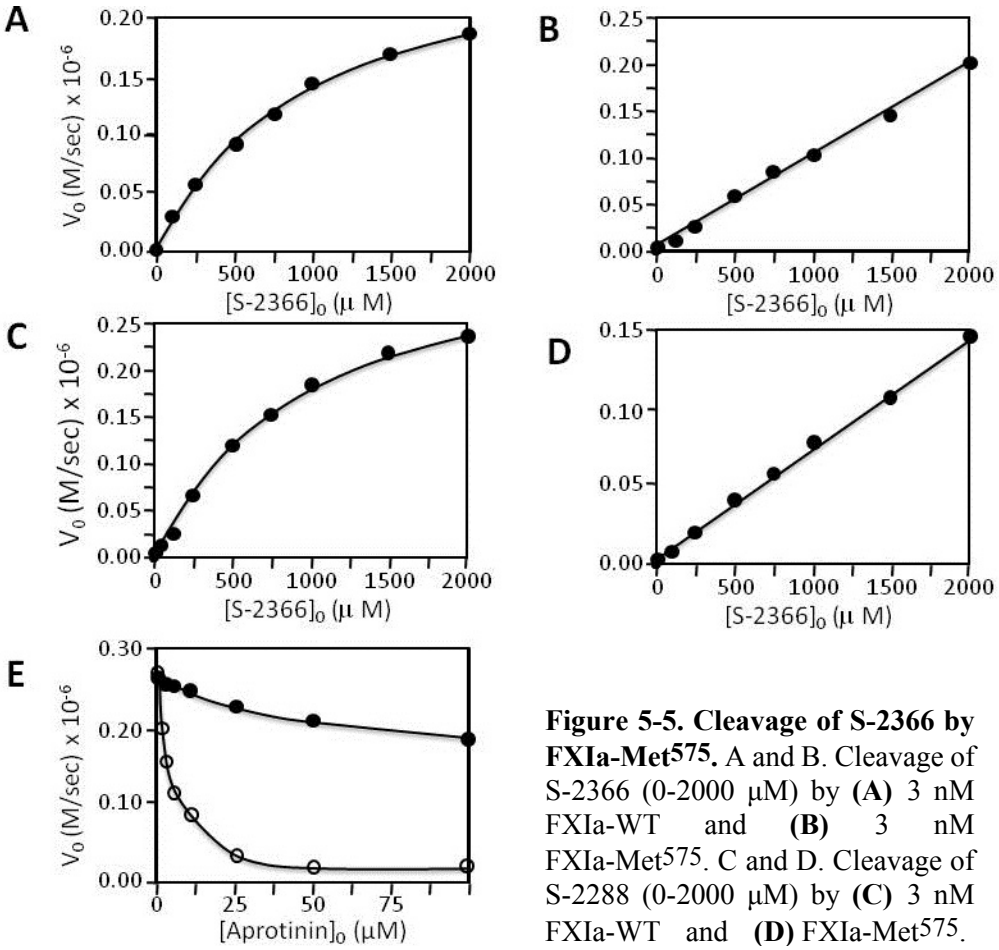

Figure 5-5. Cleavage of S-2366 by FXIa-Met^{575}. A and B. Cleavage of S-2366 (0-2000 μM) by **(A)** 3 nM FXIa-WT and **(B)** 3 nM FXIa-Met^{575}. C and D. Cleavage of S-2288 (0-2000 μM) by **(C)** 3 nM FXIa-WT and **(D)** FXIa-Met^{575}. **(E).** Cleavage of 500 μM S-2366 by 3 nM FXIa-WT (○) and FXIa-Met^{575} (●) in the presence of various concentrations of aprotinin.

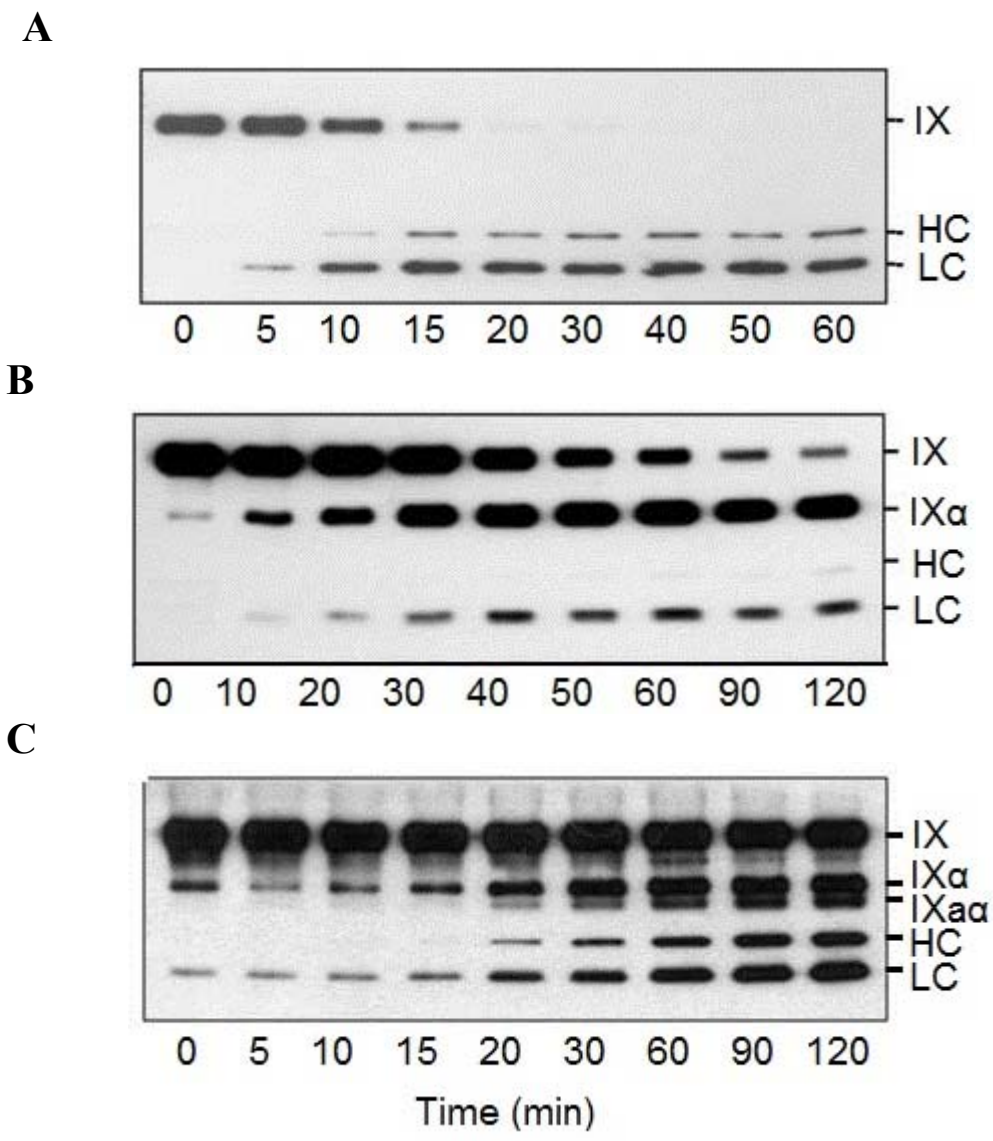

Figure 5-6. FIX activation by FXIa-Met575. Reducing western blots of time courses of 100 nM FIX incubated at room temperature with **(A)** 2 nM FXIa-WT, **(B)** 5 nM FXIa/PKA3 or **(C)** 2 nM FXIa-Met^{575}.

tripeptide substrates. This is because, as we have seen, FIX affinity and specificity are governed primarily by the exosite on the A3 domain of the FXIa heavy chain. We would anticipate, therefore, that the Thr^{575}Met would decrease k_{cat} for FIX activation by FXIa-Met^{575}, but have little effect on K_m. Consistent with the prolonged activated partial thromboplastin time (aPTT) noted in the patient homozygous for FXI-Met^{575}

(Germanos-Haddad *et al.*, 2005), the mutant protease activates FIX relatively slowly, with significant intermediate accumulation (Figure 5-6A) compared to FXIa-WT. The Kinetic parameters for FIX activation were determined, and are summarized in Table 4-1 and 4-2. As predicted the values for K_m for FIX activation by FXIa-WT and FXIa-Met^{575} are similar, indicating affinity of the mutant protease for FIX is normal. FXIa-Met^{575} cleaved FIX with a marked decrease in k_{cat} compared to FXIa-WT, most consistent with a catalytic defect. This supports the preliminary work from our group showing that FXIa with substitutions for another residue involved in active site conformation, Lys^{550} (Lys^{192} in chymotrypsin numbering), activates FIX with normal K_m and reduced k_{cat} (Schmidt *et al.*, 2008).

Interestingly, during activation of FIX by FXIa-Met^{575} we noted accumulation of an intermediate that appears to be FIXaα (FIX with a single cleavage after Arg^{180}) in addition to the previously described intermediate FIXα (Figure 5-6C). To date, we have not observed FIXaα accumulation during FIX activation by any protease with the exception of the protease from Russell Viper Venom. FIXaα is not seen in time course experiments of FIX activation by FXIa-WT or FXIa/PKA3 (Figure 5-6 A-C). The FIXaα generated with FXIa-Met^{575} appears to be a minor species. It is clearly seen on the western blot, but was not detectable on Coomassie Blue-stained gels (data not shown), and, therefore, cannot be included in kinetic analyses. However, this novel observation suggests that the ordered bond cleavage during normal FIX activation is determined by features of the FXIa active site, and this is perturbed in FXIa-Met^{575}.

Similar to FIX activation by FXIa, prothrombin activation by factor Xa, in the presence of factor Va, Ca^{2+} and phosphatidylserine-rich vesicles is a reaction that requires the

substrate to engage an exosite on the enzyme complex, followed by sequential cleavage after Arg^{320} and Arg^{271} to form the protease α-thrombin (Orcutt *et al.*, 2004). However, during the ordered bond cleavage of prothrombin, substrate interaction with the exosite appears to dictate access to the Arg^{320} bond preferentially to the Arg^{271} bond (Krishnaswamy, 2005). Our data with FXIa-Met^{575} raises the possibility that the order of bond cleavage during FIX activation by FXIa may be dictated, at least partially, by residues around the active site. This is supported by the observation that only FIXα is observed in reactions where FIX is activation by the isolated FXIa catalytic domain.

Summary

Our understanding of the mechanism of FIX activation by FXIa is enhanced by functional studies of two naturally occurring CRM+ mutations in FXI deficient patients. We found a ~3 fold higher K_m for FIX activation by FXIa-Gly^{184}, suggesting Arg^{184} is part of the exosite. In contrast, FXIa-Met^{575} activates FIX with a comparable K_m to FXIa-WT, but ~10-fold reduced k_{cat}, indicating alteration of the structure within the active site in the catalytic domain. These results are consistent with the A3 exosite of FXIa being the major determinant of substrate affinity, while the active site is responsible for substrate catalysis after initial engagement at the exosite.

Methods

Recombinant Proteins. Recombinant FXIa was expressed as described in Chapter IV. In addition to FXI-WT, several variants were prepared. In FXI-Gly^{184}, Arg^{184} is replaced with Gly, while in FXI-Met^{575}, Thr^{575} is replaced with Met.

Plasma Clotting Assay. FXI activities were determined in a partial thromboplastin time (aPTT) assay. FXI deficient plasma (30 μL George King) was mixed with 30 μL FXI (0.3 to 30 nM) in TBS with 0.1% BSA (TBSA) and 30 μL PTT-A reagent (Diagnostica Stago). After incubation at 37˚C for 5 min, 30 μL 25 mM $CaCl_2$ was added, and time to clot formation was determined on an ST4 fibrometer (Diagnostica Stago). In a separate experiment, 30 μL of FXIa diluted in TBSA (0.3 to 30 nM) was mixed with 30 μL FXI-deficient plasma and 30 μL rabbit brain cephalin (Sigma). After incubation at 37 °C for 30 sec, 30 μL 25 mM $CaCl_2$ was added, and time to clot formation determined. Results were compared to standard curves prepared with FXI-WT or FXIa-WT starting at 30 nM. Activities are percent of wild-type protein activity.

Hydrolysis of chromogenic substrate by FXIa. FXIa (6 nM) was incubated with 50-2000 μM S-2366 or S-2288 in TBS at RT. In separate experiments, FXIa (6 nM) was incubated with 500 μM S-2366 and varying concentrations of FIXaβ (FIXaβ does not cleave S-2366) in TBS with 5 mM $CaCl_2$ at RT. Generation of free p-nitroaniline (pNA) was followed by monitoring absorbance at 405 nm. Rates of pNA generation (nM/s) were determined using an extinction coefficient of 9920 M^{-1} cm^{-1} (405 nm). K_m, k_{cat} and K_i for S-2366 cleavage were determined by non-linear least squares fitting performed with MicroMath Scientific Software.

Factor IX activation followed by western blotting. Plasma FIX (100 nM) was incubated in assay buffer at room temperature with various factor XIa species. At various times, 7 μL samples were mixed with 3 μL of reducing sample buffer, fractionated on 12% SDS-polyacrylamide gels, and then transferred to nitrocellulose. The primary antibody was goat anti-human FIX polyclonal IgG, and the secondary antibody was horseradish

peroxidase-conjugated anti-goat IgG. Detection was by chemiluminescence.

The methods for FIX activation by FXIa and kinetic analysis were performed as described in Chapter IV.

References

Germanos-Haddad, M., de Moerloose, P., Boehlen, F., Peyvandi, F., Neerman-Arbez, M. (2005) Homozygosity for a Thr^{575}Met missense mutation in the catalytic domain associated with factor XI deficiency. Haematologica *90*, 418-9.

Guella, I., Soldà, G., Spena, S., Asselta, R., Ghiotto, R., Tenchini, M.L., Gastaman, G., Duga, S. (2008) Molecular characterization of two novel mutations causing factor XI deficiency: a splicing defect and a missense mutation responsible for a CRM+ defect. Thromb Haemost *99*, 523-30.

Jin, L., Pandey, P., Babine, R.E., Gorga, J.C., Seidl, K.J., Gelfand, E., Weaver, D.T., Abdel-Meguid, S.S., Strickler, J.E. (2005) Crystal structures of the FXIa catalytic domain in complex with ecotin mutants reveal substrate-like interactions. J Biol Chem *280*, 4704-4712.

Krishnaswamy, S. (2005) Exosite-driven substrate specificity and function in coagulation. J Thromb Haemost *3* 54–67.

Ogawa, T., Verhamme, I.M., Sun, M.F., Bock, P.E., and Gailani, D. (2005) Exosite-mediated substrate recognition of factor IX by factor XIa. The factor XIa heavy chain is required for initial recognition of factor IX. J Biol Chem *280*, 23523–23530.

Orcutt, S.J., and Krishnaswamy, S. (2004) Binding of substrate in two conformations to human prothrombinase drives consecutive cleavage at two sites in prothrombin. J Biol Chem *279*, 54927–54936.

Papagrigoriou, E., McEwan, P.A., Walsh, P.N., and Emsley, J. (2006) Crystal structure of the factor XI zymogen reveals a pathway for transactivation. Nat Struct Mol Biol *13*, 557-558.

Quélin, F., Trossaërt, M., Sigaud, M., Mazancourt, P.D., Fressinaud, E. (2004) Molecular basis of severe factor XI deficiency in seven families from the west of France. Seven novel mutations, including an ancient Q88X mutation. J Thromb Haemost *2*, 71-6.

Saito, H., Ratnoff, O.D., Bouma, B.N., Seligsohn, U. (1985) Failure to detect variant (CRM+) plasma thromboplastin antecedent (factor XI) molecules in hereditary plasma thromboplastin antecedent deficiency: a study of 125 patients of several ethnic backgrounds. J Lab Clin Med *106*, 718-722.

Schmidt, A.E., Agah, S., Sun, M.F., Padmanabhan, K., Cascio, D., Gailani, D., Bajaj, S.P. (2008) Structural and functional significance of amino acid lysine 192 (chymotrypsin numbering) in factor XIa and factor VIIa. Blood *112*, 708a.

Sun, M.F., Zhao, M., Gailani, D. (1999) Identification of amino acids in the factor XI apple 3 domain required for activation of factor IX. J Biol Chem *274*, 36373-8.

CHAPTER VI

STRUCTURAL BASIS FOR THE INTERACTION BETWEEN FACTOR IX AND FACTOR XIa

Structure of the Factor XI A3 Domain

The A3 domain of FXIa has been implicated in binding to heparin (Zhao *et al.*, 1998), platelet glycoprotein 1b (Baglia *et al.*, 2004), and FIX (Sun *et al.*, 1999). In Chapter IV, we presented evidence that A3 contains an exosite that binds FIX and the activation intermediate FIXα that is central to the mechanism of FIX activation by FXIa. Furthermore, in Chapter V we characterized a naturally occurring mutation within the A3 domain of FXIa, $Arg^{184}Gly$, with decreased affinity towards FIX that suggested a location for the FIX-binding exosite. To gain further insight into the structural basis of the FIX-FXIa interaction, we examined the topology of the FXIa A3 domain utilizing the crystal structure for zymogen FIX (Papagrigoriou *et al.*, 2006). Based on the kinetic analysis, a FIX binding site should be a surface epitope on the A3 domain that is not present on PK A3, and should probably not be accessible to the aqueous phase in the zymogen FXI structure, given that FIX does not bind to the zymogen.

The structural analysis software Metapocket (Zhang *et al.*, 2011), which utilizes eight predictors to identify potential surface binding sites, identified three hydrophobic pockets on the surface of FXI A3 (Figure 6-1B). Pocket 1 is formed by the alkyl groups of the side chains of Arg^{184} and Arg^{210} with additional contributions from the side chains of Ile^{186}, Leu^{262}, and Phe^{221}, and Phe^{206} from the α-helix (Figure 6-1 A and B). Charged surface

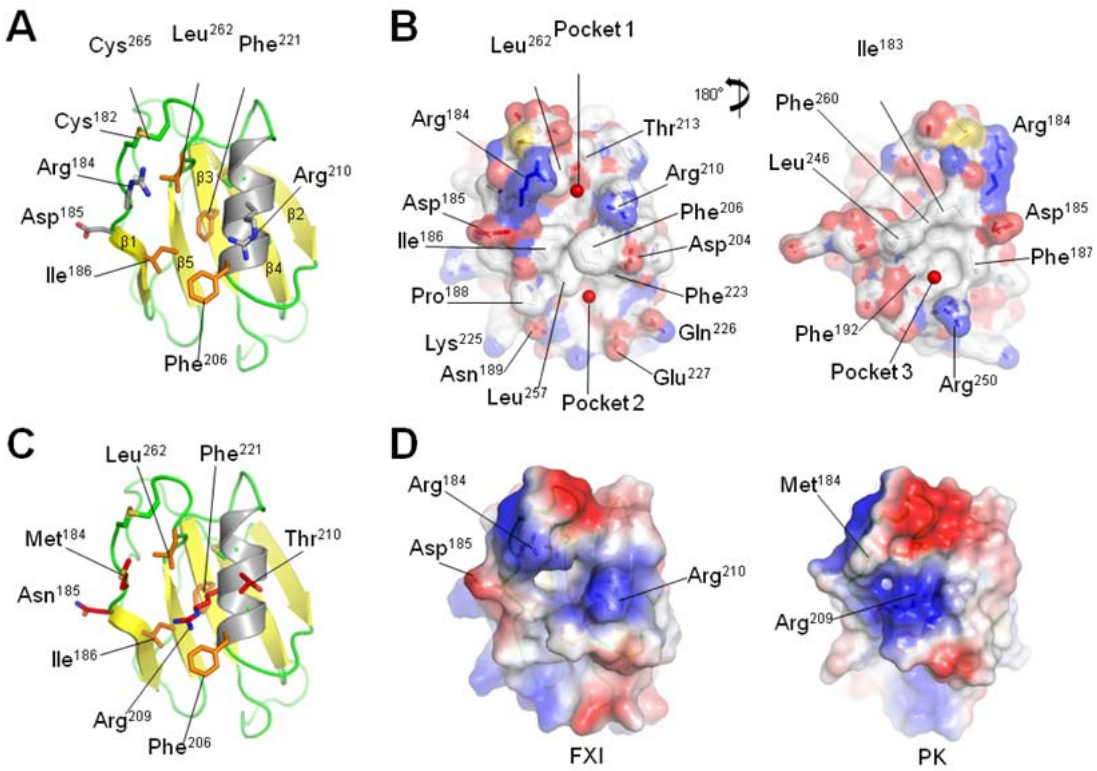

Figure 6-1. The FXI A3 domain. (A) Topological diagram showing the A3 domain of human FXI, with the β-sheet indicated in yellow and the α-helix in gray. Side chains of residues in the locality of Arg^{184} are shown as sticks. **(B)** Surface representations of the FXI A3 domain are shown with partial transparency to highlight side chains of specific residues that are colored by atom type. Two rotations are shown related by 180°. The software program METAPOCKET identified three pockets on the surface of A3 (shown as red balls). **(C)** Topological diagram of the human prekallikrein (PK) A3 domain, with side chains of non-conserved residues in the area of the pocket in FXI shown as sticks. Note that the side chain of Arg^{209} in PK occupies the site of the hydrophobic pocket in FXI. **(D)** Charged surface representations of the FXI (left) and the PK (right) A3 domains. Blue indicates positive charge, and red indicates negative charge. Note the absence of pocket 1 in the PK A3 domain model, owing to the Arg^{209} side chain.

representations (Figure 6-1B) illustrate that Arg^{184} and Arg^{210} contribute to positively charged patches on either side of pocket 1. Arg^{184} and Asp^{185} run along one side of pocket 1, with the other side formed primarily by the α-helix. Leu^{262} is in proximity to residues 184 and 185 by virtue of the Cys^{182}-Cys^{265} bond, and contributes to the wall of pocket 1 (Figure 6-1A). These residues are highly conserved across mammalian species (Fujikawa

et al., 1986; Ponczek *et al.*, 2008), consistent with this area of the domain contributing to a FXIa specific function. The Arg^{184} side chain projects upward on one face of the β-sheet (yellow) adjacent to the Cys^{182}-Cys^{265} disulfide bond. The Gly^{184} substitution would likely lead to loss of a positive charge that could contribute to electrostatic interactions with FIX, to the loss of hydrophobic interactions with the alkyl group of the Arg^{184} side chain, and would introduce flexibility into the main chain that could affect local loop conformation. Modeling of the PK structure was carried out previously utilizing the FXI crystal structure as a template (Hooley *et al.*, 2007). The model suggests that hydrophobic pocket 1 in the FXI A3 domain is not present in PK (Figure 6-1 C and D). In FXI, residue 209 on the α-helix is Gly (Figure 6-1A); while in PK it is Arg (Figure 6-1C). The PK Arg209 side chain is predicted to interfere with formation of the hydrophobic pocket in this location (Figure 6-1 C and D).

As discussed in Chapter IV, hydrophobic pocket 1 and the adjacent Arg^{184} are buried beneath the catalytic domain in zymogen FXI, with Arg^{184} forming salt bridges with Asp^{488} and Asn^{566} on the catalytic domain (Figure 5-3). This is consistent with the observation that FIX binds to FXIa but not zymogen FXI, and is consistent with the hypothesis that Arg^{184} and pocket 1 may be part of a FIX binding site that is exposed during FXI conversion to FXIa through repositioning of the catalytic domain relative to the A3 domain (Samuel *et al.*, 2007, Emsley *et al.*, 2010).

Hydrophobic pocket 2 is located on the opposite side of Phe^{206} from pocket 1 (Figure 6-1B left panel), with Asn^{189}, Phe^{223}, Ser^{225}, Gln^{226}, and Glu^{227} contributing to its formation. It would seem that this pocket is less likely to be a component of a FIX-binding site specific to FXIa, as a similar pocket (with some substitutions) is predicted to be present

on the PK A3 domain. Furthermore, pocket 2 is exposed to the aqueous phase in the zymogen structure. Hydrophobic pocket 3, which is on the opposite side of A3 from pocket 1 (Figure 6-1B right panel), is formed by Asp^{185}, Phe^{187}, Phe^{192}, Leu^{246}, Arg^{250} and Phe^{260}. While not predicted to be present in PK, this pocket is also unobstructed in zymogen FXI.

Investigations of Additional Residues on the Factor XI A3 Domain Involved in Factor IX activation

The structural analysis suggests that hydrophobic pocket 1 and/or the charged residues around the pocket may be an area on the FXIa A3 domain that interacts with FIX. This is consistent with our observation that Arg^{184} contributes to binding of FIX and FIXα to FXIa. However, the functional defect caused by the Gly^{184} substitution is modest compared to the defect observed with FXIa/PKA3, showing that residues in addition to Arg^{184} contribute to FIX binding. Residues in proximity to Arg^{184} were analyzed for their importance to FIX activation. A comparison of the amino acid sequence of the human FXI and PK A3 domains assisted us in focusing on FXIa specific sequences. A FXI variant in which residues Ile^{183}, Arg^{184} and Asp^{185} are each replaced with Ala (FXIa-$Ala^{183-185}$) demonstrated a profound defect in plasma clotting activity (< 1% clotting activity of plasma FXIa in aPTT assay). Cleavage patterns and kinetic parameters for FIX activation by FXIa-$Ala^{183-185}$ are shown in Figure 6-2A, Tables 6-1 and 6-2 (The kinetic parameters for FIX activation by FXIa-WT and FXIa/PKA3 are also listed for comparison). FXIa-$Ala^{183-185}$ exhibits a defect in FIX activation that is comparable to that of FXIa/PKA3. Thus, replacement of Ile^{183}, Arg^{184} and Asp^{185} completely disrupts the

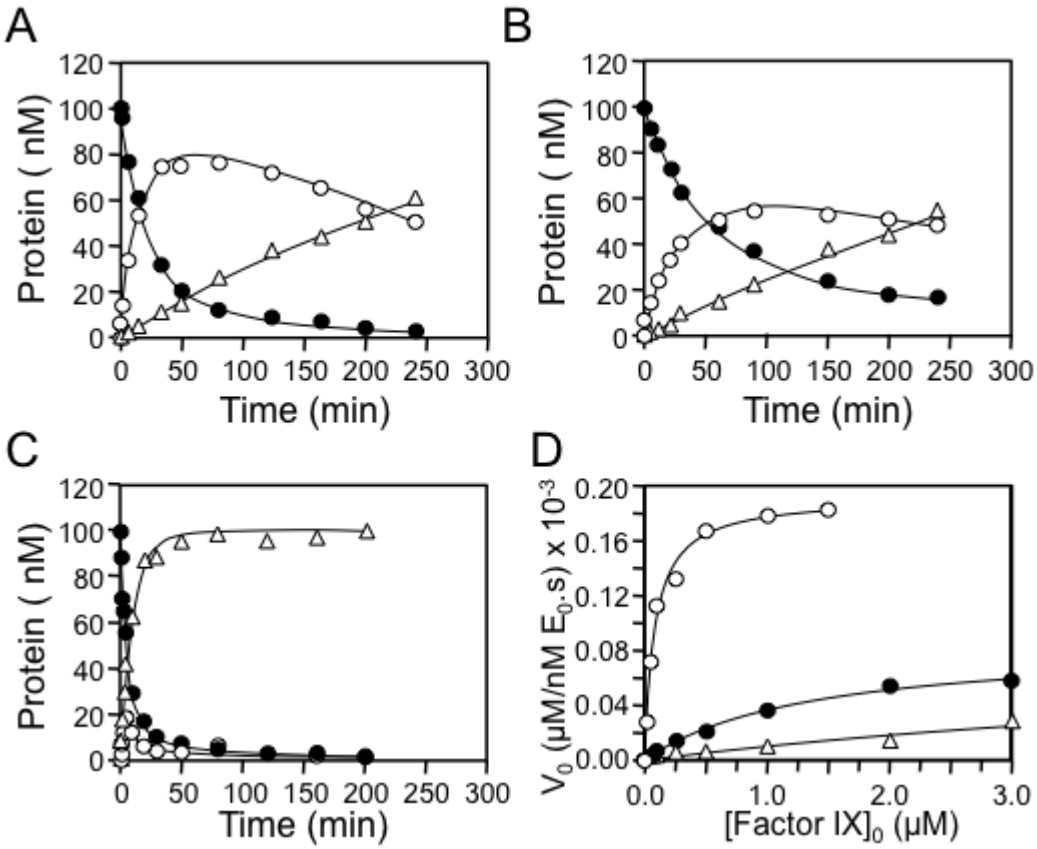

Figure 6-2. Progress curves of FIX activation by FXIa-Ala$^{183-185}$ and FXIa/PKA3 gain-of-function variants. Shown are progress curves of FIX disappearance (●), and FIXα (○) and FIXaβ (Δ) generation, for reactions containing 100 nM FIX and **(A)** 30 nM FXIa-Ala$^{183-185}$, **(B)** 3 nM FXIa/PKA3-A, and **(C)** 3 nM FXIa/PKA3-B. Note the different FXIa concentrations used in the three reactions. FXIa concentrations represent the concentrations of active subunits. **(D)** Initial velocities of cleavage of FIX after Arg^{145} (conversion of FIX to FIXa) by FXIa-Ala$^{183-185}$ (Δ), FXIa/PKA3-A (●), and FXIa/PKA3-B (○), as a function of FIX concentration.

specific interaction between the A3 domain and FIX and FIXα, and suggests that these residues in combination are a major component of the FIX-binding site.

A concern with the alanine-substitution strategy is that the replacements may alter the general conformation of A3 domain and its exosite, without actually being part of the exosite. This is a limitation of most loss-of-function strategies. As a complementary approach, FXI/PKA3 was used as a scaffold to reintroduce FXI sequence to restore activity

Table 6-1. Kinetic parameters for cleavage of FIX by FXIa.

Simulation of full-progress experimental traces was performed with KINTEK software (KINTEK EXPLORER Version 2.5), using the equation shown in methods in Chapter IV. K_m and k_{cat} for activation were calculated from individual rate constants for each step. Values are mean standard deviations for each experiment. K_i was fixed for reactions with FXIa-WT and FXIa/PKA3 on the basis of surface plasmon resonance results (Chapter IV).

Cleavage of FIX after Arg^{145}

Protease	Substrate	k_{cat} 1 (min^{-1})	Kd 1 (μM)	Km 1 (μM)	Catalytic Efficiency 1 (μM^{-1} min^{-1})	Ki 1 (μM)
FXIa-WT	FIX	12 ± 1	0.10 ± 0.01	0.20 ± 0.01	60 ± 6	0.14
FXIa-WT no Ca^{2+}	FIX	6.5 ± 0.4	4.9 ± 0.4	4.9 ± 0.4	1.3 ± 0.3	5
FXIa/PKA3	FIX	4.9 ± 0.1	4.9 ± 0.2	4.9 ± 0.2	1.0 ± 0.1	3
FXIa-$Ala^{183\text{-}185}$	FIX	9 ± 1	8 ± 1	10 ± 2	0.9 ± 0.2	6 ± 1
FXIa/PKA3-A	FIX	6.4 ± 0.2	1.3 ± 0.1	1.4 ± 0.1	4.6 ± 0.4	1.9 ± 0.1
FXIa/PKA3-B	FIX	19 ± 2	0.06 ± 0.01	0.09 ± 0.02	200 ± 30	0.5 ± 0.1

Cleavage of FIX after Arg^{180}

Protease	Substrate	k_{cat} 2 (min^{-1})	Kd 2 (μM)	Km 2 (μM)	Catalytic Efficiency 2 (μM^{-1} min^{-1})	Ki 2 (μM)
FXIa-WT	FIX	35 ± 6	0.06 ± 0.01	0.08 ± 0.01	400 ± 100	0.06
FXIa-WT no Ca^{2+}	FIX	3.6 ± 0.2	15 ± 1	15 ± 1	0.24 ± 0.04	5
FXIa/PKA3	FIX	0.6 ± 0.1	7 ± 1	7 ± 1	0.09 ± 0.02	3
FXIa-$Ala^{183\text{-}185}$	FIX	0.4 ± 0.1	3 ± 1	3 ± 1	0.13 ± 0.01	0.29 ± 0.01
FXIa/PKA3-A	FIX	1.7 ± 0.1	1.3 ± 0.1	1.3 ± 0.1	1.3 ± 0.1	0.28 ± 0.02
FXIa/PKA3-B	FIX	39 ± 4	0.04 ± 0.01	0.07 ± 0.01	600 ± 100	0.30 ± 0.03

toward FIX. The wild type PK sequence His^{183}, Met^{184} and Asn^{185} in FXIa/PKA3 was replaced with Ile^{183}, Arg^{184} and Asp^{185} from the FXIa sequence to create FXIa/PKA3-A. FXIa/PKA3-A has ~5% of FXIa-WT coagulant activity, with catalytic efficiencies for the cleavage after Arg^{145} and after Arg^{180} that are 4- and 10- fold greater, respectively, than for FXIa/PKA3 (Table 6-1). However, these values remain considerably lower than those for FXIa-WT, and accumulation of FIXα confirms that the exosite and the activation mechanism are not completely restored (Figure 6-2B).

Table 6-2. Kinetic parameters for cleavage of FIX by FXIa determined from initial velocities.

Protease	Substrate	Bond cleaved	k_{cat} 1 (min^{-1})	K_m 1 (μM)	Catalytic Efficiency 1 (μM^{-1} min^{-1})
FXIa-WT	FIX	Arg^{145}	10 ± 1	0.27 ± 0.07	40 ± 10
FXIa/PKA3	FIX	Arg^{145}	6 ± 1	3.9 ± 0.9	1.6 ± 0.4
FXIa-$Ala^{183-185}$	FIX	Arg^{145}	ND*	> 8	0.70 ± 0.10
FXIa/PKA3-A	FIX	Arg^{145}	5 ± 1	1.3 ± 0.4	4 ± 1
FXIa/PKA3-B	FIX	Arg^{145}	12 ± 1	0.08 ± 0.01	140 ± 20

* ND, not determined. The initial velocity (v_0) of cleavage of FIX after Arg^{145} was plotted against the initial substrate concentration, and analyzed with the Michaelis–Menten equation. K_m and k_{cat} were obtained from direct non-linear least squares analysis with Scientist Software. Owing to the low affinity between the enzyme and substrate in reactions with FXIa variants, we were not able to reach saturation in reactions with FXIa-$Ala^{183–185}$ or FXIa/PKA3. Thus, values for K_m are approximate, and the value for k_{cat} for FXIa-$Ala^{183–185}$ was not determined.

As discussed above, the C-terminus (residues 260-264) of the FXI A3 domain is in proximity to the N-terminus where residues 183-185 reside, due to the Cys^{182}-Cys^{265} disulfide bond that connects the N- and C-termini of the A3 domain (Figure 6-1A) (McMullen *et al.*, 1991; Papagrigoriou *et al.*, 2006). To determine if the C-terminus of the A3 domain is required for proper formation of the FIX binding site, we replaced the PK sequence Tyr^{260}-Ser^{261}-Leu^{262}-Leu^{263}-Thr^{264} in FXIa/PKA3-A with Phe^{260}-Ser^{261}-Leu^{262}-Gln^{263}-Ser^{264} from FXI, creating FXIa/PKA3-B. Superimposing these changes on the N-terminal replacements for residues 183-185 restored normal FIX activation (Figure 6-2 C and D) to FXIa/PKA3. Indeed, FXIa/PKA3-B is a modestly more efficient activator of FIX than FXIa-WT (Tables 6-1 and 6-2), with catalytic efficiencies for the first and second cleavages that are 3.3- and 1.5-fold greater, respectively, than for FXIa-WT. As with FXIa-WT, cleavage of FIX by FXIa/PKA3-B was associated with little

FIXα accumulation. Thus, replacing six amino acids in the PKA3 domain (residues 183, 184, 185, 260, 263 and 264) with the corresponding FXI residues is sufficient to restore exosite activity and the mechanism for FIX activation in FXIa/PKA3.

While our data strongly suggest the residues near hydrophobic pocket 1 are required for formation of the FIX binding exosite on FXIa, we cannot rule out a contribution from pocket 3. In the crystal structure of the A3 domain, Arg^{184} and adjacent residues form a ridge between the hydrophobic pockets 1 and 3 that is not predicted to be present in PK (Figure 6-1 B and D). The substitutions in FXIa-$Ala^{183\text{-}185}$ could disrupt the adjacent hydrophobic pockets, one or both of which could be involved in FIX binding. Residues 260 to 265 actually run underneath the chain containing 183-185 (Figure 6-1A), with Leu^{262} and Phe^{260} (Figure 6-1B) contributing to hydrophobic pockets 1 and 3, respectively. The C-terminal sequence from FXI A3 in FXIa/PKA3-B could, therefore, restore FIX binding by supplying missing components of the binding site, or by properly orienting structures such as residues 183 to 185 that are directly involved in binding.

Localization of the Factor XIa Binding Site on the Factor IX Gla Domain.

As discussed in Chapter III, the Gla domains of VKD coagulation proteases bind to phosphatidylserine-rich phospholipid membranes. These interactions are essential for formation of coagulation enzyme-substrate complexes involving these proteases. Published work from our laboratory indicates that the Gla domain of FIX may serve as a recognition site for FXIa (Aktimur *et al.*, 2003). The importance of Ca^{2+} ions to the proper conformation of the Gla domain might be the reason that FIX activation by FXIa is calcium dependent, as most of the other reactions catalyzed by FXIa do not require calcium. In the

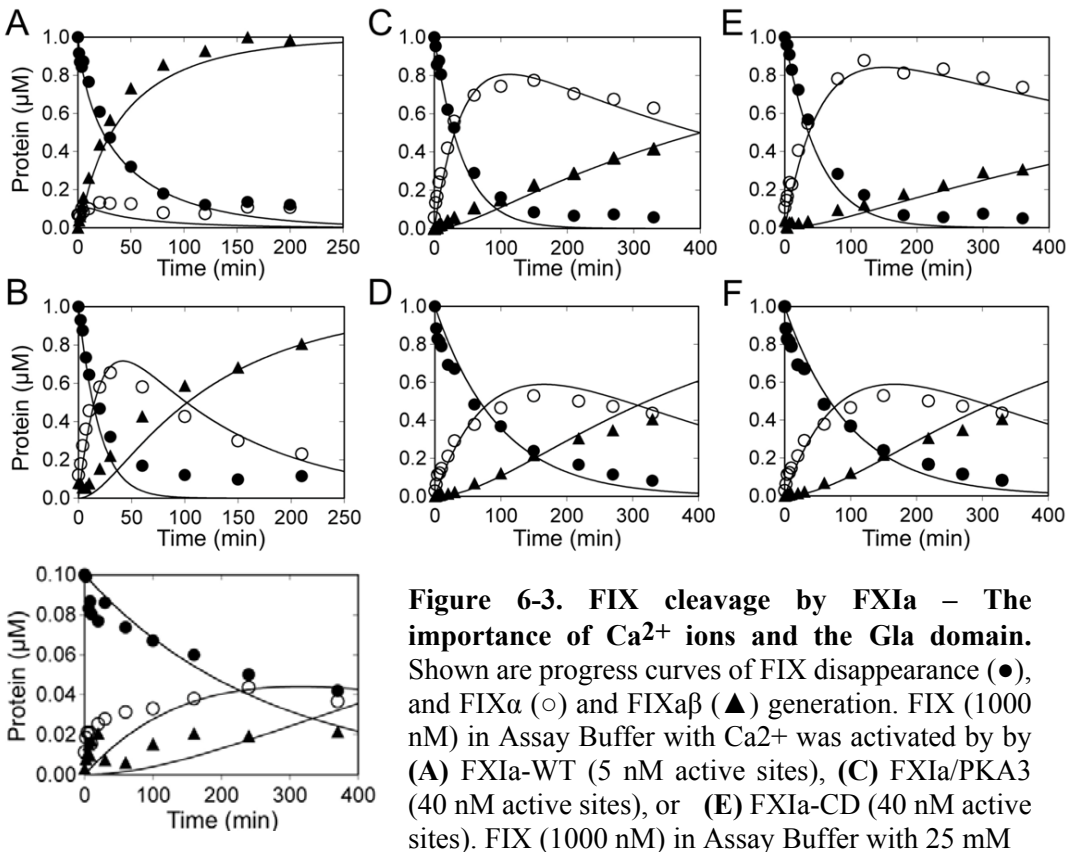

Figure 6-3. FIX cleavage by FXIa – The importance of Ca^{2+} ions and the Gla domain. Shown are progress curves of FIX disappearance (●), and FIXα (○) and FIXaβ (▲) generation. FIX (1000 nM) in Assay Buffer with Ca2+ was activated by by **(A)** FXIa-WT (5 nM active sites), **(C)** FXIa/PKA3 (40 nM active sites), or **(E)** FXIa-CD (40 nM active sites). FIX (1000 nM) in Assay Buffer with 25 mM EDTA activated at room temperature by **(B)** FXIa-WT (40 nM active sites), **(D)** FXIa/PKA3 (40 nM active sites), or **(F)** FXIa-CD (40 nM active sites). **(G)** FIX (100 nM) was activated by 3 nM FXIa-WT (active sites) in the presence of 1000 nM IgG SB 249417.

absence of Ca^{2+}, the rates of FIX bond cleavage by FXIa are significantly slower than in the presence of Ca^{2+}, with pronounced accumulation of FIXα (Figure 6-3 A and B). K_m values for FIX activation in the absence of Ca^{2+} are similar to those generated with FXIa/PKA3 in the presence of Ca^{2+} (Table 6-1). Indeed, absence of Ca^{2+} has little effect on the overall rate of FIX cleavage by FXIa/PKA3 (Figure 6-3 C and D) or FXIa-CD (Figure 6-3 E and F). The data are consistent with the premise that a Ca^{2+}-dependent interaction between the FXIa A3 domain and FIX is required for normal FIX activation. That this interaction involves the FIX Gla domain is suggested by the observation that replacing the Gla domain with the corresponding domain from FVII (Aktimur *et al.*,

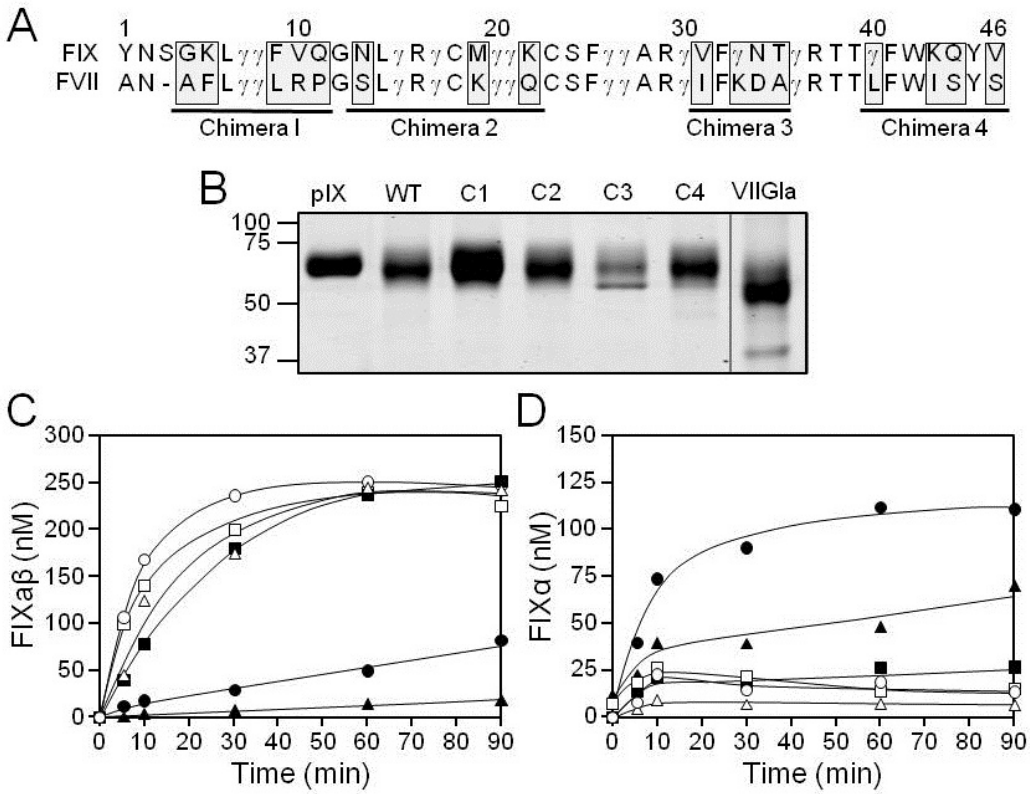

Figure 6-4. FIX with FVII sequence in the Gla-domain. (A) Primary sequences of the human FIX and FVII Gla-domains. The numbering system shown is for FIX. The symbol γ indicates the position of Gla residues. Underlined sequences were changed from the FIX sequence to the FVII sequence to generate chimeras C1, C2, C3, and C4. The residues changed in each chimera are highlighted by the gray boxes. **(B)** Stained SDS–polyacrylamide gel of purified plasma FIX (pIX), recombinant wild-type FIX (WT), FIX/FVII chimeras (C1, C2, C3, and C4), and FIX in which Gla-domain residues 1–46 are changed to the FVII sequence (FIX/FVII-Gla [VIIGla]). The weaker band running underneath FIX C3 is contaminating bovine serum albumin from conditioned media. **(C, D)** FXIa (2 nM) was incubated with 250 nM FIX-WT (○), C1 (●), C2 (□), C3 (■), C4 (Δ) and FIX/VII-Gla (▲) (250 nM) in Assay Buffer with Ca2+, as described in methods. Shown are concentrations of **(C)** FIXaβ and **(D)** FIXα at various times as determined by densitometry of SDS–polyacrylamide gels.

2003) or protein C (Ndonwi *et al.*, 2007) results in loss of FIX binding to FXIa, and that a monoclonal antibody to FIX (IgG SB 249417) that binds to FIX Gla domain inhibits FIX activation and causes significant FIXα accumulation (Figure 6-3G) (Aktimur *et al.*, 2003).

These observations suggest that a structural element specific to the FIX Gla-domain mediates binding to FXIa. The primary sequences of the human FIX and FVII

Gla-domains are compared in Figure 6-4A. Based on the comparison, FIX/VII chimeras (designated C1 to C4) were prepared in which three to five residues of sequence within the FIX Gla-domain were replaced with FVII sequence (Figure 6-4 A and B). As reported, FXIa activated FIX with a FVII Gla domain significantly more slowly than FIX-WT (Figure 6-4C), with substantial accumulation of FIXα (Figure 6-4D) (Aktimur *et al.*, 2003). FIX-WT and chimeras C2, C3, and C4 were converted to FIXaβ at roughly comparable rates (Figure 6-4 C and D), with little FIXα accumulation. However, chimera C1 demonstrated a pronounced defect in activation by FXIa with significant FIXα accumulation, similar to what is observed during FIX activation by FXIa-Ala$^{183\text{-}185}$. In binding studies using surface plasmon resonance, C1 demonstrated a major defect in binding to immobilized FXIa (K_d >2000 nM), compared to FIX-WT (K_d 350 nM) and chimeras C2 (K_d 400 nM) and C4 (K_d 350 nM). There was insufficient chimera C3 to conduct an SPR study.

The substitutions in chimera C1 are in the Ω-loop of the Gla-domain (Vadivel *et al.*, 2012)**,** as shown in the topology image of the human factor IX Gla-domain in Figure 6-5. This structure, reported by Huang *et al.*, is for the Gla-domain in complex with the conformation-specific anti-FIX IgG 10C12 (Huang *et al.*, 2004). This region was previously reported to facilitate FIX binding to phosphatidylserine (PS)-rich surfaces in a Ca^{2+}-dependent manner through a combination of charged and hydrophobic interactions (Vadivel *et al.*, 2012). Similarly, the topography of the A3 domain in the vicinity of Arg^{184} suggests that FIX binding may involve charged and hydrophobic interactions as well. This would be consistent with the hypothesis that the phospholipid-binding Ω-loop within the FIX Gla-domain is the region required for FIX binding to FXIa. The interaction between

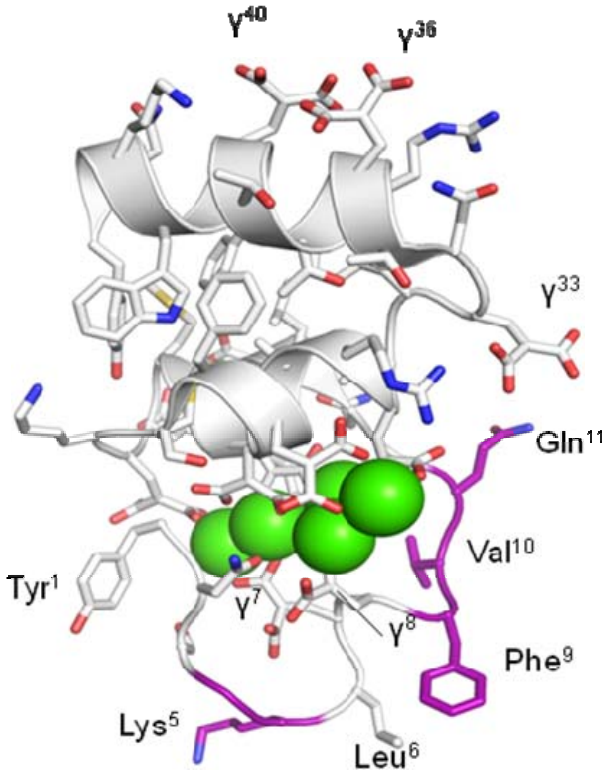

Figure 6-5. Topological diagram of the FIX Gla-domain. Shown is the Gla domain with residues in the Ω-loop (4–11) that differ from the corresponding region of the human FVII Gla-domain highlighted in magenta. The positions of certain Gla residues are indicated by the symbol 'γ'. Calcium ions in the vicinity of the Ω-loop are represented by green spheres. (Image courtesy of Dr .Jonas Emsley.)

the Gla domain of FIX and phospholipid surfaces enhances FIX activation by the FVIIa/tissue factor complex, and FX activation by FIXaβ, by reducing K_m for the reactions (Brummel-Ziedins *et al.*, 2012). Ca^{2+}-dependent binding of FIX to the FXIa A3 domain also determines K_m for FIX activation, suggesting the interaction serves a similar purpose to FIX binding to phospholipids during activation by FVIIa. Taken as a whole, the data presented in this chapter are consistent with a model in which residues in the Ω-loop of FIX and FIXα mediate Ca^{2+}-dependent binding to the FXIa A3 domain through interactions involving residues adjacent to a hydrophobic pocket formed by the N- and C- termini of A3.

Summary

Inspection of the FXI crystal structure suggests that FXI Arg^{184} and adjacent residues contribute to charged areas and hydrophobic pockets that are not present on the A3 domain of the homolog PK. Mutagenesis studies indicate that residues 183-185 at the N-terminus of A3 and residues 260-264 at the C-terminus are critical for formation of a binding site for FIX and its activation intermediate FIXα that are required for normal conversion of FIX to FIXaβ by FXIa. Replacement of FIX residues forming the Ω-loop of the Gla-domain (amino acids 4 to 11) with FVII sequence produced a defect in activation by FXIa-WT similar to the one observed with loss of the A3 domain exosite. This suggests that the FIX Ω-loop may mediate the interaction with the exosite on the FXIa A3 domain for proper activation of FIX by FXIa.

Methods

Recombinant Proteins. Recombinant FXIa was expressed as described in Chapter IV. In FXI-Ala$^{183\text{-}185}$ Ile^{183}, Arg^{184}, and Asp^{185} are replaced with alanine. In FXI/PKA3 the entire A3 domain (residues 182 to 265) is replaced with the PK A3 domain. Two modified forms of FXI/PKA3 were prepared. In FXI/PKA3-A, FXI sequence is restored at amino acids 183 to 185. In FXI/PKA3-B FXI sequence is restored at amino acids 183 to 185 and 260 to 264.

Recombinant FIX was expressed in HEK293 cells grown in media containing 10 μg/mL vitamin K1 (for proper γ-carboxylation of Gla domain). FIX was purified from conditioned media by antibody affinity chromatography (Aktimur *et al.*, 2003; Smith *et al.*, 2008). In addition to wild type FIX (FIX-WT), four FIX chimeric proteins were prepared

in which Gla-domain residues are replaced with corresponding residues from human FVII (C1 – residues 4, 5, 9, 10 and 11; C2 – 13, 19 and 22; C3 – 30, 32, 33, and 34; and C4 – 41, 43, 44, and 46).

The methods for FIX activation by FXIa and surface plasmon resonance were performed as described in Chapter IV.

References

Aktimur, A., Gabriel, M. A., Gailani, D., and Toomey, J. R. (2003) The factor IX γ-carboxyglutamic acid (Gla) domain is involved in interactions between factor IX and factor XIa. J Biol Chem *278*, 7981–7987.

Baglia, F.A., Gailani, D., López, J.A., Walsh, P.N. (2004) Identification of a binding site for glycoprotein Ib-α in the Apple 3 domain of factor XI. J Biol Chem *279*, 45470-6.

Brummel-Ziedins, K., and Mann, K.G. (2012) Molecular basis of blood coagulation, In: Hematology: basic principles and practice, 6th Ed., Churchill Livingstone-Elsevier, Philadelphia, pp 1821-41

Emsley, J., McEwan, P.A., Gailani, D. (2010) Structure and function of factor XI. Blood *115*, 2569-2577.

Fujikawa, K., Chung, D.W., Hendrickson, L.E., Davie, E.W. (1986) Amino acid sequence of human factor XI, a blood coagulation factor with four tandem repeats that are highly homologous with plasma prekallikrein. Biochemistry *25*, 2417-24.

Hooley, E., McEwan, P.A., and Emsley, J. (2007) Molecular modeling of the prekallikrein structure provides insights into high-molecular-weight kininogen binding and zymogen activation. J Thromb Haemost *5*, 2461-2466.

Huang, M., Furie, B.C., Furie, B. (2004) Crystal structure of the calcium-stabilized human factor IX Gla domain bound to a conformation-specific anti-factor IX antibody. J Biol Chem *279*, 14338-46.

McMullen, B.A., Fujikawa, K., Davie, E.W. (1991) Location of the disulfide bonds in human coagulation factor XI: the presence of tandem apple domains. Biochemistry *30*, 2056-2060.

Ndonwi, M., Broze, G.J., Agah, S., Schmidt, A.E., Bajaj, S.P. (2007) Substitution of the Gla domain in factor X with that of protein C impairs its interaction with factor VIIa/tissue

factor: lack of comparable effect by similar substitution in factor IX. J Biol Chem *282*, 15632-44.

Papagrigoriou, E., McEwan, P.A., Walsh, P.N., and Emsley, J. (2006) Crystal structure of the factor XI zymogen reveals a pathway for transactivation. Nat Struct Mol Biol *13*, 557-558.

Ponczek, M.B., Gailani, D., Doolittle, R.F. (2008) Evolution of the contact phase of vertebrate blood coagulation. J Thromb Haemost *6*, 1876-1883.

Samuel, D., Cheng, H., Riley, P.W., Canutescu, A.A., Nagaswami, C., Weisel, J.W., Bu, Z., Walsh, P.N., and Roder, H. (2007) Solution structure of the A4 domain of factor XI sheds light on the mechanism of zymogen activation. Proc Natl Acad Sci USA *104*, 15693-15698.

Sun, M.F., Zhao, M., Gailani, D. (1999) Identification of amino acids in the factor XI apple 3 domain required for activation of factor IX. J Biol Chem *274*, 36373-8.

Vadivel, K., Schmidt, A.E., Marder, V.J., Krishnaswamy, S., Bajaj, S.P. (2012) Structure and function of vitamin K-dependent coagulation and anticoagulation proteins, In: Hemostasis and Thrombosis: basic principles and clinical practice, 6th Ed., Lippincott, Williams & Wilkins, Philadelphia, pp 208-32

Zhang, Z., Li, Y., Lin, B., Schroeder, M., Huang, B. (2011) Identification of cavities on protein surface using multiple computational approaches for drug binding site prediction. Bioinformatics *27*, 2083-8.

Zhao, M., Abdel-Razek, T., Sun, M.F., Gailani, D. (1998) Characterization of a heparin binding site on the heavy chain of factor XI. J Biol Chem *273*, 31153–9.

CHAPTER VII

THE DIMERIC STRUCTURE OF FACTOR XI AND ZYMOGEN ACTIVATION

FXI is a dimer in all mammals in which it has been studied (Ponczek *et al.*, 2008). This is an atypical structure for a trypsin-like enzyme, and unique among clotting proteases. That the dimeric structure is so highly conserved, and that its parent homolog (PK) is a monomer, implies that dimerization is critical for one or more specific aspects of FXI function. The FXIa substrate FIX must be cleaved at two sites to form the protease FIXaβ, raising the possibility that the two protease domains of a FXIa dimer facilitate FIX activation. However, work with 1/2-FXIa and monomeric FXIa showed that a single FXIa subunit is sufficient for FIX activation.

Like FXIa, granzyme A, a cell-death inducing protein secreted by cytotoxic T lymphocyte, is a homodimeric serine protease. In granzyme A, the dimeric interface forms a recognition site for macromolecular substrates (an exosite) that is not present in the protease monomer (Bell *et al.*, 2003). While this is not the case for FXIa activation of FIX, it is possible that the dimeric interface harbors, or helps to form, a binding site for FXI activating proteases or FXIa inhibitors. Supporting this hypothesis is an observation that FXI monomers are converted to FXIa significantly more slowly than FXI dimers (Wu *et al.*, 2008). This suggests that dimerization facilitates normal activation of FXI. Based on their observation, a *trans*-activation mechanism was proposed in which the activating protease (FXIIa, thrombin or FXIa) binds to one FXI subunit within a dimer while

activating the opposite subunit (Samuel *et al.*, 2007; Wu *et al.*, 2008). We questioned this hypothesis, as PK, the homolog of FXI, is a monomer and is effectively activated by FXIIa. We investigated the importance of the FXI dimer to protease activation, using forms of plasma FXI with one or two activated subunits, and recombinant dimeric and monomeric FXI.

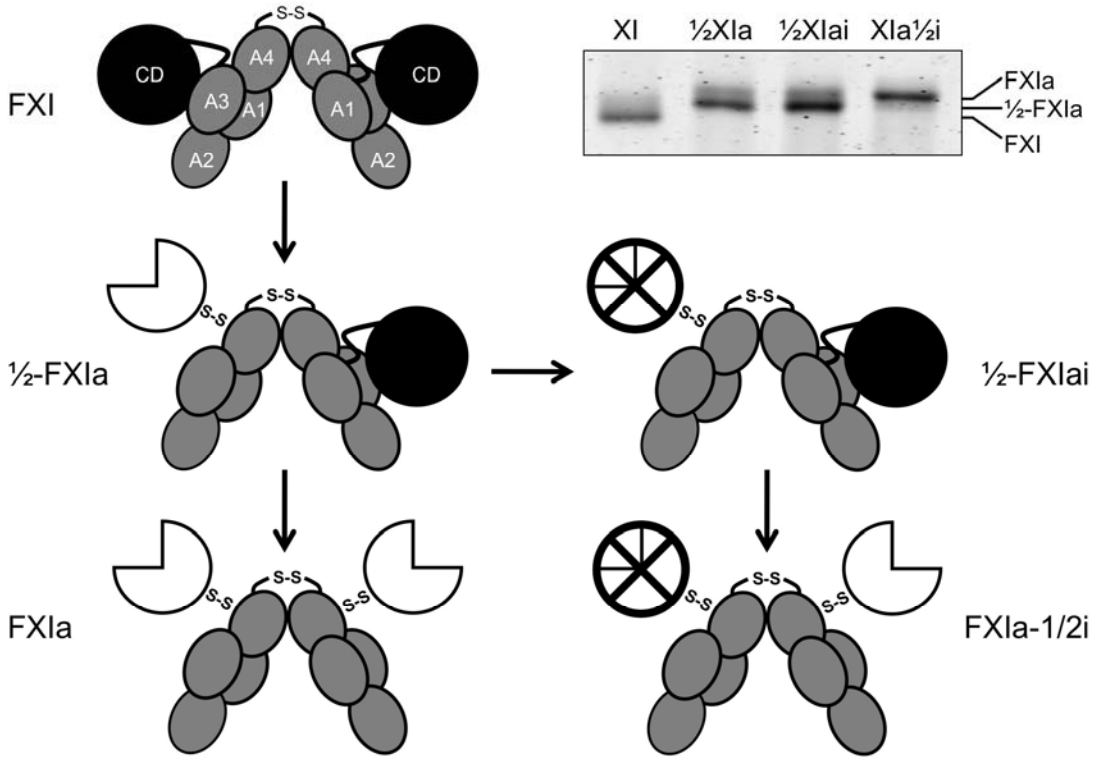

Figure 7-1. Schematic diagrams of species generated during FXI activation. The gray ellipses represent the 4 apple domains (A1–A4) and the black circles represent the catalytic domains (CD) of zymogen FXI. The 2 subunits of the FXI dimer are connected by a hydrophobic interface involving the A4 domains and a disulfide bond involving Cys^{321}. Activation of 1 FXI subunit by cleavage of the Arg^{369}-Ile^{370} bond results in a species with 1 active site, referred to as 1/2-FXIa. The white three-quarter circle represents the activated protease domain. Subsequent cleavage of the Arg^{369}-Ile^{370} bond on the second subunit results in generation of FXIa. FXI, 1/2-FXIa, and FXIa migrate slightly differently on SDS-PAGE (inset), facilitating their identification and purification. The preparation of 1/2-FXIa shown in the inset has approximately 10% contamination with FXIa (upper of the 2 bands). Inhibition of the active protease domain (⊗) of 1/2-FXIa yields a species called 1/2-FXIai. Activation of the second subunit of 1/2-FXIai results in a species with 2 activated subunits, 1 of which is inhibited called FXIa-1/2i.

Activation of Factor XI subunits

As described in Chapter II, activation of a FXI subunit involves cleavage of the Arg^{369}-Ile^{370} bond; a process that can be mediated by several proteases including FXIIa, various forms of thrombin, or trypsin. Previously, we showed that conversion of zymogen FXI (no activated subunits) to FXIa (two activated subunits) by FXIIa or α-thrombin proceeds through a form with only one activated subunit (1/2-FXIa) (Figure 7-1) (Smith *et al.*, 2008). 1/2-FXIa has identical activity on an active site basis to FXIa in terms of its ability to activate FIX and to induce clot formation in plasma. Because activated FXIa only requires one activated subunit to activate FIX, it is possible that a FXI subunit in each

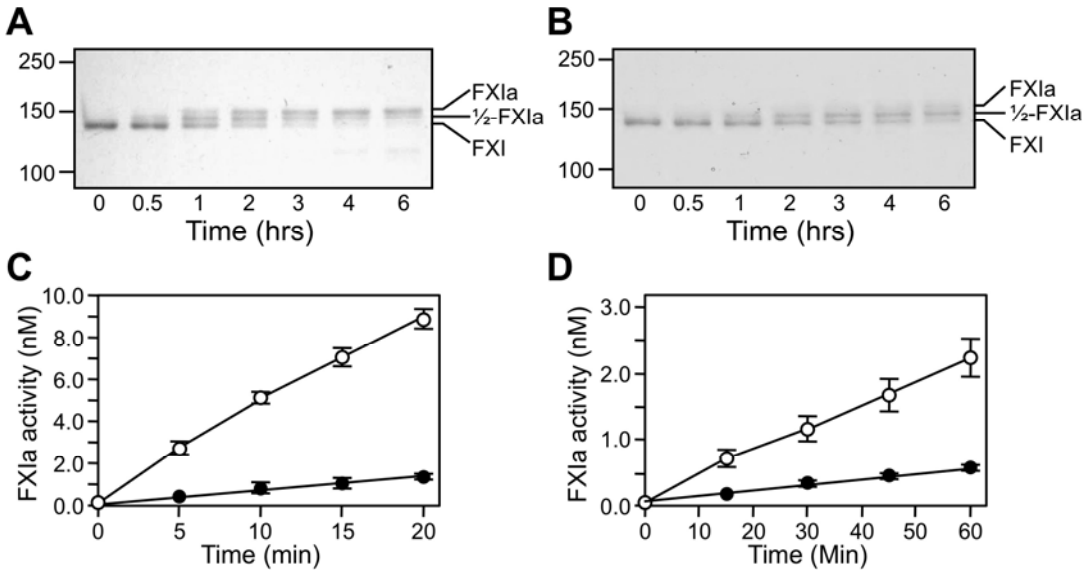

Figure 7-2. Activation of plasma FXI. (A and **B)** Plasma FXI (600nM) was incubated at 37 °C with **(A)** 60 nM FXIIa or **(B)** 600nM α-thrombin. Samples of each reaction were quenched in non-reducing sample buffer at the indicated times and size fractionated on 6% polyacrylamide-SDS gels. Positions for markers, and protein standards for factor XI (FXI), factor XIa (FXIa) and 1/2-FXIa are indicated. **(C** and **D)** Activation of 100 nM FXI (○) or 200 nM 1/2-FXIai (●) by (**C**) FXIIa (10 nM) or (**D**) α-thrombin (50 nM). At various times samples were tested for enzymatic activity by measuring cleavage of the chromogenic substrate S-2366 (500 μM) as described under Methods. Error bars represent one SD. The concentration of 1/2-FXIai was 200 nM in the activation assay to generate sufficient signal to detect in the chromogenic substrate assay. Reactions performed with 100 nM 1/2-FXIai would have slopes half as large as those for the progress curves shown.

dimer may have a function unrelated to catalysis, and that it may not need to be in an active conformation to perform that function.

There is little information available regarding generation of 1/2-FXIa or its conversion to FXIa. It is difficult to distinguish the singly activated species from FXIa during activation time course experiments because of their comparable molecular masses. FXI activation is thought to be accompanied by a significant conformational change in the activated subunit (Samuel *et al.*, 2007). Consistent with this, we noted that, 1/2-FXIa migrates slightly differently than FXI and FXIa (Figure 7-1 and 7-2) on non-reducing 6% SDS-PAGE, running in between the zymogen and fully activated species. FXI activation by FXIIa (Figure 7-2A) or α-thrombin (Figure 7-2B) is a slow process in the absence of a polyanion. With both proteases, 1/2-FXIa was noted to form prior to FXIa, and it appeared that conversion of FXI to 1/2-FXIa was a more rapid process than conversion of 1/2-FXIa to FXIa (Figure 7-2 A and B). Indeed, complete conversion of FXI to FXIa with α-thrombin is difficult to achieve, even with extended incubation.

The relative rates of activation of the two subunits of dimeric FXI were compared. Conversion of plasma FXI to 1/2-FXIa was studied by measuring reaction rates at early time points prior to the appearance of fully active FXIa (compare open circles in Figure 7-2 C and D). Activation of the first FXI subunit was 60-fold faster with FXIIa (15000 M^{-1} sec^{-1}) than with α-thrombin (250 M^{-1} sec^{-1}). Activation of the second FXI subunit (conversion of 1/2-FXIa to FXIa) was assessed using a preparation of purified 1/2-FXIa as substrate (Figure 7-1). 1/2-FXIa was produced by limited digestion of FXI with α-thrombin (Smith *et al.*, 2008). The reaction mixture, which contained a mixture of FXI and 1/2-FXIa, with a trace of FXIa, was applied to a benzamidine-Sepharose column.

1/2-FXIa bound to the column, while FXI passed through the column and appeared in the flow through. 1/2-FXIa was eluted from the resin with benzamidine. After purification, the active site of the activated subunit of 1/2-FXIa was irreversibly blocked by treatment with DIP (1/2-FXIai –Figure 7-1). This prevents this subunit from contributing to chromogenic substrate cleavage.

Cleavage of the unactivated subunit of 1/2-FXIai was 40-fold faster with FXIIa than with α-thrombin (1200M^{-1} sec^{-1} and 30 M^{-1} sec^{-1}, respectively). Cleavage of the first subunit was 12-fold faster than cleavage of the second subunit with FXIIa and 8- fold faster with α-thrombin (Compare closed circles to open circles in Figure 7-2 C and D), indicating that conformational changes accompanying activation of a subunit affect activation of the second subunit within a dimer.

Activation of monomeric FXI

The interface between FXI subunits has been discussed in detail in Chapter II. While Cys^{321} forms a disulfide bond connecting the A4 domains, FXI is a dimer even in the absence of this bond (Cheng *et al.*, 2003). Leu^{284}, Ile^{290}, and Tyr^{329} form the hydrophobic core of the dimer interface (Papagrigoriou *et al.*, 2006). We expressed FXI with Cys^{321} replaced by serine, with or without alanine replacement for Leu^{284} or Ile^{290}, as described by Wu *et al.* (Wu *et al.*, 2008). On nonreducing denatured SDS-PAGE, FXI-WT, as expected, is a 160-kDa dimer (Figure 7-3A), while FXI-Ser^{321}, FXI-Ser^{321},Ala^{284}, and FXI-Ser^{321},Ala^{290} migrate as 80-kDa monomers because they lack the Cys^{321}-Cys^{321} disulfide bond that connects the two subunits in FXI-WT. On size exclusion chromatography, the peak retention volumes for FXI-WT (11.7 mL) and FXI-Ser^{321}

(12.1 mL) are similar, indicating FXI-Ser^{321} is a non-covalently associated dimer despite lacking Cys^{321} (Figure 7-3B). In contrast, retention volumes for FXI-Ser^{321},Ala^{284} (13.5 mL) and FXI-Ser^{321},Ala^{290} (13.7 mL) are similar to PK (13.3 mL), the monomeric homolog of FXI (Figure 7-3C), consistent with these molecules existing largely in a monomeric state.

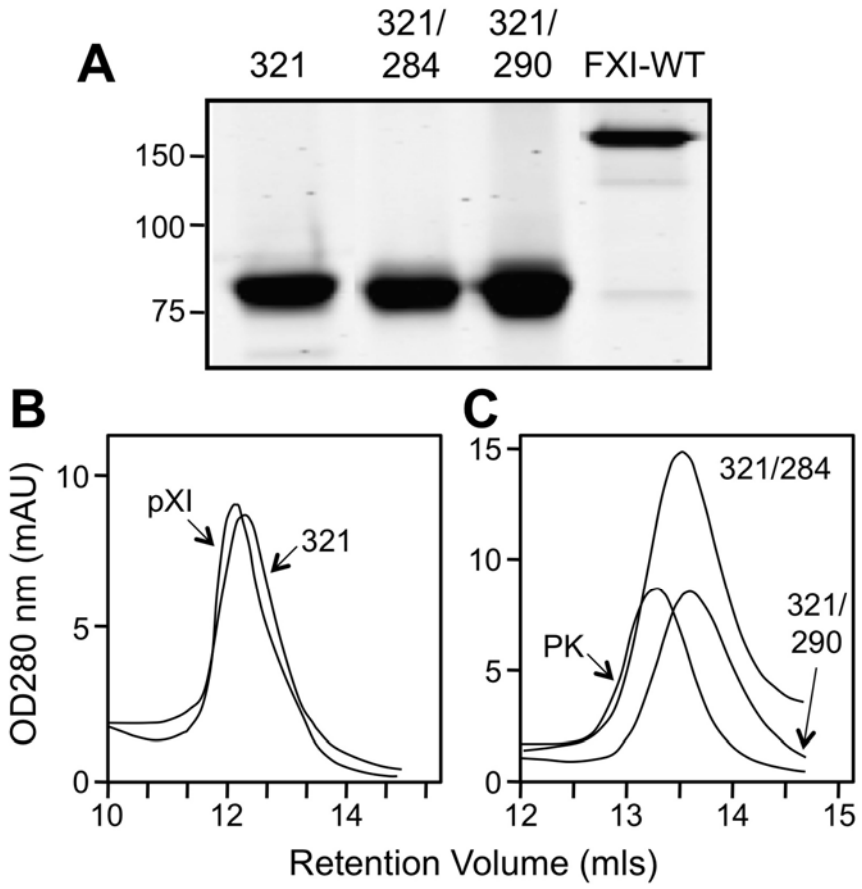

Figure 7-3. Recombinant FXI. (A) Recombinant FXI-Ser^{321} (321), FXI-Ser^{321},Ala^{284} (321/284) and FXI-Ser^{321},Ala^{290} (321/290) appear as 80 kDa monomers on 7.5% non-reducing SDS-PAGE because they lack the Cys^{321}-Cys^{321} inter-chain disulfide bond that connects the two subunits of the dimer in FXI-WT (160 kDa band at right). Positions of molecular mass standards (kDa) are indicated at the left of the panel. Size-exclusion chromatography of **(B)** plasma FXI (pXI) and FXI-Ser^{321} (321) or **(C)** FXI-Ser^{321},Ala^{284} (321/284) and FXI-Ser^{321},Ala^{290} (321/290) and plasma prekallikrein (PK). Shown are continuous readouts of optical density (280 nm) of solutions exiting a Superose-12 size exclusion column (flow rate 1.0 ml/min). Protein retention volumes in mls are indicated below the curves.

Activation of monomeric FXI in the absence of polyanions

Wu *et al*. showed that the monomeric FXI-Ser^{321},Ala^{284} and FXI-Ser^{321},Ala^{290} are activated more slowly than FXI-WT or FXI-Ser^{321} at low enzyme-to-substrate (E:S) ratios (Wu *et al.*, 2008). Consistent with this, we observed slower monomer activation by FXIIa at an E:S ratio of 1:20 (Figure 7-4A). However, this discrepancy became smaller as the E:S ratio increased, and disappeared at a E:S ratio of 1:1 (Figure 7-4 B-D). Rates of FXI-WT activation by FXIIa exhibited a linear dependence on FXIIa concentration up to 30 nM, consistent with a second-order rate constant of 14000 M^{-1} sec^{-1} for the FXI-WT dimer, which is in agreement with the value determined for conversion of plasma FXI to 1/2-FXIa. However, the rate with 100 nM FXIIa was approximately 2-fold higher than expected from the linear dependence, suggesting facilitated activation when FXIIa occupies both subunits. FXI monomers were poorer substrates at low FXIIa concentrations, but similar rates for monomer and dimer activation were observed with FXIIa >30 nM.

Modeling of FXI activation over a range of FXIIa concentrations suggests that FXI subunits harbor two productive binding sites with different affinities for FXIIa. The lower-affinity site would be contained within a subunit, while a higher-affinity site may extend onto the neighboring subunit. This is supported by the higher FXI activation rates at 100 nM FXIIa than expected from the second-order rate constant calculated for activation by FXIIa at 5 to 30 nM. The behavior of the monomer at low FXIIa concentrations can be explained by absence of the higher-affinity site. As FXIIa concentration increases, the low-affinity sites common to monomers and dimers are saturated, resulting in comparable activation rates.

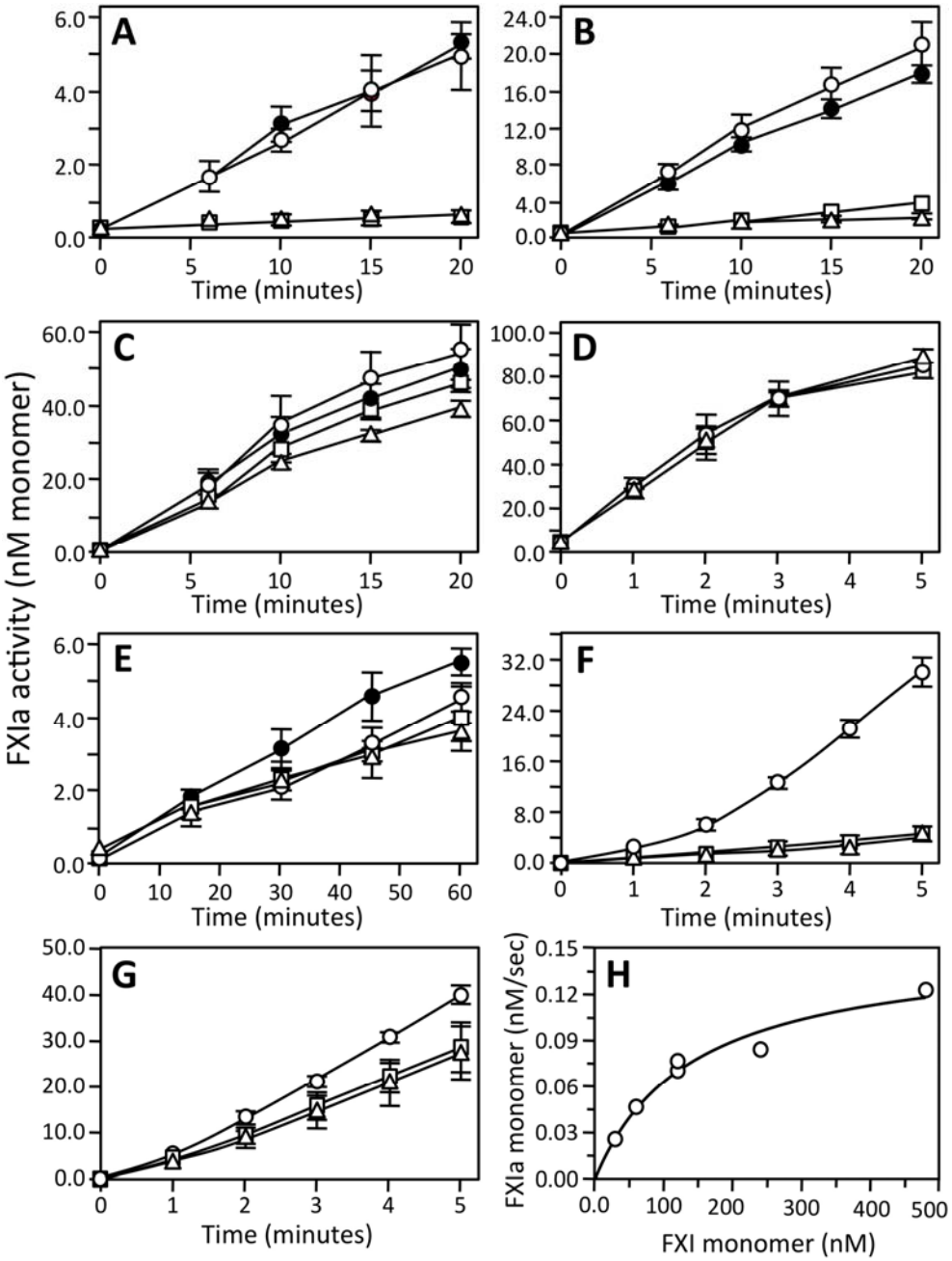

Figure 7-4. Activation of FXI. A-D. FXI-WT (○), FXI-Ser^{321} (●), FXI-Ser^{321},Ala^{284} (□), or FXI-Ser^{321},Ala^{290} (△), 200 nM subunits for each protein, were incubated with FXIIa at **(A)** 5 nM, **(B)** 10nM, **(C)** 30 nM, or **(D)** 100 nM concentration. **(E)** FXI species in panels A-D (200 nM subunits) activated by 50 nM α-thrombin. **F-G.** Activation of FXI-WT (○), FXI-Ser^{321},Ala^{284} (□) or FXI-Ser^{321},Ala^{290} (△), 120 nM subunits each incubated with **(F)** 3 nM FXIIa or **(G)** 3 nM α-thrombin in the presence of 50 nM poly-P. For panels A through G, samples of reactions were tested at various times for FXIa activity by measuring cleavage of S-2366 (500 μM). **Panel H.** Michaelis-Menten nonlinear least squares analysis of the substrate concentration dependence of FXI-WT subunit activation by 3 nM α-thrombin in the presence of 50 nM poly-P. For all panels, error bars show one standard deviation (SD).

In contrast to FXI activation by FXIIa, similar activation rates were observed for FXI dimers and monomers in reactions with α-thrombin (Figure 7-4E), indicating that catalytic efficiencies for activation of monomer and a subunit within a dimer are comparable. However, a relatively high E:S ratio (1:4) was required, as slow activation rates precluded studying the process at lower ratios.

Activation of monomeric FXI in the presence of polyanions

FXI activation can be accelerated by polyanions such as dextran sulfate (DS) (Gailani and Broze, 1991). Recently, Choi *et al.* showed that polyP released from platelet dense granules is a potent enhancer of FXI activation by thrombin and autoactivation, and is a strong candidate for a physiologic cofactor for FXI activation (Choi *et al.*, 2011). We examined FXI activation by FXIIa or α-thrombin in the presence of polyP with a size distribution comparable to platelet polyP. PolyP increased the initial rate of FXI activation by FXIIa approximately 30-fold (500,000 M^{-1} sec^{-1}, Figure 7-4F) and by α-thrombin approximately 3000-fold (700,000 M^{-1} sec^{-1}, Figure 7-4G) compared with reactions without polyP (Figure 7-4 A-E). Michaelis–Menten analysis of FXI-WT activation by thrombin with polyP gave a rate of ~700,000 M^{-1} sec^{-1} with k_{cat} 0.05 ± 0.01 s^{-1} and K_m 70 ± 10 nM FXI dimer (Figure 7-4H). During the reactions, a mixture of 1/2-FXIa and FXIa is formed, and it is likely that modest FXI activation by these proteases (autoactivation) is responsible for the curvature of some time courses (Figure 7-4 G and H).

We noted that the defect in FXIIa-mediated activation of FXI monomers in the absence of a polyanion remained evident in the presence of polyP (Figure 7-4F). The results with polyP are also consistent with the premise that FXI does not need to be a dimer to be activated by thrombin. The latter observation seems to be incompatible with a

trans-activation mechanism based on an analysis of the crystal structure of zymogen FXI (Papagrigoriou *et al.*, 2006). It was proposed that the protease domain of FXI is interposed between a putative α-thrombin binding site on the A1 domain (Baglia *et al.*, 1996) and the activation cleavage site. It was predicted that this would interfere with a thrombin molecule that bound to a FXI subunit activating that same subunit. However, our results clearly show that any binding site for α-thrombin likely lies within the FXI subunit undergoing activation (*cis*-activation). The reason for the discrepancy between our data and the previously published work is not clear. One possibility is that a significant conformational change occurs in a FXI subunit upon initial binding of thrombin, rendering the activation cleavage site accessible to the protease. Alternatively, the proposed thrombin binding site on A1 may not be correct. Additional work with site-directed mutants may help clarify this situation.

Autoactivation of FXI

Polyanions, including DS and polyP, induce FXI activation in the absence of an activating protease. The process is probably initiated by traces of FXIa in FXI preparations and probably requires FXI and an activated FXI species to bind in proximity on the polyanion (a template mechanism). The process has been referred to as FXI autoactivation. The effect of DS on plasma FXI is shown in Figure 7-5A (open circles). After a lag phase in which 1/2-FXIa formation predominates, there is rapid conversion to FXIa (Figure 7-5B). Bands representing degradation products are observed on SDS-PAGE at later time points. It has been proposed that FXI autoactivation may involve an activated subunit in a dimer activating the other subunit within the same dimer (Wu *et al.*, 2010). We tested this

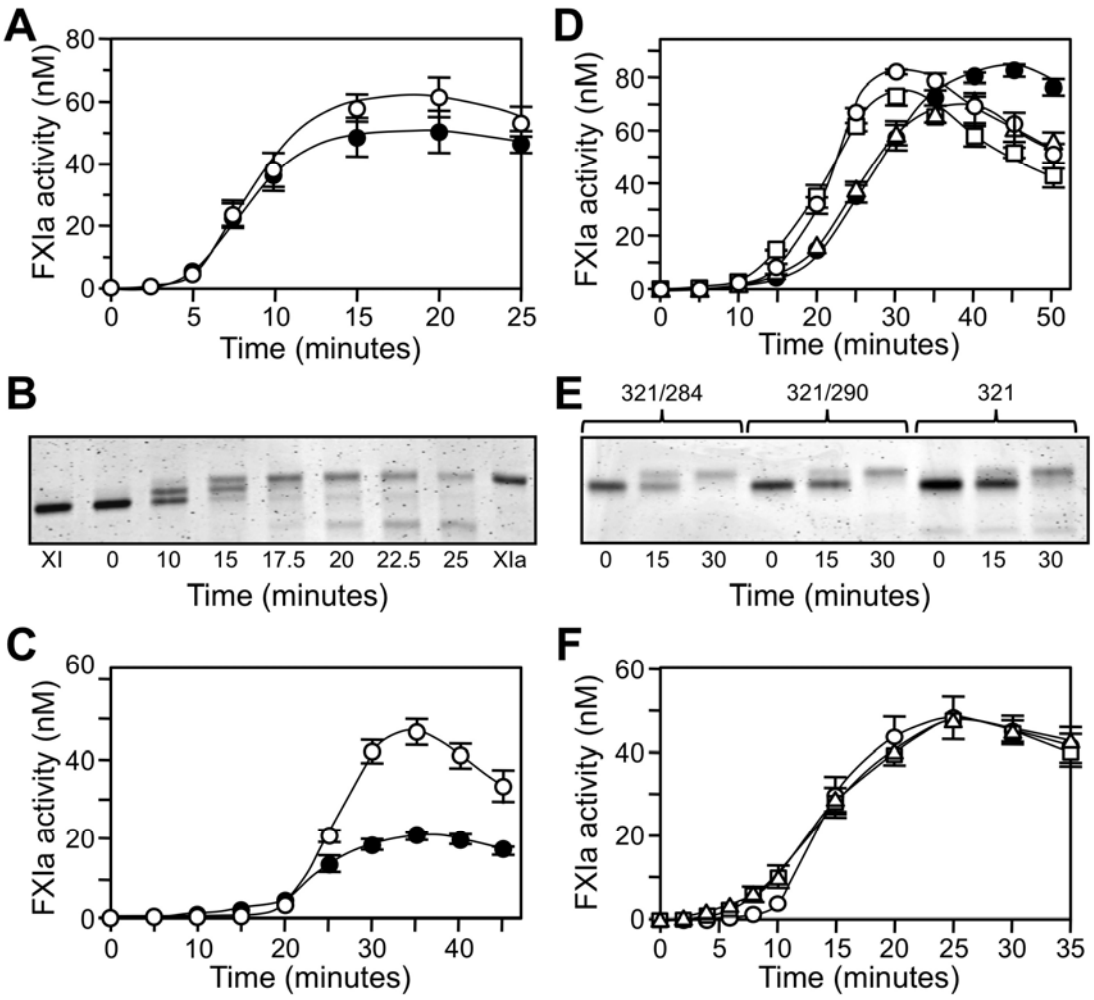

Figure 7-5. FXI autoactivation. (A) Plasma FXI (120 nM subunits) was incubated with 1 μg/ml DS (●) or 50 nM poly-P (○). At various times FXIa generation was determined by chromogenic substrate assay. **(B)** Plasma FXI (120 nM subunits) was incubated with 1 μg/ml DS. Samples were collected into non-reducing sample buffer at the indicated time points and size fractionated on 6% polyacrylamide gels, then stained with GelCode blue **(C)** 120 nM subunits of plasma FXI (○) or 1/2-FXIai (●) were incubated with 1 μg/ml dextran sulfate. At various times FXIa generation was determined chromogenic substrate assay. The FXI preparations in this panel were treated with DIP to inactivate contaminating FXIa, accounting for the longer lag phase compared to progress curves in panel A. **(D)** FXI-WT (○), FXI-Ser^{321} (●), FXI-Ser^{321},Ala^{284} (□) or FXI-Ser^{321},Ala^{290} (△), all 120 nM subunits, were incubated with 1 μg/ml dextran sulfate. At various times FXIa generation was determined by chromogenic substrate assay. **(E)** FXI-Ser^{321},Ala^{284} (321/284), FXI-Ser^{321},Ala^{290} (321/290) or FXIC^{321}S (321) 120 nM subunits was incubated with 1 μg/ml dextran sulfate. Samples were collected into non-reducing sample buffer at the indicated time points and size fractionated on 7.5% polyacrylamide gels, then stained with GelCode blue. **(F)** FXI-WT (○),FXI-Ser^{321},Ala^{284} (□) or FXI-Ser^{321},Ala^{290} (△), each at a concentration of 120 nM subunits, was incubated with 50 nM poly-P. At various times FXIa generation was determined. For all panels error bars represent one S.D.

hypothesis by comparing the effects of DS on activation of FXI and 1/2-FXIai. Intra-subunit activation shouldn't occur in 1/2-FXIai because its single activated subunit is irreversibly inhibited. In this study, FXI and 1/2-FXIai were treated with DIP to neutralize active subunits on contaminating FXIa. This likely accounts for the longer lag phases than those in Figure 7-5A. DS promoted autoactivation of the unactivated subunit of 1/2-FXIai in a similar manner to conversion of FXI to FXIa (Figure 7-5C). The amount of FXIa activity produced from 1/2-FXIai was half that generated from FXI, consistent with the difference in the maximum number of possible activated subunits. These data do not support the hypothesis that one activated FXI subunit in a dimer is required to activate the other subunit. Also, in contrast to published data suggesting that FXI monomers do not undergo autoactivation (Wu *et al.*, 2008), we observed comparable activation rates for FXI dimers (FXI-WT and FXI-Ser^{321}) and monomers (FXI-Ser^{321},Ala^{284} and FXI-Ser^{321},Ala^{290}) in the presence of DS (Figure 7-5D). The SDS-PAGE gel in Figure 7-5E shows changes in migration that occurred as zymogen monomer is activated. Note that there is no band representing an intermediate because the proteins are monomers.

While the polyanion DS is not a candidate for a physiologic cofactor for FXI activation, polyP is. In the presence of polyP, sigmoidal progress curves for FXIa generation were observed that are similar to those with dextran sulfate (Figure 7-5A, black circles). This is consistent with a template mechanism in which polyP enhances FXI activation by bringing an activating protease and the substrate into proximity, and perhaps by inducing conformational changes in the protease and/or substrate. The activation profiles for FXI-WT, FXI-Ser^{321},Ala^{284} and FXI-Ser^{321},Ala^{290} with polyP were comparable (Figure 7-5F). Furthermore, direct binding studies using SPR confirmed that FXI-Ser^{321},Ala^{284}

and FXI-Ser^{321},Ala^{290} bind to polyP with K_d of 25 to 50 nM (FXI-WT K_d 5–25 nM). These results support the conclusion that the capacity to undergo polyanion-induced autoactivation is intrinsic to a FXI subunit, and does not require the dimeric conformation.

Results of our *in vitro* analysis with polyP support the *trans*-activation hypothesis for FXI activation by FXIIa, but not for activation by thrombin or FXIa. The discrepancy between our data and the published work of Wu *et al.* showing defective monomer activation regardless of the activating protease may partly reflect functionally important differences between polyP (a linear molecule), and DS (a complex branched polymer of sulfated sugar residues). However, this does not completely explain the disparate results. In our study, FXI need not be a dimer to undergo autoactivation with DS or polyP. Our data indicate that FXI must be a dimer for normal activation by FXIIa in the presence or absence of a polyanion, but need not be a dimer for activation by thrombin. This points to different activation mechanisms for the two proteases.

Monomeric FXI in Blood Coagulation

Our *in vitro* data indicate that the dimeric structure of FXI is important for proper activation by FXIIa. We tested this hypothesis in a plasma-based system and in animal models. Obviously, as the complexity of the experimental system increases, our ability to account for all reactions and interactions involving the molecules of interest decreases (*e.g.* polyP has multiple effects on various coagulation factors and the fibrinolytic system). Therefore, we cannot attach direct causality from what is concluded in the purified system to the *in vivo* study. However, a consistency between *in vitro* and *in vivo* studies would support our predictions for mechanisms of FXI activation.

FXI monomers in FXI-dependent plasma coagulation

The aPTT assay, which uses a non-physiologic trigger such as silica to initiate FXII activation, is widely used in clinical practice to test the integrity of the intrinsic pathway of coagulation. As Wu *et al.* observed, the monomeric FXI species FXI-Ser^{321},Ala^{284} and FXI-Ser^{321},Ala^{290} have similar capacity (116% and 117% of the FXI-WT, respectively) to reconstitute clot formation when used to supplement FXI-deficient plasma in the aPTT (Figure 7-6A). Note that in the aPTT FXI is activated by FXIIa. As discussed above, we demonstrated that FXI monomers are activated slowly by FXIIa at low enzyme to substrate ratios. The normal activities of the monomers in the aPTT can be attributed to the high FXIIa concentration generated in aPTT assay, which would mask the monomer activation defect, as indicated by results in Figure 7-4D. If we dilute the silica activator to reduce FXIIa generation, we seen longer clotting times in plasma reconstituted with monomers compared to dimers (Figure 7-6B). We see similar results if we use polyP to initiate clotting in plasma. In addition to enhancing FXI activation, polyP, like silica, promotes FXII activation (Müller *et al.*, 2009). PolyP of 70 to 85 phosphate units is a relatively weak inducer of FXII activation. Similar to results with diluted PTT reagent, polyP-induced clot formation was slower in plasma containing FXI monomers than dimers (Figure 7-6C).

The effect of polyP on thrombin-mediated FXI activation was tested in plasma containing the FXIIa inhibitor corn trypsin inhibitor (CTI). Clotting was induced with β-thrombin (Matafonov *et al.*, 2011), a form of thrombin that converts fibrinogen to fibrin poorly due to disruption of anion-binding exosite I (Soslau *et al.*, 2004). As this exosite is not involved in FXI activation, β-thrombin and α-thrombin activate FXI similarly (Matafonov *et al.*, 2011). In the reactions shown in Figure 7-6D, β-thrombin activates FXI

bound to polyP, leading to α-thrombin generation from plasma prothrombin and clot formation. β-thrombin induced clot formation more rapidly in the presence of FXI-WT (~100 seconds) than in its absence (~750 seconds), confirming the system's FXI dependence (Figure 7-6D). FXI monomers and dimers support β-thrombin–initiated

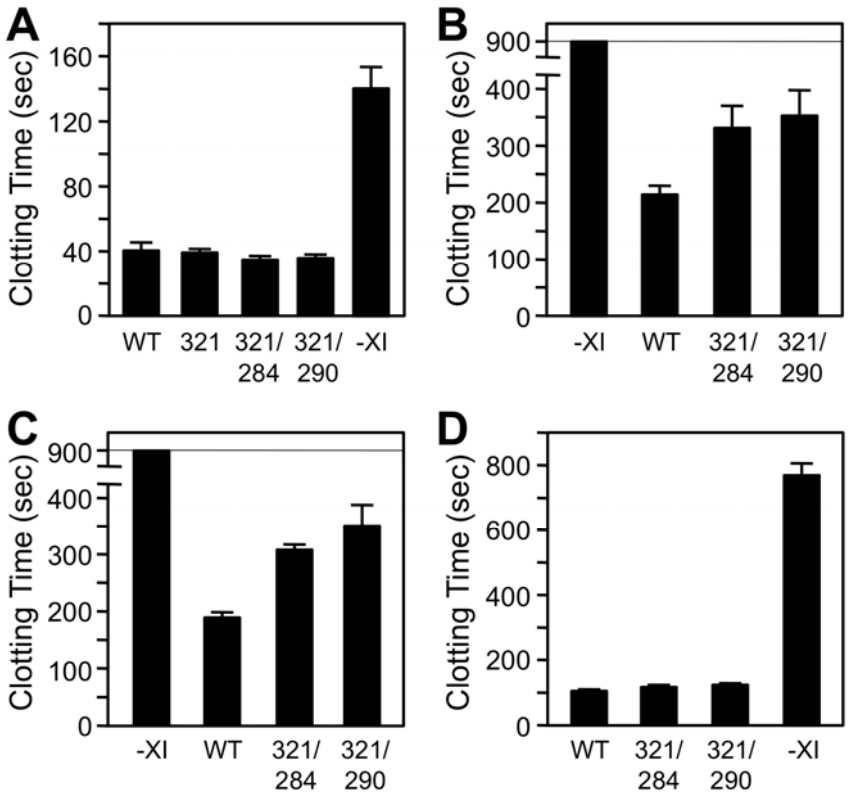

Figure 7-6. Plasma clotting assays. (A) FXI-WT (WT), FXI-Ser^{321} (321), FXI-Ser^{321},Ala^{284} (321/284), or FXI-Ser^{321},Ala^{290} (321/290) was added to FXI-deficient human plasma anticoagulated with 0.32% sodium citrate to a final concentration of 30 nM. –XI indicates vehicle treated control plasma. Plasma containing FXI (30 μL) was mixed with an equal volume of PTT reagent, followed by incubation for 5 minutes at 37°C. Thirty microliters of 25 mM $CaCl_2$ was added and time to fibrin clot formation was determined. Proteins were tested in triplicate. **(B-C)** FXI-deficient plasma-containing vehicle or 30 nM FXI-WT, FXI-Ser^{321},Ala^{284}, or FXI-Ser^{321},Ala^{290} supplemented with 60 μM PC–PS vesicles was incubated with **(B)** 30 μL 1:256 dilution of PTT-reagent or **(C)** 30 μL poly-P (final concentration 50 nM). Mixtures were incubated for 1 minute at 37°C before addition of $CaCl_2$ and measuring time to clot formation, as above. **(D)** FXI-deficient plasma containing 8 μM corn trypsin inhibitor (to inhibit FXIIa), 60 μM PC–PS vesicles, and 200 nM poly-P (final concentration 50 nM) was mixed with an equal volume of 30 nM FXI-WT, FXI-Ser^{321},Ala^{284}, or FXI-Ser^{321},Ala^{290}. β-thrombin was added to a final concentration of 1.5 nM, followed by incubation for 1 minute at 37°C. $CaCl_2$ was added and the time to clot formation was measured. For all panels, error bars represent 1 SD.

clotting similarly (Figure 7-6D), consistent with data in Figure 7-4G and in support of the hypothesis that FXI need not be a dimer for activation by thrombin in plasma in the presence of polyP.

FXI Monomers in a Model of Arterial Thrombosis

FXI deficient (FXI$^{-/-}$) mice are relatively resistant to injury-induced arterial thrombosis (Cheng *et al.*, 2010; Wang *et al.*, 2005), and infusion of human plasma-derived FXI into these animals restores the wild type phenotype in thrombosis models (Wang *et al.*, 2005). Several lines of evidence suggest that FXI is activated by FXIIa during these experimentally-induced thromboses in mice (Wang *et al.*, 2005; Cheng *et al.*, 2010). Physiologic counterparts to the non-biologic polyanions used *in vitro* have been proposed to be involved in the thrombotic process. In particular, polyP released from platelets appears to play a role (Müller *et al.*, 2009), possibly by activating FXII, and enhancing FXI activation. As the *in vitro* studies described above indicate that the dimeric structure of FXI is involved in activation by FXIIa, we postulated that FXI monomers would not reconstitute FXI$^{-/-}$ mice as well as dimeric FXI in a model of carotid artery thrombosis induced by application of concentrated ferric chloride to the exterior of the vessel (Wang *et al.*, 2005; Cheng *et al.*, 2010).

Recombinant FXI-WT expressed in HEK293 cells has a very short plasma half-life (<20 minutes) compared to human plasma FXI (> 3 hours) after infusion into mice, likely as a consequence of differences in glycosylation or other post-translational modifications. This makes it difficult to establish a stable plasma concentration of protein during the 45-minute time frame of the carotid artery thrombosis model. Instead, we transiently expressed human FXI-WT, FXI-Ser^{321},Ala^{284}, and FXI-Ser^{321},Ala^{290} in FXI$^{-/-}$

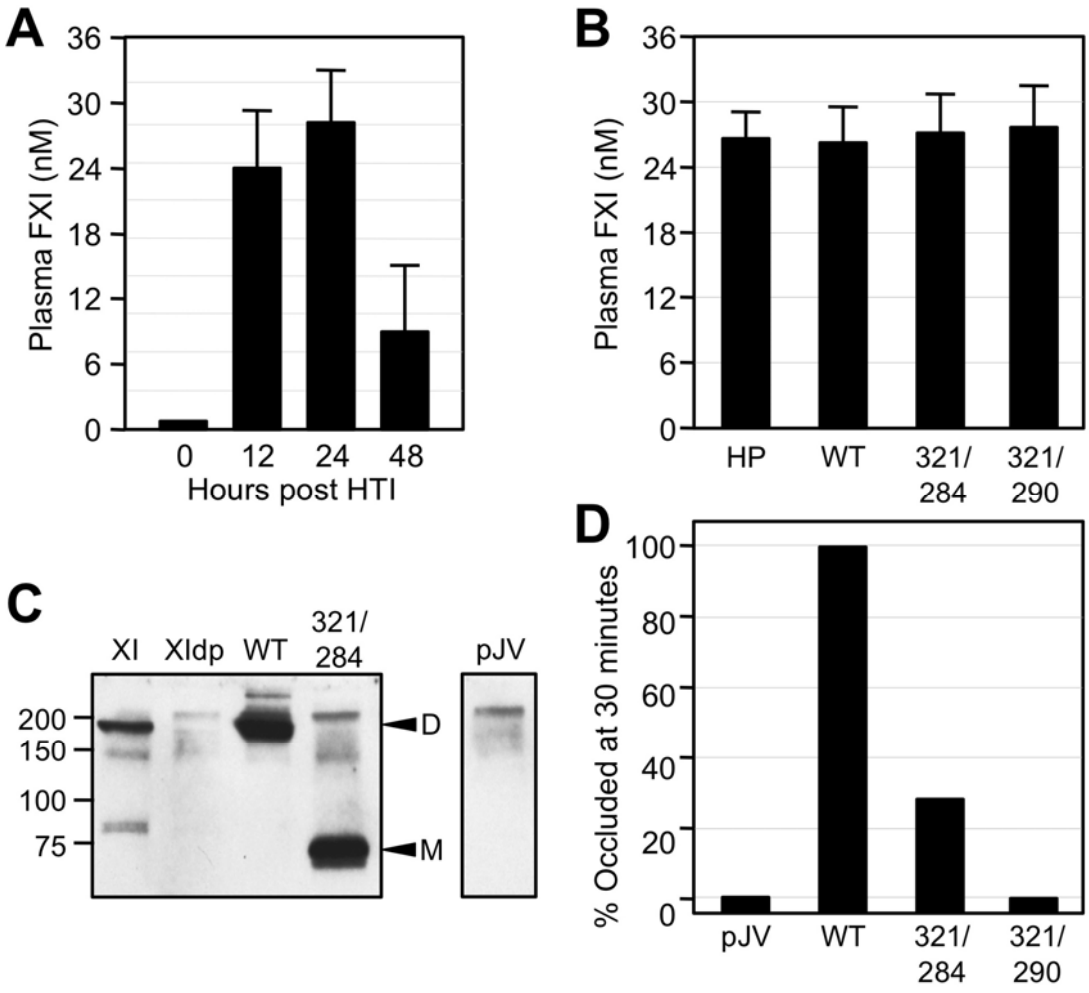

Figure 7-7. $FeCl_3$-induced carotid artery occlusion in FXI-deficient mice expressing human FXI. (A) FXI-/- mice underwent HTI with human FXI-WT cDNA in expression vector pJVCMV. Shown are concentrations of human FXI in mouse plasma at various times post-HTI. **(B)** Concentrations of FXI levels in plasma from FXI-/- mice 24 hours post-HTI with constructs for human FXI-WT (WT), FXI-Ser^{321},Ala^{284} (321/284), or FXI-Ser^{321},Ala^{290} (321/290). Normal human plasma is shown for comparison. For panels A and B, error bars represent 1 standard deviation. **(C)** Western blot of mouse plasmas 24 hours post-HTI with constructs for human FXI-WT, FXI-Ser^{321},Ala^{284}, or empty vector control (pJV). A sample of pure human FXI (XI) and a sample of FXI-deficient mouse plasma (XIdp) are shown for comparison. Positions of molecular mass standard (kDa) are shown at the left of the blot. Positions for FXI dimer (D) and monomer (M) are indicated on the right. **(D)** Groups of 10 FXI-/- mice underwent HTI with constructs for FXI-WT, FXI-Ser^{321},Ala^{284}, FXI-Ser^{321},Ala^{290}, or empty vector control (pJV). Twenty-four hours later, the animals were tested in a carotid artery thrombosis model in which thrombus formation is induced by exposing the vessel to 3.5% $FeCl_3$. Each bar indicates the percent of mice in each group with occluded arteries 30 minutes after applying $FeCl_3$. Plasma FXI levels of the mice in this study are shown in panel B.

mice using the technique of hydrodynamic tail-vein injection (HTI) (Liu *et al.*, 1999; Zhang *et al.*, 1999; Sebesty´en *et al.*, 2006). Here, the cDNA constructs used to express protein in HEK293 cells are rapidly infused into the tail vein of the mouse in a large volume of fluid (2 mL of lactated Ringer solution). The process results in swelling of the liver, and a transient transfection of hepatocytes (among other tissues) with the construct. Infusion of 15 μg FXI-WT construct into FXI$^{-/-}$ mice reproducibly results in expression of human FXI-WT reaching a peak 12-24 hours post DNA infusion (Figure 7-7A), with plasma concentrations comparable to the FXI level in normal human plasma (15-45 nM, avg. 30 nM; Figure 7-7B). Larger amounts of DNA did not result in a further increase in plasma levels, indicating a maximum expression level was reached with 15 μg of construct. Using this technique, peak plasma concentrations of FXI-Ser^{321},Ala^{284} and FXI-Ser^{321},Ala^{290} were achieved that were similar to those for FXI-WT (Figure 7-7B), consistent with the conclusion that the dimeric structure is not required for protein secretion (Wu *et al.*, 2008). Western blots of mouse plasma 24 hours post-infusion confirmed the presence of human FXI species of appropriate size (Figure 7-7C). The aPTTs of plasmas from mice expressing FXI-WT, FXI-Ser^{321},Ala^{284}, and FXI-Ser^{321},Ala^{290} (25–33 seconds) were similar to those of plasma from wild-type mice, and shorter than plasma from untreated FXI$^{-/-}$ mouse (>45 seconds).

Wild type C57Bl/6 mice consistently develop occlusive platelet-rich thrombi in the carotid arteries after the vessel is exposed to a 3.5% solution of $FeCl_3$, while FXI$^{-/-}$ mice do not form occlusive thrombi at this concentration. All FXI$^{-/-}$ mice expressing FXI-WT developed occlusion within 15 minutes of $FeCl_3$ exposure, consistent with experiments using infusions of human plasma FXI (Wang *et al.*, 2005). Mice treated with pJVCMV

control (no FXI cDNA) remained resistant to thrombus formation (Figure 7-7D). Interestingly, arteries of 70% of FXI$^{-/-}$ mice expressing FXI-Ser^{321},Ala^{284} and 100% expressing FXI-Ser^{321},Ala^{290} remained patent (Figure 7-7D). These results demonstrate that FXI monomers can be synthesized and circulate *in vivo*. However, dimeric FXI, but not monomeric FXI, reconstitutes the wild-type phenotype in FXI$^{-/-}$ mice in a FXIIa-dependent thrombosis model, suggesting that the dimeric structure of FXI plays a role in FXIIa-dependent thrombosis.

The reason for the different capacities of FXI-Ser^{321},Ala^{284} and FXI-Ser^{321},Ala^{290} to support arterial thrombus formation after vessel injury with $FeCl_3$ (Figure 7-7D) may reflect subtle differences between the 2 proteins that are not obvious in *in vitro* assays. It is not surprising that a monomer would exhibit some activity in the thrombosis model, as the defect in FXIIa-mediated activation observed *in vitro*, while significant, is not total. Interestingly, FXI$^{-/-}$ mice expressed FXI dimers and monomers comparably. In the past, it was suspected that intracellular processing and secretion of FXI required dimerization. Meijers *et al.* noted that the FXI A4 domain mutation Phe^{283}Leu found in patients with FXI deficiency causes a partial defect in dimerization, with monomers retained within the transfected cells (Meijers *et al.*, 1992). Similar results were reported for the A4 mutation Glu^{350}Gly (FXI Nagoya III), which causes a severe dimerization defect (Kravtsov *et al.*, 2004). However, most missense mutations causing FXI deficiency result in poor protein secretion, regardless of the effect on dimer formation. Subsequent work with mutations targeting the FXI dimer interface, and the data presented here show that dimerization is not a prerequisite for protein secretion.

This study suggests that the dimeric structure of FXI is important for protease activity

in vivo, at least under the conditions of the model. Based on this, it is tempting to postulate that FXI dimerization is an adaptation to enhance zymogen activation. However, there are reasonable objections to this proposal. *In vitro*, FXI monomers were defective only when FXIIa was the activating protease. Given the absence of hemostatic abnormalities associated with FXII deficiency, there is no compelling evidence indicating FXI activation by FXIIa is required for hemostasis. Thrombin may be the more important FXI activator during hemostasis (Furie and Furie, 2009; Spronk *et al.*, 2009), while FXIIa may contribute to pathologic coagulation through FXI activation. PK is a monomer with a domain structure identical to that of FXI, and PK is efficiently activated by FXIIa *in vitro* (Gailani *et al.*, 2010). Reducing FXII expression in mice with antisense oligonucleotides results in decreased PK activation, indicating FXIIa activates PK *in vivo* (Revenko *et al.*, 2011). Cumulatively, these observations raise the possibility that aspects of protease function unrelated to zymogen activation drove the evolution of the FXI dimer. There is evidence that FXI needs to be dimeric to function properly in the presence of platelets. FXI may bind to a platelet through one subunit, while binding to its substrate factor IX through the other (Gailani *et al.*, 2001). In this scenario, the dimer may be an adaptation to facilitate proper protease localization and function in flowing blood.

Summary

During activation, FXI is initially converted to a species with one active subunit (1/2-FXIa). For both FXIIa and thrombin, the rate of conversion of FXI to 1/2-FXIa is 3-4 fold faster than conversion of 1/2-FXIa to XIa, indicating that 1/2-FXIa accumulates during coagulation and may be an important species. PolyP released from platelets can

enhance FXI activation. FXI monomers were activated more slowly than dimers by FXIIa in the presence of polyP. However, this defect was not observed when thrombin was the activating protease, nor during FXI autoactivation, suggesting that FXIIa and thrombin activate FXI by different mechanisms. Consistent with this, monomeric FXIs were defective in reconstituting FXII-initiated clot formation, while functioned normally in thrombin-initiated clot formation. Transient expression of human FXI in FXI$^{-/-}$ mice restores the wild type phenotype in a ferric chloride-induced carotid artery thrombosis model, but monomeric variants are defective in this model. These results indicate that the dimeric structure of FXI is required for proper activation by FXIIa, but not by thrombin or FXIa. This may contribute to a protective effect for thrombus formation *in vivo*.

Methods

Recombinant FXI. Recombinant FXI-WT, FXI with serine replacing Cys^{321} (FXI-Ser^{321}), or FXI-Ser^{321} with alanine replacing Leu^{284} or Ile^{290} (FXI-Ser^{321},Ala^{284}, FXI-Ser^{321},Ala^{290}) were expressed in HEK293 cells as described (Wu *et al.*, 2008). FXI was treated with 500 μM diisopropylfluorophosphate (DIP) to inhibit traces of FXIa, then dialysis into TBS. FXI (20 μg) was passed over a Superose-12 column equilibrated with 50 mM sodium phosphate, pH 7.4, 150mM NaCl (Cheng *et al.*, 2003). Retention volumes were compared with protein standards and with plasma FXI and PK. FXI binding to immobilized polyP was determined by SPR, as described in the published paper (Choi *et al.*, 2011).

Polyphosphate. Sodium phosphate glass from Sigma-Aldrich. PolyP (75 to 100 phosphate units) was prepared by gel electrophoresis, as described (Smith *et al.*, 2010), except that a

model 491 Prep cell (Biorad) was used for continuous elution electrophoresis. PolyP concentrations are given based on an average polymer of 80 phosphate units.

Plasma FXI and FXIa Species with one Active Site. FXI purified from human plasma (HP; 600 nM) was incubated with thrombin (900 nM) for 6 hours at 37°C. Reactions were terminated with 20 μM hirudin, applied onto a SBTI-agarose column, and eluted with TBS containing 200 mM benzamidine, 1 mM EDTA. Eluate contained 1/2-FXIa (Smith *et al.*, 2008). 1/2-FXIa (500 nM) in TBS was incubated with 500 μM DIP, irreversibly inhibiting the active site(s) of 1/2-FXIa and contaminating FXIa (confirmed by chromogenic substrate assay). The inhibited preparation is referred to as 1/2-FXIai.

FXI Activation. FXI (200 nM subunits [100 nM dimer]) was incubated with FXIIa (5 to 100 nM) or α-thrombin (50 nM) in 30 mM HEPES pH 7.4, and 50 mM NaCl with 0.1% BSA (HBSA) at 37°C. For FXI (120 nM subunits) activation in the presence of polyP (50 nM), 3 nM FXIIa, or α-thrombin was used. At various times, 1.5 μM corn trypsin inhibitor (FXIIa) or hirudin (α-thrombin) was added to aliquots to terminate activation, mixed with an equal volume of 1 mM S-2366. pNA generation was monitored at 405 nm, and activation rates were determined by linear regression of time dependences of FXIa active site generation. Second order rate constants k_{cat}/K_m ($M^{-1}s^{-1}$) were obtained by dividing initial rates (v_0) by protease and substrate concentrations and by measuring initial slopes of FXIIa or FXI concentration dependences of v_0. FXI-WT activation by FXIIa (5 to 100 nM) was modeled by numerical integration using KinTek Explorer version 2.5 software (Johnson *et al.*, 2009). For FXI-WT activation by thrombin in the presence of polyP, a FXI concentration dependence (30–480 nM subunits) was established to define the extent of saturation.

FXI autoactivation was induced by incubating FXI (120 nM subunits) with DS (1 μg/mL, 500,000 Da) or polyP (50 nM) in HBSA at 37°C. At various times, 18 μL samples were mixed with an equal volume of 1 mM S-2366, 4 μg/mL polybrene. Conversion of FXI to FXIa was followed by monitoring at a wavelength of 405 nm. FXI activation was also analyzed by SDS-PAGE. FXI (120 nM subunits) in HBS containing 1 mg/mL PEG 8000 was incubated at 37°C with 1 μg/mL DS. At various times, aliquots were removed and placed into nonreducing sample buffer, size-fractionated on 7.5% polyacrylamide-SDS gels, and stained with GelCode Blue (Pierce). Gels were imaged with an Odyssey infrared imaging system.

FXI Activity in Plasma. FXI-deficient plasma (30 μL, George King) was mixed with 30 μL FXI (0.3–30 nM) in TBSA. Contact activation was initiated with 30 μL PTT-A reagent (Diagnostica Stago, undiluted, or diluted 1:256 in TBSA with 60 μM phosphatidylcholine–phosphatidylserine [PC–PS] vesicles) or 200 nM polyP (with 60 μM PC–PS). After incubation at 37°C (5 min for PTT reagent, 1 min for 1:256 PTT reagent or polyP), 30 μL of 25 mM calcium chloride ($CaCl_2$) was added, and time to clot formation was determined on an ST4 fibrometer (Diagnostica Stago). In separate experiments, 30 μL FXI (5 μg/mL) in TBSA was mixed with equal volumes of FXI-deficient plasma containing 8 μM corn trypsin inhibitor, 60 μM PC–PS, and 200 nM polyP. β-thrombin (1.5 nM) was added and incubated for 1 min at 37°C. Clotting was initiated with 30 μL of 25 mM $CaCl_2$.

Expression of FXI in Mice by Hydrodynamic Tail-Vein Injection. The C57Bl/6 FXI–deficient ($FXI^{-/-}$) mice (24–27 g) were anesthetized with 50 mg/kg intraperitoneal pentobarbital. pJVCMV/FXI constructs (15 μg) in 2 mL lactated Ringer's solution were

infused over 20 sec into the tail vein. Plasma was prepared from 25 μL blood samples collected at various times post hydrodynamic tail-vein injection (HTI), and FXI concentration was determined by enzyme-linked immunosorbent assay (ELISA). Western blots of plasma FXI (1 μL per lane) were prepared using anti-FXI IgG 14E11 (Cheng *et al.*, 2010).

Carotid Artery Thrombosis Model. The FXI$^{-/-}$ mice underwent HTI with pJVCMV/FXI constructs. Twenty four hours post-HTI, mice were anesthetized, and the right common carotid artery was fitted with a Doppler flow probe (model 0.5 VB; Transonic System). Thrombus formation was induced by applying 3.5% ferric chloride ($FeCl_3$) to the artery, as described (Wang *et al.*, 2005; Cheng *et al.*, 2010) Flow was monitored for 30 minutes. After the experiment, blood was collected and plasma FXI concentration was determined by ELISA.

References

Baglia, F.A. and Walsh, P.N. (1996) A binding site for thrombin in the apple 1 domain of factor XI. J Biol Chem *271*, 3652-3658.

Bell, J.K., Goetz, D.H., Mahrus, S., Harris, J.L., Fletterick, R.J., Craik, C.S. (2003) The oligomeric structure of human granzyme A is a determinant of its extended substrate specificity. Nat Struct Biol *10*, 527-34.

Cheng, Q., Sun, M.F., Kravtsov, D.V., Aktimur, A., Gailani, D. (2003) Factor XI apple domains and protein dimerization. J Thromb Haemost *1*, 2340-2347.

Cheng, Q., Tucker, E.I., Pine, M.S., Sisler, I., Matafonov, A., Sun, M.F. White-Adams, T.C., Smith, S.A., Hanson, S.R., McCarty, O.J., Renné, T., Gruber, A., Gailani, D. (2010) A role for factor XIIa-mediated factor XI activation in thrombus formation *in vivo*. Blood *116*, 3981-3989.

Choi, S.H., Smith, S.A., Morrissey, J.H. (2011) Polyphosphate is a cofactor for the activation of factor XI by thrombin. Blood *118*, 6963-70.

Furie, B., and Furie, B.C. (2009) Molecular basis of blood coagulation. In: Hematology: Basic Principles and Practice. 5th ed. Philadelphia: Churchill Livingstone-Elsevier; pp1819-1836.

Gailani, D., and Broze, G.J. (1991) Factor XI activation in a revised model of blood coagulation. Science *253*, 909-912.

Gailani, D., Ho, D., Sun, M.F., Cheng, Q., Walsh, P.N. (2001) Model for a factor IX activation complex on blood platelets: dimeric conformation of factor XIa is essential. Blood *97*, 3117-3122.

Kravtsov, D.V., Wu, W., Meijers, J.C., Sun, M.F., Blinder, M.A., Dang, T.P., Wang, H., Gailani, D. (2004) Dominant factor XI deficiency caused by mutations in the factor XI catalytic domain. Blood *104*, 128-134.

Liu, F., Song, Y.K., Liu, D. (1999) Hydrodynamics-based transfection in animals by systemic administration of plasmid DNA. Gene Ther *6*, 1258-1266.

Matafonov, A., Sarilla, S., Sun, M.F., Sheehan, J.P., Serebrov, V., Verhamme, I.M., Gailani D. (2011) Activation of factor XI by products of prothrombin activation. Blood *118*, 437-445.

Meijers, J.C., Davie, E.W., Chung, D.W. (1992) Expression of human blood coagulation factor XI: characterization of the defect in factor XI type III deficiency. Blood *79*, 1435-1440.

Müller, F., Mutch, N.J., Schenk, W.A., Smith, S.A., Esterl, L., Spronk, H.M., Schmidbauer, S., Gahl, W.A., Morrissey, J.H., Renné, T. (2009) Platelet polyphosphates are proinflammatory and procoagulant mediators *in vivo*. Cell *139*, 1143-1156.

Papagrigoriou, E., McEwan, P.A., Walsh, P.N., and Emsley, J. (2006) Crystal structure of the factor XI zymogen reveals a pathway for transactivation. Nat Struct Mol Biol *13*, 557-558.

Ponczek, M.B., Gailani, D., Doolittle, R.F. (2008) Evolution of the contact phase of vertebrate blood coagulation. J Thromb Haemost *6*, 1876-1883.

Revenko, A.S., Gao, D., Crosby, J.R., Bhattacharjee, G., Zhao, C., May, C., Gailani, D., Monia, B.P., MacLeod, A.R. (2011) Selective depletion of plasma prekallikrein or coagulation factor XII inhibits thrombosis in mice without increased risk of bleeding. Blood *118*, 5302-5311.

Samuel, D., Cheng, H., Riley, P.W., Canutescu, A.A., Nagaswami, C., Weisel, J.W., Bu, Z., Walsh, P.N., and Roder, H. (2007) Solution structure of the A4 domain of factor XI sheds light on the mechanism of zymogen activation. Proc Natl Acad Sci USA *104*, 15693-15698.

Sebestyén, M.G., Budker, V.G., Budker, T., Subbotin, V.M., Zhang, G., Monahan, S.D., Lewis, D.L., Wong, S.C., Hagstrom, J.E., Wolff, J.A. (2006) Mechanism of plasmid delivery by hydrodynamic tail vein injection. I. Hepatocyte uptake of various molecules. J Gene Med *8*, 852-873.

Smith, S.B., Verhamme, I.M., Sun, M.F., Bock, P.E., Gailani, D. (2008) Characterization of novel forms of coagulation factor XIa: independence of factor XIa subunits in factor IX activation. J Biol Chem *283,* 6696-6705.

Soslau, G., Goldenberg, S.J., Class, R., Jameson, B. (2004) Differential activation and inhibition of human platelet thrombin receptors by structurally distinct α-, β- and γ-thrombin. Platelets *15*, 155-166.

Spronk, H.M.H., Wilhelm, S., Heemskerk, H. (2009) Feedback activation of factor XI by thrombin is essential for haemostasis *in vivo*. J Thromb Haemost *7*, Abstract PL-TU-003.

Wang, X., Cheng, Q., Xu, L., Feuerstein, G.Z., Hsu, M.Y., Smith, P.L., Seiffert, D.A., Schumacher, W.A., Ogletree, M.L., Gailani, D. (2005) Effects of factor IX or factor XI deficiency on ferric chloride-induced carotid artery occlusion in mice. J Thromb Haemost *3*, 695-702.

Wu, W., Roder, H., Walsh, P.N. (2010) Conformational changes facilitate FXI autoactivation to FXIa. Blood *116*. [Abstract 19]

Wu, W., Sinha, D., Shikov, S., Yip, C.K., Walz, T., Billings, P.C., Lear, J.D., Walsh, P.N. (2008) Factor XI homodimer structure is essential for normal proteolytic activation by factor XIIa, thrombin, and factor XIa. J Biol Chem *283*, 18655-18664.

Wu, W., Sinha, D., Shikov, S., Yip, C.K., Walz, T., Billings, P.C., Lear, J.D., Walsh, P.N. (2008) Factor XI homodimer structure is essential for normal proteolytic activation by factor XIIa, thrombin, and factor XIa. J Biol Chem *283*, 18655-18664.

Zhang, G., Budker, V., Wolff, J.A. (1999) High levels of foreign gene expression in hepatocytes after tail vein injections of naked plasmid DNA. Hum Gene Ther *10*, 1735-1737.

CHAPTER VIII

EXPRESSION OF FACTOR XI HETERODIMERS: A NOVEL APPROACH TO INVESTIGATING THE DIMERIC STRUCTURE

The preliminary work presented in this chapter will serve as the basis for future investigation into the functional significance of FXI's unique dimeric structure in flowing blood. FXI(a) is thought to bind to platelet receptors through the A2 and A3 domains. This interaction may be essential for keeping FXI localized to an injury site in flowing blood. Interestingly, binding sites for FIX and the platelet receptor GP Ibα are in proximity to each other on the A3 domain of FXI (Sun *et al.*, 1999; Baglia *et al.*, 1995), suggesting that a FXIa subunit could not bind to its substrate and the platelet surface simultaneously. We postulate that the dimeric structure may offer a solution to this conundrum. FXI could bind to the platelet through one subunit, while interacting with the substrate FIX through the other (Figure 8-1).

As discussed in the previous chapter, monomeric FXI is activated poorly by low concentrations of FXIIa, which may make interpretations of results in complex systems difficult. It has been observed that patients with a single allele coding for a non-secretable FXI variant can have a bleeding disorder inherited in a dominant manner because the product of this allele can form a heterodimer with normal FXI subunits, trapping them within cells (Kravtsov *et al.*, 2004). This inspired us to develop a new strategy to produce recombinant FXI carrying different mutations on each subunit (FXI heterodimers). Recombinant FXI heterodimers will be used in the future to test the hypothesis that one FXIa subunit binds to a surface while the other binds to FIX in flowing blood.

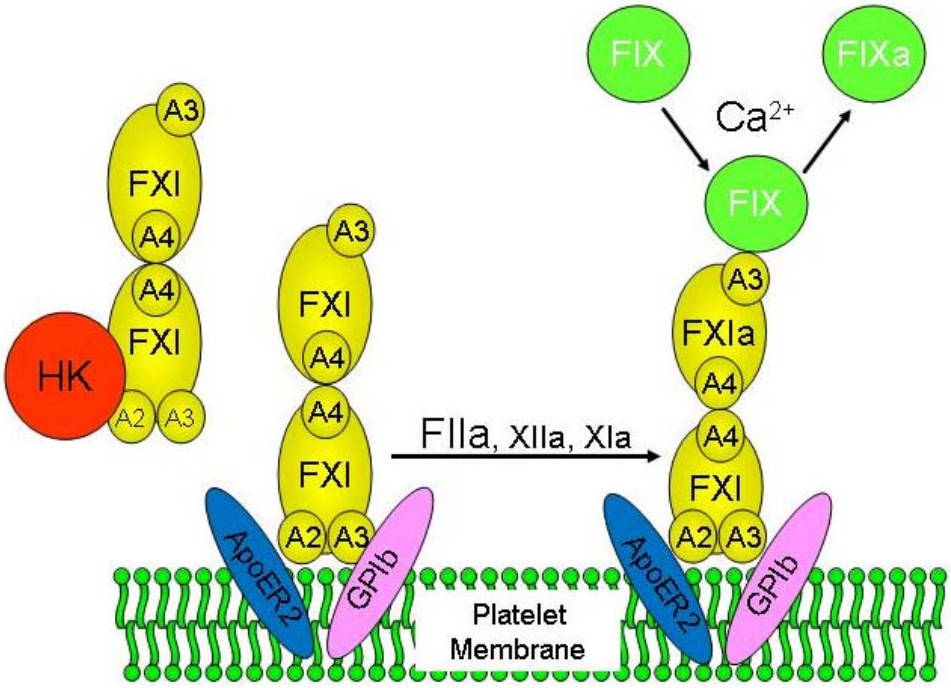

Figure 8-1 Postulated model of factor XI activity on the platelet surface. The FXI dimer binds to platelet GPIb and ApoER2 complex through A3 and A2, and becomes activated on the platelet surface. FXIa may then bind to FIX, possibly through the A3 domain that is not involved in binding to platelets, and converts FIX to FIXaβ.

Generation of a Factor XI Heterodimer with an Unactivatable Subunit

Purification of FXI heterodimers with different mutations on each subunit requires labeling one or each subunit with protein tags that enables the selection of heterodimeric FXI by sequential chromatography steps. As described in Chapter II, FXI has a relatively compact structure, and placing tags in FXI has a high chance of affecting apple domain folding, leading to abnormal structure and poor secretion. We chose a polyhistidine (polyHis) tag because of its relatively small size and charge. The polyHis tag can bind to metal ions such as Co^{2+} or Ni^{2+} immobilized on a matrix. The efficiency of this purification system is dependent on the length of the tag as well as the availability of the

tag on the protein surface. Usually a minimum of six histidine residues is required for optimal purification.

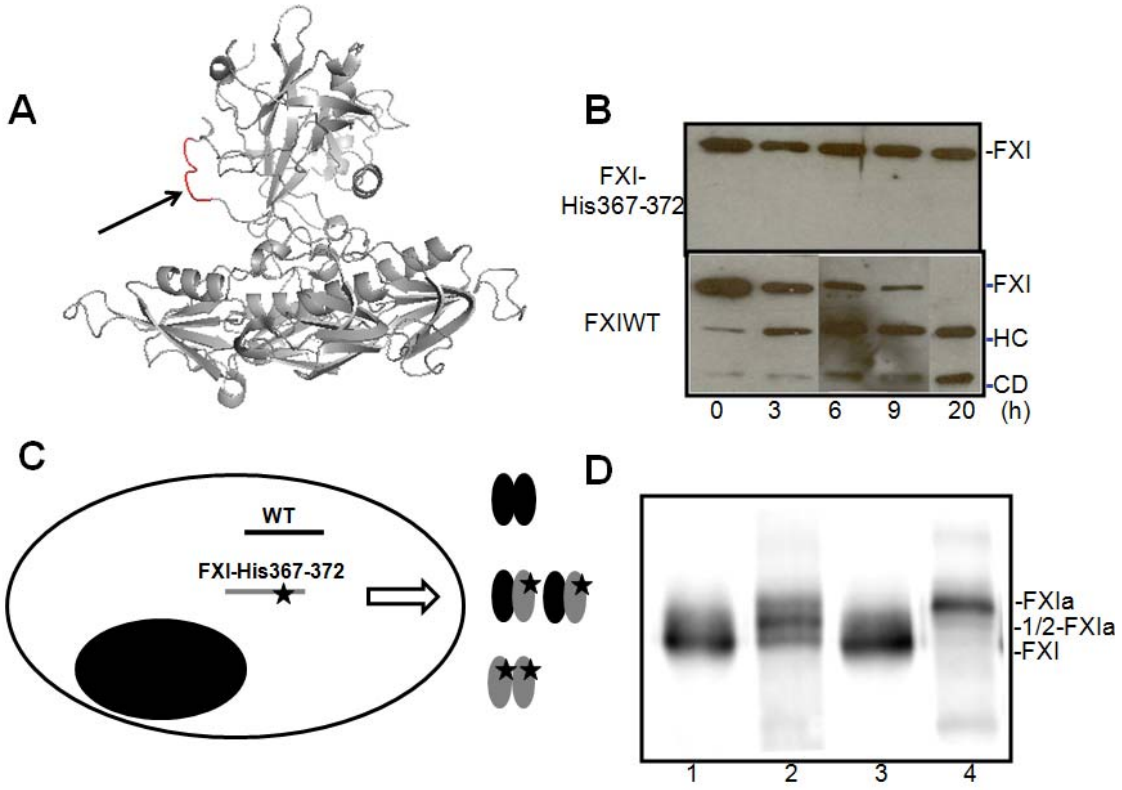

Figure 8-2. Preparation of FXI heterodimer. (A) Topology diagram showing FXI zymogen structure. Residues 367-372 that were changed to histidine are labeled in red (where the arrow points to). Note that this region is solvant-exposed and relatively flexible. **(B)** FXI-WT and FXI- FXI-His$^{367\text{-}372}$ (both 300nM) were activated by FXIIa (30nM). Aliquots were taken from the reaction mix at indicated times into reducing sample buffer, fractionated on 12% polyacrylamide-SDS gels, and analyzed by western blotting. **(C)** Schematic of the strategy for expression of FXI heterodimers. 293-6E cells were transfected with FXI-WT (WT, black line) and FXI- FXI-His$^{367\text{-}372}$ (grey line with star, star stands for the His-tag). Theoretically the cell will express FXI-WT, heterodimer, and homodimeric FXI-His$^{367\text{-}372}$ in a 1:2:1 ratio. **(D)** Conditioned medium containing FXI-WT homodimers, FXI His 367-372 homodimers and the heterodimers (lane 1) were activated by FXIIa overnight, and visualized by western blotting (lane 2). As a control, recombinant FXIa-WT expressed in conditioned medium under same conditions was also activated and shown on the blot (lane 3 and 4). Positions for standards for FXI zymogen, FXIa and the half activated heterodimer are shown to the right of the blot.

In the FXI crystal structure, the activation loop connecting the heavy chain and catalytic domain appears to have a relatively loose structure that is separate from the tightly packed apple domains and the catalytic domain (Figure 8-2A). This flexible loop is solvent exposed, and forms fewer interactions with other parts of the protein. A tag placed in this loop could be used to remove the activation cleavage site (Arg^{369}-Ile^{370}) rendering the subunit not activatable. We replaced FXI residues 367-372 on FXI with histidine to create the protein FXI-$His^{367-372}$. Since zymogen FXI will not bind to FIX, A FXI heterodimer with one subunit fixed in the zymogen state will be a useful tool to investigate the importance of dimeric structure in protease function.

FXI-$His^{367-372}$ homodimer (two unactivatable subunits in each FXI molecule) was expressed in HEK293 fibroblasts. The protein was expressed at a comparable level, and migrated at the same position on SDS-PAGE, as FXI-WT, indicating that the histine substitution did not disrupt overall protein conformation. As we predicted, reducing western blots of time courses of FXI-$His^{367-372}$ activation by FXIIa revealed dramatically impaired activation compared to FXI-WT (Figure 8-2B).

The FXI heterodimer with one wild type subunit and one subunit containing the His-tag at the activation loop was generated by co-expressing FXI-WT and FXI-$His^{367-372}$ cDNA in HEK293 cells. Most of the recombinant proteins in our lab are produced by cells stably transfected with vectors containing FXI cDNA, using resistance to a drug as a selection strategy. However, attempts to stably co-transfect HEK293 cells with equal amounts of vectors encoding two selection markers, or to transfect the cell line already stably expressing FXI-WT with FXI-$His^{367-372}$ cDNA, resulted in clones primarily expressing only one FXI variant. Based on the study by Kravtsov *et al.*, we decided to cotransfect

293-6E cells (293 cells growing in suspension to ensure high throughput protein production) with equal amounts of vectors containing a cDNA for FXI-WT or FXI-His$^{367\text{-}372}$ (Kravtsov *et al.*, 2004). Hypothetically, wild type and mutant FXI polypeptides should be synthesized in equal amounts. Therefore, wild type homodimer (both subunits can be activated), heterodimer (only the wild type subunit can be activated) and mutant homodimer (both subunits cannot be activated) should be produced and secreted into medium in a 1:2:1 ratio (Figure 8-2C). When conditioned medium containing a mixture of heterodimers and homodimers is fully activated by FXIIa, FXI-WT homodimer will be converted to FXIa, the heterodimer will be converted to ½-FXIa, and mutant homodimer will remain in the zymogen form. This was confirmed by western blotting on non-reducing PAGE in Figure 8-2D.

Labeling the C-terminus of Factor XI with a Polyhistidine-tag

Purification of FXI heterodimers with different mutations on each subunit requires labeling one or each subunit with different protein tags, enabling the selection of heterodimers by sequential chromatography steps. Labeling the activation loop results in an unactivatable FXI subunit. A different strategy is required for tagging a FXI subunit without interfering with FXI function. In the FXI crystal structure the C-terminus of the protein is a relatively flexible region that is surface exposed.

A FXI variant with six histidine residues added onto the C-terminus (FXI-His^{CT}) was expressed in 293-6E cells (HEK293 cells growing in suspension). FXI-His^{CT} was present in conditioned medium at a concentration of ~2 μg/mL. This is similar to the expression level of FXI-WT. On non-reducing SDS-PAGE, FXI-His^{CT} and FXI-WT migrate as 160

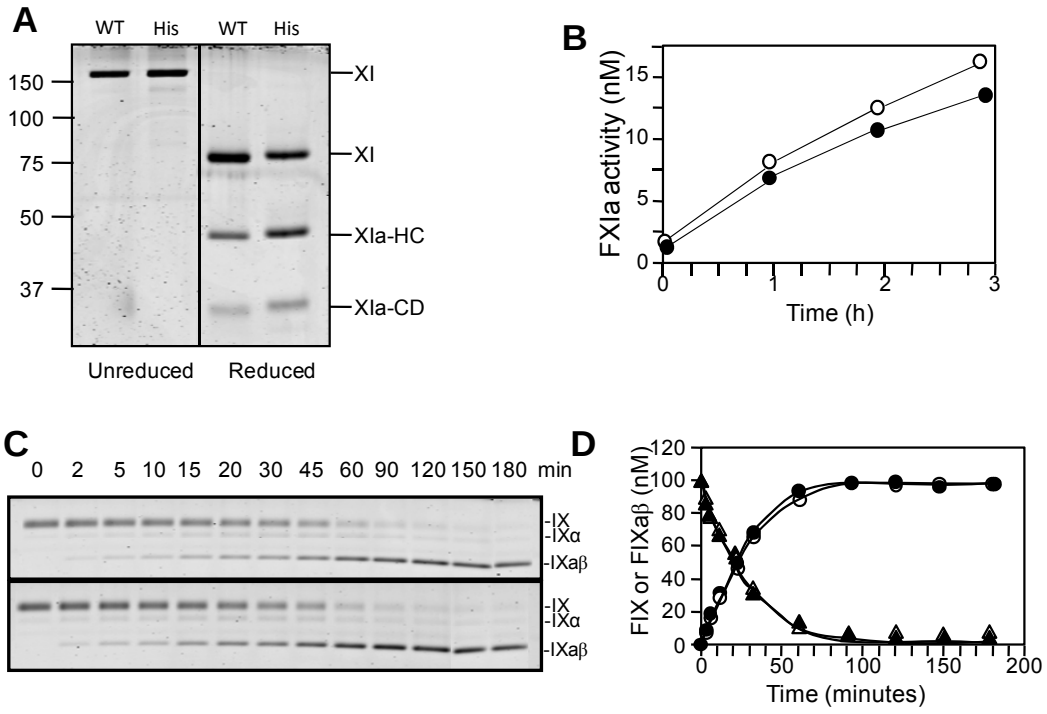

Figure 8-3. Characterization of FXI-His^{CT}. (A) Left: non-reducing SDS-PAGE of recombinant FXI-WT (WT) and FXI-His^{CT} (His) stained with GelCode blue. Right panel: reducing SDS-PAGE of the zymogen (FXI) and protease (FXIa) forms of the proteins in the left panel. The positions of FXI zymogen (XI) and the heavy chain (XIa-HC) and catalytic domain (XIa-CD) of FXIa are shown to the right of the panel. The positions of molecular mass standards for both gels are indicated on the left in kilodaltons.**(B)** 300 nM FXI-WT (○) and FXI-His^{CT} (●) were activated by 30 nM FXIIa, FXIa activity was determined by cleavage of S-2366. **(C and D)** FIX (100 nM) was activated by FXIa-WT (○) and FXI-His^{CT} (●) (2 nM active site). FIX and FIXaβ in the reaction mix were measured by the infrared intensity of corresponding bands on SDS-PAGE.

kDa proteins (Figure 8-3A). After complete activation, both proteases appear as a pair of 45 kDa and 35 kDa bands on reducing SDS-PAGE (Figure 8-3A). Attempts to put a His-tag at N-terminus of FXI resulted in low protein levels in the conditioned medium, and this strategy was not pursued further.

The protein with a C-terminal His-tag was added to FXI-deficient plasma and tested in an aPTT assay. FXI-His^{CT} had comparable activity to FXI-WT (clotting time 33.4 ± 0.85s

for FXI-WT, 34 ± 0.3s for FXI-His^{CT}). FXI-His^{CT} and FXI-WT were activated by FXIIa similarly (Figure 8-3B), and the activated proteases had similar capacities to cleave the tripeptide chromogenic substrate S-2366 (data not shown). In addition, FXIa-CTHis and FXIa-WT activated FIX with similar reaction rates and cleavage patterns (Figure 8-3 C and D). These findings indicate that attaching a small tag to the C-terminus of FXI can be done without compromising protease function. We are testing other small peptide tags (like FLAG and c-myc) in the same position.

The data discussed in this chapter provide a foundation for future development of a useful strategy for testing the dimeric structure of FXI. To test the hypothesis that FXI needs to be a dimer to simultaneously interact with the substrate FIX and platelets, FXI heterodimer with a wild type subunit and a subunit that lacks the capacity to bind to both FIX and a platelet will be expressed. We anticipate that such a heterodimer would fail to function in a FXI-dependent flow system if the dimer is required for simultaneous binding to platelets and FIX. The heterodimer should, however, function normally in a static plasma clotting assays such as the aPTT because the single wild type subunit would be sufficient to perform the required functions of the protein. A variety of FXI heterodimers with defects in various funcrtions can be created to facilitate investigation of the role of the FXI dimer in interactions with blood and blood vessel components.

Summary

While the results in Chapter VII indicate that the FXI dimeric structure is required for proper zymogen activation in some situations, the possibility that the dimer is an adaptation for binding to a surface and substrate simultaneously is an alternative

explanation that needs to be persued. We developed a strategy to express FXI heterodimers with different mutations on each subunit. Attaching a small tag to the C-terminus of FXI allows purification of heterodimers from homodimers. Utilizing this strategy, we will evaluate the importance of FXI's dimeric structure to thrombus formation in flowing blood in the future.

Methods

His-tag Fused FXI cDNA. Mutations to introduce a His-tag consisting of six histidine substitutions for FXI residues 367-372 (FXI-His$^{367\text{-}372}$) were introduced into the wild-type FXI in pJVCMV. In addition, six His residues were added to the C-terminus of FXI (FXI-His^{CT}).

Expression of FXI in Suspension. 293-6E human embryonic kidney cells were transfected with 19 μg FXI-His^{CT}, FXI-WT or FXI-His$^{367\text{-}372}$ in pJVCMV, together with 1 μg pEGFP vector. In the co-transfection assay, 293-6E cells were transfected with 9.5 μg FXI-His$^{367\text{-}372}$ and 9.5 μg FXI-WT, together with 1 μg pEGFP vector. Transfection complexes were generated by incubating vectors with 40 μg polyethyleneiminie (PEI) in 2 mL F17 medium for 10 minutes at room temperature. Cells were directly dispensed in 125 mL flasks at 1×10^6 cells/mL before transfection. Flasks were shaken constantly at 37°C in a 5% CO_2 incubator. Twenty-four hours following transfection the cells received a peptone feed of 0.5% TN-1. Cells were sampled for growth rate, viability and GFP expression daily. 120 hours after transfection, conditioned media was collected by centrifugation at 1500 g for 5 minutes, and stored at -20°C pending purification.

Purification of FXI-His^{CT} by Co^{2+}-Charged Affinity Resin. The conditioned medium

was passed over a 1 mL Co^{2+}-charged affinity resin column. After loading, the column was washed with 10 volumes of 50mM sodium phosphate (pH7.4), 100 mM NaCl, 5 mM Benzamidine (washing buffer), followed by elution with 150 mM Imidazole in washing buffer. Protein-containing fractions were pooled and concentrated in an ultra-filtration concentrator (Amicon, Inc, Beverly, MA), dialyzed against TBS, and stored at -80°C. Proteins were analyzed by SDS-polyacrylamide gel electrophoresis for purity, and protein concentration was measured by dye binding assay (Bio-rad). Activation of FXI by FXIIa, activation of plasma derived FIX by FXIa, and the coagulant activity of FXI in aPTT assay were performed as described in previous chapters.

References

Baglia, F., Jameson, B., Walsh, P. (1995) Identification and characterization of a binding site for platelets in the apple 3 domain of coagulation factor XI. J Biol Chem *270*, 6734-6740.

Kravtsov, D.V., Wu, W., Meijers, J.C., Sun, M.F., Blinder, M.A., Dang, T.P., Wang, H., Gailani, D. (2004) Dominant factor XI deficiency caused by mutations in the factor XI catalytic domain. Blood *104*, 128-134.

Rapaport, S., Proctor, R., Patch, M., Yettra, M. (1961) The mode of inheritance of PTA deficiency: evidence for the existence of major PTA deficiency and minor PTA deficiency. Blood *18*, 149-165.

Sun, M.F., Zhao, M., Gailani, D. (1999) Identification of amino acids in the factor XI apple 3 domain required for activation of factor IX. J Biol Chem *274*, 36373-8.

CHAPTER IX

FACTOR XI ANION-BINDING SITES ARE REQUIRED FOR PRODUCTIVE INTERACTIONS WITH POLYPHOSPHATE

The rates for FXI activation by FXIIa or thrombin are relatively low in solution, suggesting that a cofactor is required to enhance the rate of activation *in vivo*. Choi and coworkers demonstrated that polyP released from platelet dense granules enhance FXI activation by thrombin, and promote FXI activation by FXIa, through a mechanism requiring both activating protease and substrate to bind to polyP (Choi *et al.*, 2011). This is consistent with an observation made 40 years ago that activated platelets support FXI activation (Walsh, 1972). We subsequently showed that polyP enhances FXI activation by α-thrombin and FXIIa by ~3000 and ~30-fold respectively (in Chapter VII), further supporting the hypothesis that polyP is a physiologic enhancer of FXI activation.

PolyP in human platelets contain 60-100 phosphate groups, and have a number of procoagulant and pro-inflammatory properties (Müller *et al.*, 2009). Previous work indicates that a minimum polyP chain length is required to support FXI activation, consistent with the notion that a single polyP chain must be long enough to allow FXI and an activating protease to bind to it (Choi *et al.*, 2011). PolyP is highly negatively-charged, suggesting that it may interact with FXI through electrostatic interactions. Electrostatic interactations are also involved in FXI and FXIa binding to heparin (Zhao *et al.*, 1998; Yang *et al.*, 2009). Heparin enhances the inhibition of several coagulation proteases by the serpin antithrombin (AT) through allosteric and ternary (template) mechanisms (Tollefsen

and Zhang, 2013). The latter typically involve binding of the catalytic domain to heparin through electrostatic interactions involving a specific anion binding site (ABS) comprised of lysine and arginine residues (Vadivel *et al.*, 2012). The heparin binding site on α-thrombin is referred to as anion binding exosite II (ABE II), and is comprised of Arg^{89}, Arg^{98}, Arg^{245}, Lys^{248} and Lys^{252} (chymotrypsin numbering) (Sheehan and Sadler, 1994). The same site is involved in α-thrombin binding to polyP (Mutch *et al.*, 2010). In FXIa there is an ABS on the catalytic domain 170-loop containing residues Lys^{529}, Arg^{530} and Arg^{532} (Figure 2-6) (Yang *et al.*, 2009). In addition, FXIa has a novel ABS on its A3 domain (Arg^{250}, Lys^{252}, Lys^{253} and Lys^{255}) (Figure 2-6) (Zhao *et al.*, 1998). Both ABSs bind heparin, and both are required for full expression of heparin cofactor activity during AT inhibition of FXIa. The FXI homolog PK contains basic residues in the catalytic domain 170-loop in the same locations as in FXI (McMullen *et al.*, 1991), and heparin enhances AT inhibition of activated PK (α-kallikrein) (Venneröd and Laake, 1975). However, PK lacks the ABS on the A3 domain found in FXI, suggesting this feature supports specific FXI functions. In this chapter, experiments evaluating the importance of the FXI ABSs to the interaction with polyP are presented.

Activation of Factor XI in the Presence of Polyanions

We expressed and purified recombinant FXI-WT, FXI with alanine replacing Arg^{250}, Lys^{252}, Lys^{253} and Lys^{255} (FXI-ABS1), FXI with alanine replacing Lys^{529}, Arg^{530} and Arg^{532} (FXI-ABS2), or FXI with both sets of substitutions (FXI-ABS1/2) HEK293 cells. The proteins all migrate at the appropriate 160 (unreduced) and 80 (reduced) kDa positions on SDS-PAGE (Figure 9-1). After conversion to FXIa, the proteases cleave the substrate S-2366 with similar K_m and k_{cat} (not shown).

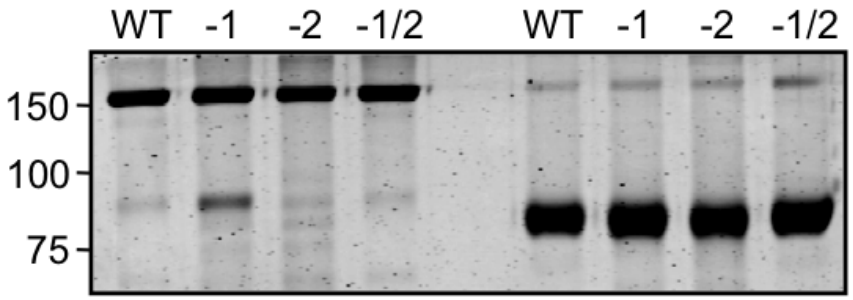

Figure 9-1. Recombinant FXI ABS mutants. Purified FXI-WT, FXI-ABS1 (-1), FXI-ABS2 (-2) and FXI-ABS1/2 (-1/2) run under non-reducing (left) and reducing (right) conditions on a 10% polyacrylamide-SDS gel. Positions of molecular mass standards in kilodaltons are on the left.

Factor XI Autoactivation

Dextran sulfate (DS), heparin and polyP induce FXI activation through a mechanism requiring FXI binding to the polyanion (Gailani and Broze, 1991; Choi *et al.*, 2011). As discussed in Chapter VII, a sigmoidal progress curve is observed during FXI activation induced by these polyanions (Figure 9-2). We suspect activation is initiated by traces of FXIa in the FXI preparations. Treating the preparations with DFP to inhibit contaminating FXIa can prolong the lag phase in the activation curve, but does not prevent activation.

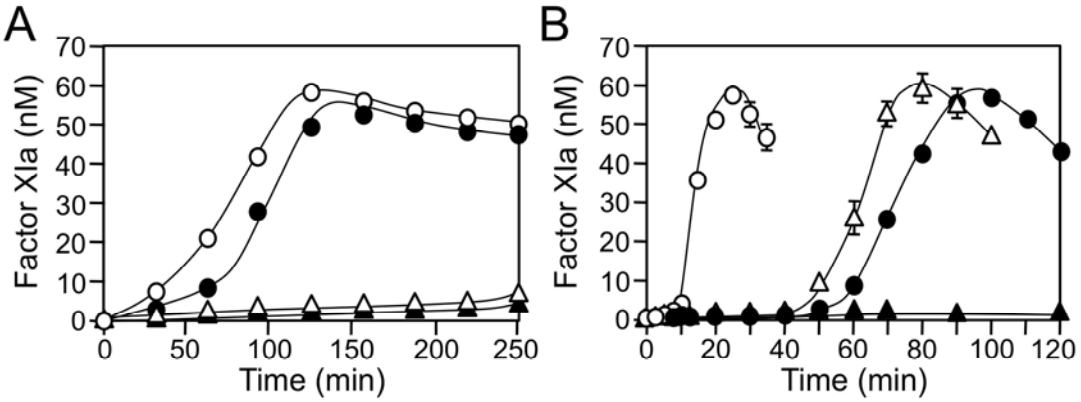

Figure 9-2. FXI activation in the presence of heparin or polyP. FXI-WT (○), FXI-ABS1 (△), FXI-ABS2 (●) or FXI-ABS1/2 (▲) incubated with **(A)** 400 nM heparin or **(B)** 50 nM polyP. FXIa generation was determined by chromogenic assay.

However, DFP-treated FXI preparations still cleave S-2366 at a low but detectable rate suggesting persistent FXIa contamination in the picomolar range for a solution of 100 nM FXI zymogen. In the presence of heparin, FXI-WT and FXI-ABS2 were activated similarly, while FXI-ABS1 and FXI-ABS1/2 demonstrated significant activation defects (Figure 9-2A). Comparable results were obtained with dextran sulfate (data not shown), indicating that the A3 domain ABS, but not the catalytic domain ABS, is required to support autoactivation induced by these polyanions. In reactions with polyP, in contrast, both FXI-ABS1 and FXI-ABS2 demonstrated longer lag phases than FXI-WT, while ABS-1/2 failed to activate (Figure 9-2B). This indicates that polyP must interact with both ABSs to promote optimal activation, and suggests that the autoactivation reactions differ in some way from those supported by heparin or DS.

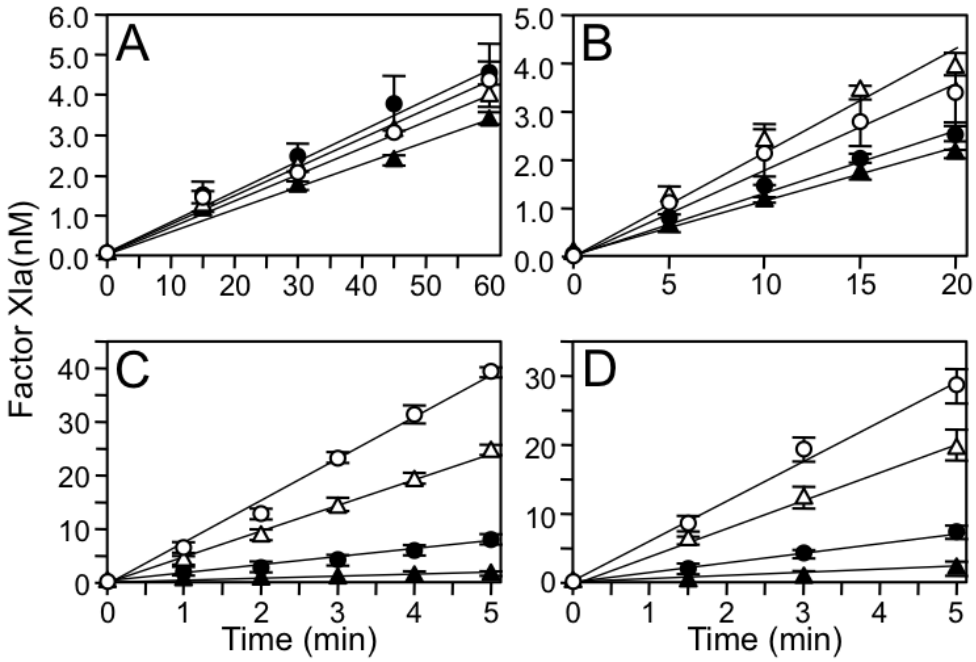

Figure 9-3. FXI activation by α-thrombin or FXIIa. (A and B) FXI-WT (○), FXI-ABS1 (△), FXI-ABS2 (●) or FXI-ABS1/2 (▲), 200 nM subunits, incubated with **(A)** 50 nM α-thrombin or **(B)** 5 nM FXIIa. **(C and D)** Activation of 120 nM subunit of FXI (symbols same as in panels A and B) by 3 nM **(C)** α-thrombin or **(D)** FXIIa in the presence of 50 nM polyP. FXIa generation was determined by chromogenic assay.

Factor XI Activation by Thrombin and FXIIa

Work presented in Chapter VII shows that FXI activation by thrombin and FXIIa is enhanced by polyP. To test the importance of the FXI ABSs in this process, we compared activation rates for FXI-WT and the FXI ABS mutants by thrombin and FXIIa. In the absence of polyP, second order rate constants for FXI-WT activation by α-thrombin (Figure 9-3A, 240 M^{-1} sec^{-1}) or FXIIa (Figure 9-3B, 16,600 M^{-1} sec^{-1}) were roughly comparable to those for FXI ABS mutants (Table 9-1). PolyP enhanced FXI-WT activation by α-thrombin ~3000-fold (Figure 9-3C, 713,000 M^{-1} sec^{-1}) and by FXIIa ~30-fold (Figure 9-3D, 543,000 M^{-1} sec^{-1}). Rates were moderately reduced for FXI-ABS1 activation by α-thrombin (34%) and FXIIa (42%). There were greater reductions for FXI-ABS2 (5-fold for α-thrombin, 3-fold for FXIIa). With FXI-ABS1/2, rate constants were ~20- and ~7-fold lower, respectively, demonstrating the importance of both FXI ABSs to polyP enhancement of FXI activation by these proteases.

Table 9-1. The effect of polyP on rates of FXI activation by thrombin and FXIIa.

Shown are second order rate constants derived from curves in figure 9-3 for activation of FXI by α-thrombin or FXIIa in the absence or presence of 50 nM polyP.

	α-Thrombin			FXIIa		
Protein	No PolyP	With PolyP	Fold-Increase	No PolyP	With PolyP	Fold-Increase
FXI-WT	240	714,000	2975	16,600	543,000	33
FXI-ABS1	230	450,000	1957	20,000	375,000	19
FXI-ABS2	270	153,000	567	12,100	135,000	11
FXI-ABS1/2	190	29,000	152	10,600	49,000	5

The activation rate of FXI was plotted against a range of polyP concentrations. PolyP-dependences of FXI activation by α-thrombin (Figure 9-4A) and FXIIa (Figure 9-4B) have bell-shaped distributions, with an optimal concentration of polyP for the maximal rate of enhancement. This is consistent with a template mechanism requiring protease and substrate to bind to polyP. To confirm this, we looked at FXI activation by a recombinant α-thrombin with residue 89 changed from Arg to Glu (rIIa^{R89E}). Residue 89 is part of the ABE II on thrombin, and is essential for normal binding to heparin and polyP

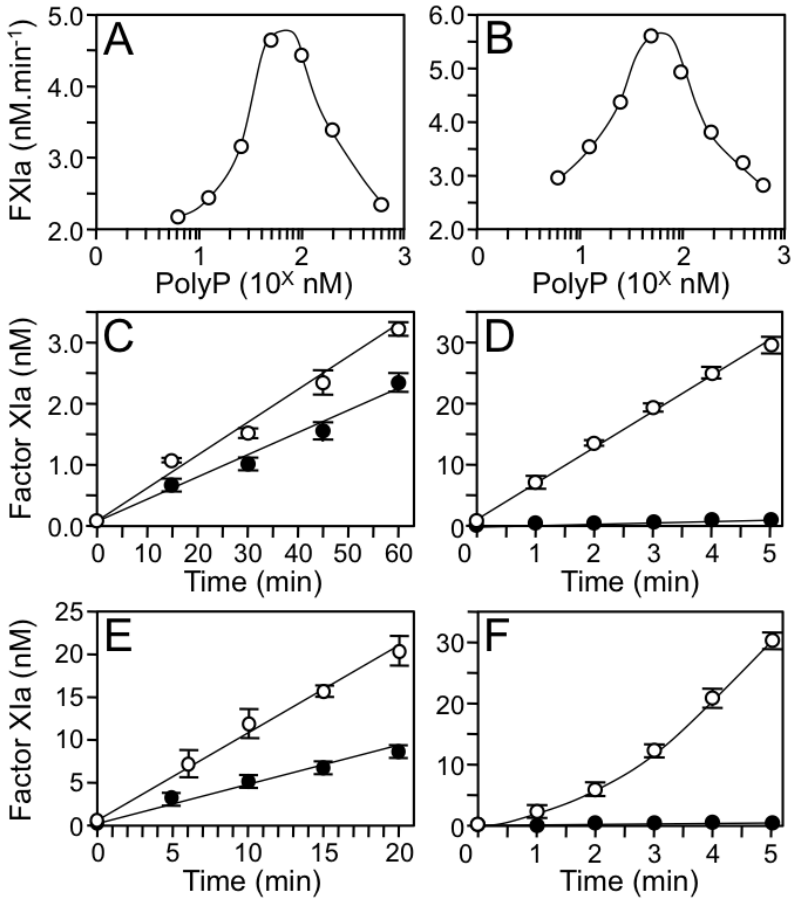

Figure 9-4. FXI activation by thrombin or FXIIa variants. (A and B) Concentration dependence of polyP-enhanced FXI-WT (120 nM subunits) activation by 3 nM **(A)** α-thrombin or **(B)** FXIIa. **(C)** FXI-WT (200 nM subunits) incubated with 50 nM (○) rIIa^{WT} or (●) rIIaR^{89}E. **(D)** FXI-WT (120 nM subunits) was activated by 3 nM (○) rIIa^{WT} or (●) rIIaR^{89}E in the presence of 50 nM polyP. **(E)** FXI-WT (200 nM subunits) was incubated with 10 nM (○) FXIIa or (●) β-FXIIa. **(F)** FXI-WT (120 nM subunits) incubated with 3 nM (○) FXIIa or (●) β-FXIIa in the presence of 50 nM polyP. FXIa generation was determined by chromogenic assay.

(Olson, 1988; Sheehan and Sadler, 1994; Mutch, *et al.*, 2010). In the absence of polyP, FXI is activated comparably by wild type α-thrombin (rIIa^{WT}) and rIIa^{R89E} (Figure 9-4C. 177 and 124 M^{-1} sec^{-1}, respectively); however, in the presence of polyP the rate constant for rIIaR^{89}E (16,500 M^{-1} sec^{-1}) was ~35-fold lower than for rIIa^{WT} (573,000 M^{-1} sec^{-1}) (Figure 9-4D). This demonstrates the importance of α-thrombin binding to polyP during FXI activation. β-FXIIa, a degradation product of FXIIa, lacks the anion-binding heavy chain. β-FXIIa activates FXI at ~40% of the rate of FXIIa (7,300 and 17,100 M^{-1} sec^{-1}, respectively) without polyP (Figure 9-4E), but showed a more profound defect with polyP (Figure 9-4F. 13,600 and 293,000, respectively; a >20-fold difference). Again, this is consistent with a template mechanism requiring FXIIa to bind to polyP during this reaction.

The data demonstrate that polyP enhances FXI activation by α-thrombin, FXIIa or autoactivation through a template mechanism that requires FXI and the activating protease to bind to polyP. Both FXI ABSs are required to observe optimal enhancement. This contrasts with reactions in the presence of DS or heparin, where the A3 ABS alone is required to support activation, even though both ABSs are known to bind to these polyanions. An examination of the FXI structure suggests that ABSs are positioned on the FXI zymogen subunit in a manner that would allow a single polymer to span both sites (Figure 2-6). We postulate that the difference we observed between polyP and other polyanions may be related to specific structural features of the polyanions, or perhaps may reflect different affinities for FXI. While our studies strongly implicate a template mechanism is involved in FXI activation in the presence of polyP, we cannot rule out additional mechanisms, including allosteric changes in FXI or the protease upon polyP

binding that increase the catalytic efficiency of the reaction.

Effects of PolyP on Factor XIa Activity and Inhibition

Hydrolysis of S-2366 by FXIa in the presence of polyanions

Previously, we noted that FXIa-mediated cleavage of the tripeptide S-2366 is partially inhibited by heparin. This appears to be due to an allosteric effect of the polyanion on the protease active site. We investigated the effect of heparin and polyP on the cleavage of S-2366 by FXIa-WT, FXIaABS-1, FXIaABS-2 and FXIaABS-1/2. We observed that both heparin and polyP inhibit the cleavage of S-2366 by FXIa-WT in a concentration dependent manner (Figure 9-5A). PolyP produces a less pronounced effect than heparin (Figure 9-5B). For both polyanions, the catalytic domain ABS is required to observe inhibition, as polyanions do not affect S-2366 cleavage by FXI-ABS2 or FXI-ABS1/2. Interestingly, the absence of the A3 domain ABS (FXI-ABS1) reduces inhibition somewhat, perhaps by changing the manner in which polyanions bind to the catalytic domain ABS. The results are consistent with the conclusion that heparin and polyP engage both ABSs on FXIa.

Activation of FIX by FXIa in the presence of polyanions

As discussed in Chapter IV, FXIa-WT activates FIX by cleaving the protein after Arg^{145} to produce FIXα (Figure 9-5C), and then after Arg^{180} to form FIXaβ (Figure 9-5D) (Vadivel, *et al.*, 2012). As mentioned, the catalytic efficiency of the second cleavage is greater than the first, limiting FIXα accumulation. Central to this mechanism is the FIX binding exosite on the FXIa A3 domain. When FIX is activated by FXIa-WT in the presence of heparin or DS, there is significant FIXα accumulation (Figure 9-5C) and

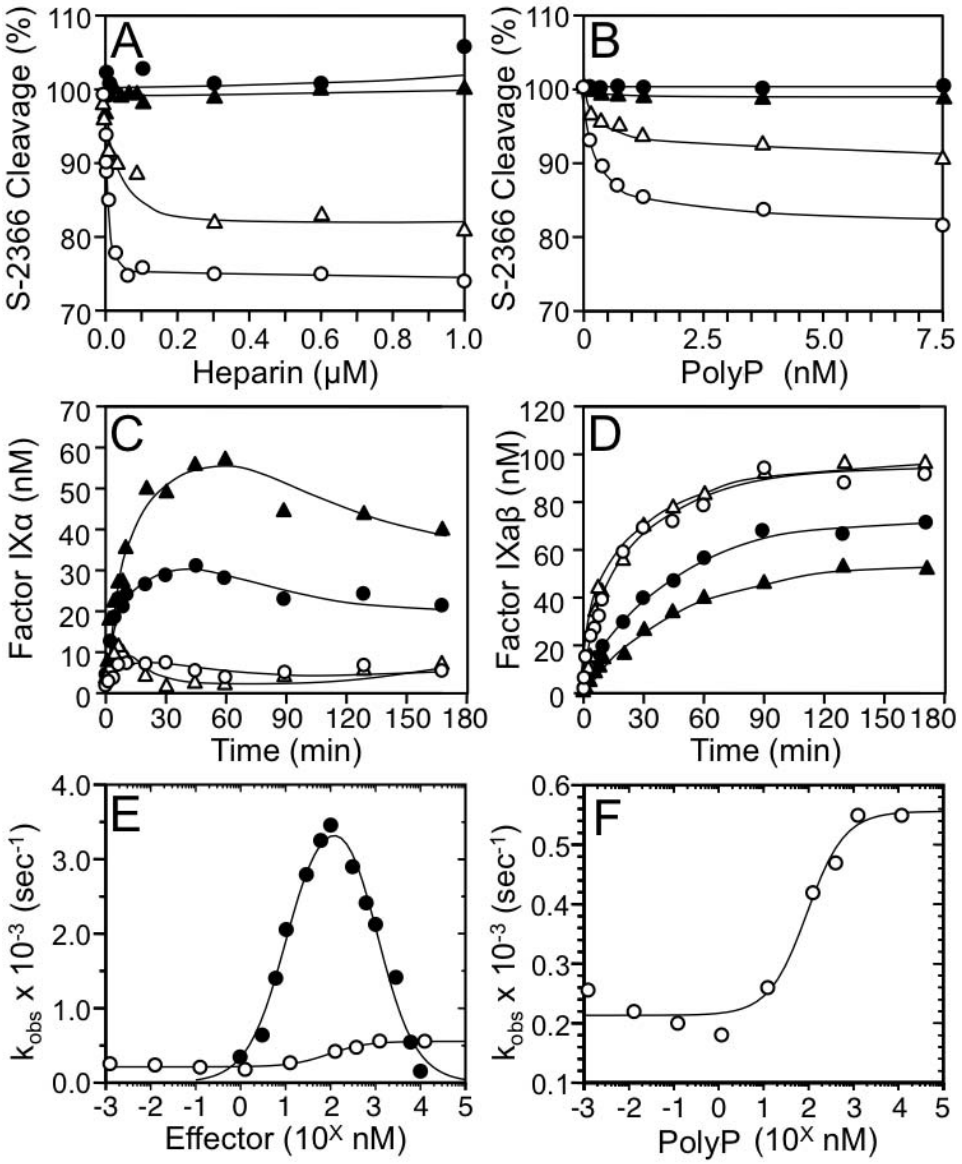

Figure 9-5. Effects of polyanions on FXIa activity. (A and B) FXIa-WT (○), FXIaABS-1 (△), FXIaABS-2 (●) or FXIaABS-1/2 (▲), 6 nM active sites, was supplemented with **(A)** heparin or **(B)** polyP, then tested for its ability to hydrolyze S2366. **(C and D)** FIX (100 nM) was incubated in Assay Buffer at RT with 3 nM (active sites) FXIa-WT with (○) vehicle, (●) 400 nM unfractionated heparin, (▲) 1 μg/ml dextran sulfate or (△) 50 nM polyP. Samples were removed into nonreducing SDS-sample buffer and size-fractionated on 17% polyacrylamide-SDS. Conversion of FIX to (**C**) FIXα and (**D**) FIXaβ was determined by densitometry of stained gels. **(E and F)** FXIa-WT (6 nM active sites) incubated in TBSA with antithrombin (130 nM) and (●) unfractionated heparin or (○) polyP. *k*obs for each polyanion concentration was determined as described under methods.

reduced rates of FIXaβ formation (Figure 9-5D). These data suggest that the polyanions sterically interfere with FIX binding to the A3 exosite. PolyP, in contrast, does not alter FIX activation. This is consistent with the premise that polyP interacts differently with FXIa than does dextran sulfate or heparin, despite using the same binding sites. It is possible that FIX can displace polyP from the A3 domain more easily than other polyanions. Alternatively, the geometry of binding may be different enough to prevent interference with the factor IX binding exosite.

Effects of Polyanions on Antithrombin-Mediated Inhibition of FXIa

In plasma, FXIa activity is regulated by several members of the serpin family of protease inhibitors, including AT. FXIa inhibition by AT is enhanced 40-fold by heparin at therapeutic concentrations (Zhao *et al.*, 1998). The heparin-dependence of AT inhibition of FXIa (Figure 9-5E) is bell-shaped, indicating the FXIa and AT both bind to the heparin (Olson, 1988; Zhao *et al.*, 1998). PolyP has little effect on AT inhibition of FXIa (Figure 9-5E). At polyP concentrations >1 μM a modest saturable inhibition is observed (Figure 9-5F), consistent with an allosteric effect due to polyP binding to FXIa. AT up to 6 μM did not bind to polyP in surface plasmon resonance studies (S.A. Smith and J.H. Morrissey, Univ. of Illinois-Urbana, personal communication), consistent with results reported by Church and coworkers (Church *et al.*, 1988).

Both heparin and polyP appear to interact with the same general areas on FXI and thrombin. Although it has the capacity to enhance FXI activation specifically, and contact activation in general, heparin produces a net anticoagulant effect in plasma because it serves as a cofactor for AT-mediated protease inhibition. PolyP, on the other hand, is procoagulant *in vivo*. The interaction between heparin and AT involves a well-defined

pentasaccharide sequence within the heparin molecule, which is absent in polyP (van Boeckel *et al.*, 1994). As a result, polyP does not bind AT, and predictably lacks the capacity to function as a cofactor for AT. Our results showing that polyP does not significantly accelerate FXIa inhibition by AT, and does not interfere with FIX activation by FXIa, support the hypothesis that polyP is, on balance, a promoter of coagulation.

The Importance of Factor XI ABSs in Blood Coagulation

Factor XI in Plasma Assays

To understand the importance of the FXI interaction with polyanions in plasma coagulation, we performed aPTT assays using silica as a triggering agent in FXI-deficient plasma supplemented with recombinant FXI. FXI-WT and FXI-ABS1 restored clotting times of FXI-deficient plasma comparably, while FXI-ABS2 and FXI-ABS1/2 gave slightly longer clotting times (1.2 and 1.35 times of FXI-WT, respectively) (Figure 9-6A).

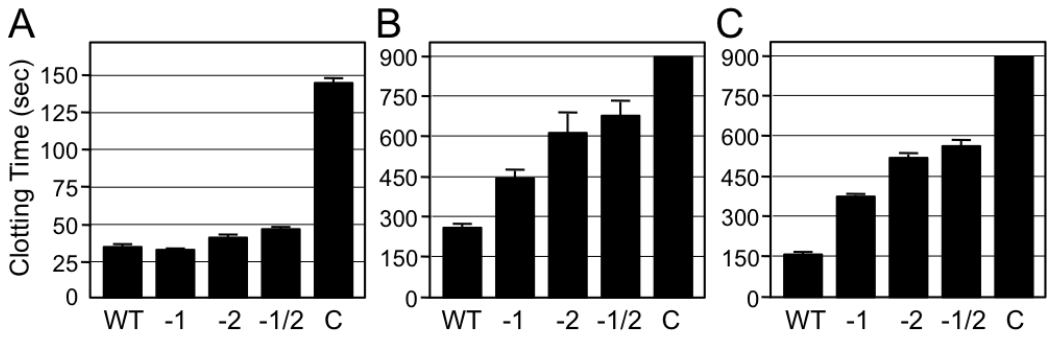

Figure 9-6. Plasma clotting assays. (A) FXI-deficient plasma supplemented with 30 nM FXI-WT, FXI-ABS1, FXI-ABS2, FXI-ABS1/2, or vehicle (C) and incubated aPTT reagent. After recalcification, time to clot formation was measured on a coagulometer. **(B)** Clotting times of FXI-deficient plasma supplemented with FXI as in panel A incubated for 3 min with 50 nM polyP and 10 μM PC/PS vesicles. **(C)** Clotting times of FXI-deficient plasma supplemented with FXI incubated for 3 min with 50 nM polyP, 10 μM PC/PS vesicles, and 1.5 nM β-thrombin. CTI (4 μM) was used to block contributions from FXII/XIIa in experiments in panel C. For all panels, proteins were tested in triplicate. Error bars represent one standard deviation.

Replacing silica with polyP resulted in longer clotting times (Figure 9-6B), because polyP of ~80 phosphate units are relatively weak FXII activators (Smith *et al.*, 2010). With polyP, differences in clotting times between plasma supplemented with different FXI variants are evident, and in line with the results in Figure 9-3D. In Figure 9-6C, FXII activation and FXIIa activity are blocked in plasma with CTI, and FXI is activated in the presence of polyP by adding β-thrombin. As discussed in Chapter II, β-thrombin is a cleavage product of α-thrombin that converts fibrinogen to fibrin poorly (Matafonov *et al.*, 2011). While β-thrombin and α-thrombin activate FXI similarly in solution, β-thrombin is a more potent FXI activator in plasma than is α-thrombin, because fibrinogen does not compete with FXI for the enzyme (Emsley *et al.*, 2010). As with polyP-enhanced FXIIa activation of FXI (Figure 9-6B), polyP-dependent β-thrombin activation of FXI in plasma is compromised by loss of the FXI ABSs. These results indicate that the ability of polyP to enhance α-thrombin-mediated or FXIIa-mediated FXI activation in plasma also requires both ABSs.

Thrombus Formation in vivo

As discussed in Chapter VII, FXI-WT can be transiently expressed in FXI$^{-/-}$ mice by HTI. FXI ABS mutants were expressed in FXI$^{-/-}$ mice using this technique (Figure 9-7A). Twenty-four hours post-HTI, the plasma FXI concentrations of ABS mutants are comparable to the normal FXI level in human plasma (30 nM), while FXI-WT concentrations were modestly lower (Figure 9-7B). Carotid arteries of wild type mice occlude within 15 minutes of exposure to 3.5% $FeCl_3$, while FXI$^{-/-}$ mice are resistant to occlusion (consistent with the results in Figure 7-7D). All FXI$^{-/-}$ mice expressing FXI-WT developed arterial occlusion after $FeCl_3$ exposure (Figure 9-7C). However, despite plasma

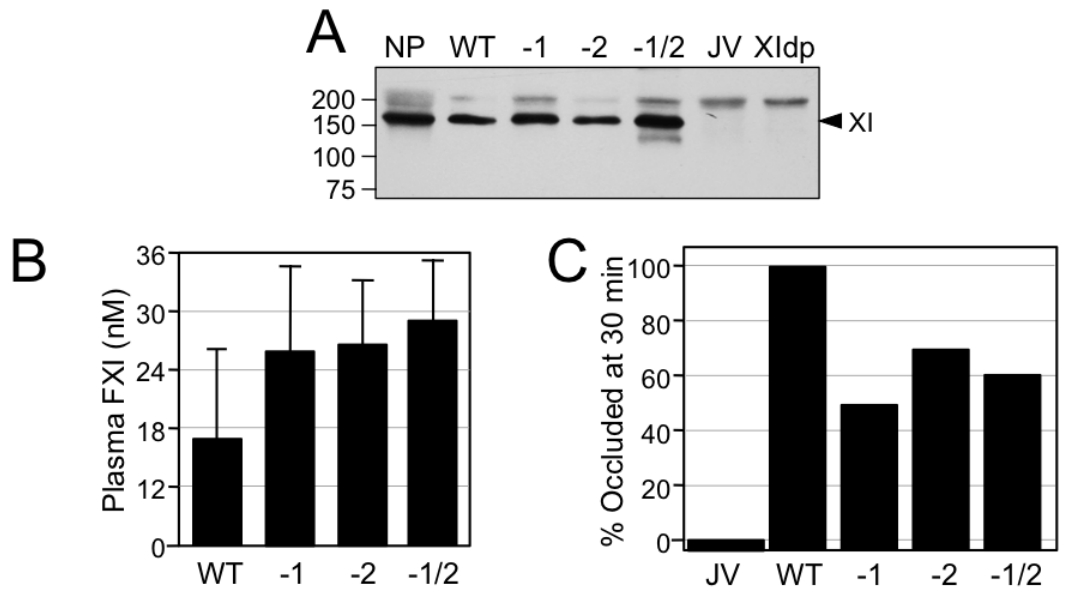

Figure 9-7. FeCl3-induced carotid artery occlusion. (A) FXI western blot of mouse plasmas 24 hours post-HTI with constructs for FXI-WT, FXI-ABS1 (-1), FXI-ABS2 (-2), FXI-ABS1/2 (-1/2) or empty vector (JV). Normal human plasma (NP) is in the left lane and FXI-deficient mouse plasma (XIdP) in the right lane. Positions of molecular mass standard (kDa) are shown on the left, and FXI is indicated on the right. **(B)** Concentrations of FXI in mouse plasma 24 hours post-HTI. Error bars indicate 1 SD (n=10 per construct). **(C)** FXI-/- mice underwent HTI with FXI constructs (n=10 per construct). 24 hours post-HTI, mice were tested in a model in which thrombus formation in the carotid artery is induced with 3.5% $FeCl_3$. Bars indicate percent of mice with occluded arteries 30 min post-$FeCl_3$ application.

FXI levels that were ~40% higher on average than FXI-WT expressing mice, only about half of the mice expressing FXI lacking one or both anion-binding sites developed arterial occlusion (Figure 9-7C).

PolyP appears to contribute to thrombus formation in the mouse arterial thrombosis model used in this study. In this model, an antithrombotic effect can be produced by treating mice with alkaline phosphatase to destroy polyP (Müller *et al.*, 2009), or by administering compounds that neutralize polyP (Smith *et al.*, 2012; Jain *et al.*, 2012).

Based on the importance of the FXI anion-binding sites to interactions with polyP and heparin (and presumably heparin-like molecules), hypothetically, loss of one or both sites could result in (1) an enhanced sensitivity to $FeCl_3$-induced thrombosis because of reduced AT-mediated inhibition, (2) a decrease in sensitivity to $FeCl_3$-induced thrombosis due to decreased affinity for polyP, or (3) a combination of the effects leading to an intermediate result. The results presented here indicate, on balance, that loss of the FXI ABSs produces an antithrombotic effect, supporting the notion that targeting the FXI interaction with polyanions such as polyP may be a useful antithrombotic strategy.

Summary

PolyP is released from activated platelets and produces procoagulant effects in plasma. Several laboratories, including our own have reported that polyP accelerates FXI activation by thrombin, FXIIa and FXIa. Our results indicate that the two anion binding sites (ABSs) found on each subunit of FXI are required for productive interactions with polyP. This contrasts to some extent with the FXI interaction with polyanions such heparin and DS, which only require the ABS on the A3 domain for autoactivation. Interestingly, unlike heparin and DS, polyP does not interfere with FIX activation by FXIa, consistent with the impression that polyP is, on balance, a promoter of thrombin generation and coagulation. Studies with FXI ABS mutants in plasma and in a mouse thrombosis model support the hypothesis that the FXI ABSs are required for expression of the cofactor effect of polyP during FXI activation. Given this, therapeutic targeting of the interaction between the FXI ABSs and polyP may prevent FXI from contributing to thrombotic processes.

Methods

Recombinant FXI. Recombinant wild type FXI (FXI-WT), FXI with alanine replacing Arg^{250}, Lys^{252}, Lys^{253} and Lys^{255} in the A3 domain (FXI-ABS1) (Zhao *et al.*, 1998), FXI with alanine replacing Lys^{529}, Arg^{530} and Arg^{532} in the catalytic domain (FXI-ABS2) (Yang *et al.*, 2009), or both sets of substitutions (FXI-ABS1/2) were expressed and purified as described. FXI was incubated with 500 μM DIP on ice for 1 hr to inhibit traces FXIa, followed by dialysis into TBS. FXI was activated with FXIIa (20:1 FXI:FXIIa) at 37 ˚C for 24 hrs in TBS.

Recombinant Thrombin. Wild type α-thrombin ($rIIa^{WT}$) and α-thrombin with Arg^{89} replaced by Glu ($rIIa^{R89E}$) were prepared as described (Sheehan and Sadler, 1994). Prothrombin forms of both proteins were expressed in BHK cells, and purified from medium by barium sulfate precipitation and chromatography on DEAE-Sephacel. α-Thrombin was generated by incubating Prothrombin with *Oxyuranus scutellatus* venom, and purified by ion-exchange chromatography. Thrombin active sites were titrated with hirudin.

Hydrolysis of S-2366 by FXIa. FXIa-WT (12 nM active sites) was incubated with 50-2000 μM S-2366 in TBS with 0.1% BSA (TBSA) at RT. Rates of *p*NA generation were determined as in Chapter V. In a separate experiment, 12 nM FXIa-WT was incubated with S-2366 (500 μM) and varying concentrations of heparin or polyP.

FXI Activation. FXI autoactivation was performed as described in Chapter VI. In the absence of polyP, FXI (200 nM subunits) was incubated with FXIIa (10 nM) or thrombin (50 nM) in HBSA at 37 ºC. Reactions in the presence of polyP (50 nM) contained FXI (120

nM subunits) and 3 nM FXIIa or thrombin.

FIX Activation by FXIa. FIX (100 nM) in Assay Buffer was incubated at RT with FXIa (3 nM active sites) with vehicle, 1 μg/mL dextran sulfate, 400 nM heparin, or 50 nM polyP. At various times, aliquots were removed into non-reducing SDS-sample buffer, size fractionated on 17% polyacrylamide gels, and stained with GelCode Blue (Pierce). Gels were imaged under infrared wavelengths, and conversion of FIX to FIXα and FIXaβ was assessed by densitometry as described in Chapter IV.

Inhibition of FXIa by Antithrombin. FXIa (6 nM active sites) was incubated with AT (130 nM), and heparin (10^0 to 10^4 nM) or polyP (10^{-3} to 10^4 nM) in TBSA at 37°C. At various times, 50 μL was removed into 50 μL of TBSA containing 1 mM S-2366 and 4 μg/mL polybrene. FXIa activity was determined by monitoring changes at a wavelength of 405 nm. Initial linear rates of *p*NA formation were expressed as mOD/min for 100 μl reactions. Progress curves of residual FXIa activity (E/E_0) were analyzed by direct nonlinear least squares fitting to a first-order decay equation, $E/E_0 = e^{-k_{obs}.t}$ in which k_{obs} is the first-order inactivation rate constant (s^{-1}) and t is time (s). The semi-logarithmic dependence of k_{obs} on [heparin] was analyzed with a model in which heparin forms a ternary complex with FXIa and AT (Olson, 1988). The data for polyP were analyzed by a quadratic equation $k_{obs} = k_{obs,unc} + F(k_{obs,lim} - k_{obs,unc})$, where

$$F = \frac{([FXIa]_o + [P]_o + K_{FXIa,P}) - \sqrt{([FXIa]_o + [P]_o + K_{FXIa,P})^2 - 4[FXIa]_o[P]_o}}{2[FXIa]_o}$$

$k_{obs,unc}$ is the rate constant for AT inactivation in the absence of polyP, and $k_{obs,lim}$ is the limiting rate constant at high polyP concentration. $[FXIa]_o$ and $[P]_o$ are

concentrations of FXIa active sites and polyP, and $K_{FXIa,P}$ is the apparent dissociation constant for polyP binding to the FXIa subunit, assuming 1 binding site for the polyP chain on each FXIa subunit.

The methods for testing FXI activity in plasma and FXI deficient mice were described in Chapter VII.

References

Choi, S.H., Smith, S.A., Morrissey, J.H. (2011) Polyphosphate is a cofactor for the activation of factor XI by thrombin. Blood *118*, 6963-70.

Church, F.C., Pratt, C.W., Treanor, R.E., Whinna, H.C. (1988) Antithrombin action of phosvitin and other phosphate-containing polyanions is mediated by heparin cofactor II. FEBS Lett *237*, 26-30.

Emsley, J., McEwan, P.A., Gailani, D. (2010) Structure and function of factor XI. Blood *115*, 2569-2577.

Gailani, D., and Broze, G.J. (1991) Factor XI activation in a revised model of blood coagulation. Science *253*, 909-912.

Jain, S., Pitoc, G.A., Holl, E.K., Zhang, Y., Borst, L., Leong, K.W., Lee, J., Sullenger, B.A. (2012) Nucleic acid scavengers inhibit thrombosis without increasing bleeding. Proc Natl Acad Sci USA *109*, 12938-43.

Matafonov, A., Sarilla, S., Sun, M.F., Sheehan, J.P., Serebrov, V., Verhamme, I.M., Gailani D. (2011) Activation of factor XI by products of prothrombin activation. Blood *118*, 437-445.

McMullen, B.A., Fujikawa, K., Davie, E.W. (1991) Location of the disulfide bonds in human coagulation factor XI: the presence of tandem apple domains. Biochemistry *30*, 2056-2060.

Müller, F., Mutch, N.J., Schenk, W.A., Smith, S.A., Esterl, L., Spronk, H.M., Schmidbauer, S., Gahl, W.A., Morrissey, J.H., Renné, T. (2009) Platelet polyphosphates are proinflammatory and procoagulant mediators *in vivo*. Cell *139*, 1143-1156.

Müller, F., Mutch, N.J., Schenk, W.A., Smith, S.A., Esterl, L., Spronk, H.M., Schmidbauer, S., Gahl, W.A., Morrissey, J.H., Renné, T. (2009) Platelet polyphosphates are proinflammatory and procoagulant mediators *in vivo*. Cell *139*, 1143-1156.

Mutch, N.J., Myles, T., Leung, L.L.K., Morrissey, J.H. (2010) Polyphosphate binds with high affinity to exosite II of thrombin. J Thromb Haemost *8*, 548-55.

Olson, S.T. (1988) Transient kinetics of heparin-catalyzed protease inactivation by antithrombin III. Linkage of protease-inhibitor-heparin interactions in the reaction with thrombin J Biol Chem *263*, 1698–708.

Sheehan, J.P., and Sadler, J.E. (1994) Molecular mapping of the heparin-binding exosite of thrombin. Proc Natl Acad Sci USA. *91*, 5518-5522.

Smith, S.A., Choi, S.H., Collins, J.N., Travers, R.J., Cooley, B.C., Morrissey, J.H. (2012) Inhibition of polyphosphate as a novel strategy for preventing thrombosis and inflammation. Blood *120*, 5103-10.

Smith, S.A., Choi, S.H., Davis-Harrison, R., Huyck, J., Boettcher, J., Rienstra, C.M., Morrissey, J.H. (2010) Polyphosphate exerts differential effects on blood clotting, depending on polymer size. Blood *116*, 4353-4359.

Tollefsen, D.M., Zhang, L. (2013) Heparin and vascular glycosaminoglycans, In: Marder VJ, Aird WC, Bennet JS, Schulman S, White GC. Hemostasis and Thrombosis: basic principles and clinical practice, 6th Ed., Lippincott, Williams & Wilkins, Philadelphia, pp 585-597

Vadivel, K., Schmidt, A.E., Marder, V.J., Krishnaswamy, S., Bajaj, S.P. (2012) Structure and function of vitamin K-dependent coagulation and anticoagulation proteins, In: Hemostasis and Thrombosis: basic principles and clinical practice, 6th Ed., Lippincott, Williams & Wilkins, Philadelphia, pp 208-32

van Boeckel, C.A., Grootenhuis, P.D., Visser, A. (1994) A mechanism for heparin-induced potentiation of antithrombin III. Nat Struct Biol *1*, 423-5.

Venneröd, A.M., and Laake, K. (1975) Inhibition of purified plasma kallikrein by antithrombin III and heparin. Thromb Res *7*, 223–226.

Walsh, P.N. (1972) The effects of collagen and kaolin on the intrinsic coagulant activity of platelets. Evidence for an alternative pathway in intrinsic coagulation not requiring factor XII. Br J Haematol. *22*, 393-405.

Yang, L., Sun, M.F., Gailani, D., Rezaie, A.R. (2009) Characterization of a heparin-binding site on the catalytic domain of factor XIa: Mechanism of heparin acceleration of factor XIa inhibition by the serpins antithrombin and C1-inhibitor. Biochemistry *48*, 1517–24.

Zhao, M., Abdel-Razek, T., Sun, M.F., Gailani, D. (1998) Characterization of a heparin binding site on the heavy chain of factor XI. J Biol Chem *273*, 31153–9.

CHAPTER X

IMPLICATIONS OF THE RESEARCH AND FUTURE DIRECTIONS

Despite research over the course of six decades, the functions of the proteins that make up the plasma contact system (FXII, FXI, PK and HK) in normal health and in disease are not well understood. To some extent this is due to the long practice of studying these proteins in systems triggered with non-physiologic substances. This contributed to the impression that contact reactions are *in vitro* artifacts that do not reflect the physiologic roles of the proteins. Another contributing factor is, until recently, a general lack of enthusiasm for studying contact proteins, because of the unimpressive phenotypes associated with their deficiencies. While contact activation was originally thought to be a physiologically relevant trigger for coagulation in certain situations, it is now established that only FXI is required for normal hemostasis, and its role is relatively minor compared to the VKD coagulation proteases. The observation that FXI can be activated by thrombin further reinforced the impression that FXII, PK and HK were not likely to contribute to coagulation in a substantial way.

There has a been resurgence in interest in a role for contact activation in coagulation, initially based on observations indicating that FXI contributes to thrombosis in humans and in animal models, and then by work revealing that mice lacking FXII (Renné *et al.*, 2005; Kleinschnitz *et al.*, 2006), HK (Merkulov *et al.*, 2008), or PK (Revenko *et al.*, 2011; Bird *et al.*, 2012) are resistant to thrombosis. The data suggest that a process similar to classic contact activation contributes to pathologic clot formation and/or growth. A case is

building for a mechanism in which FXI is activated on or near the surface of aggregating platelets, possibly by FXIIa, leading to inappropriate thrombin generation, fibrin production and platelet activation within a blood vessel lumen. The ability of polyP, a polyanion released from platelet dense granules, to enhance FXI activation, and to some extent FXII activation, provides a convincing link between activated platelets and the contact system. Several polyP binders, including cationic proteins, polymers and small molecules have demonstrated anti-thrombotic properties *in vitro* and *in vivo* (Smith *et al.*, 2012), consistent with the importance of polyP in pathologic processes.

With the realization that FXI contributes to thrombosis, there is active interest in targeting the protein for therapeutic purposes. A major underlying goal of the work presented in this thesis is to provide data that will inform rational design of therapeutic approaches targeting FXI. Specifically, we wanted to (1) establish the mechanism and structural basis of FIX activation by FXIa, (2) determine the mechanism by which FXI/XIa interacts with polyP, and (3) investigate the importance of FXI's dimeric structure to zymogen activation. FXI's unusual structure (for a coagulation protease) makes it difficult to predict structure-function relationships by extrapolating from the large literature for VKD proteins. During the course of the work, we came to appreciate the complexities of studying a protease that can have one or two active sites, interacting with a substrate that must be cleaved at more than one location. We hope that our results will provide a foundation for future work on the roles of FXI in vascular biology.

Factor IX Activation by Factor XIa

We demonstrated that FIX activation by FXIa involves an exosite-mediated

release-rebind mechanism (Geng *et al.*, 2012). Similar processes have been reported for activation of prothrombin by FXa (Orcutt and Krishnaswamy, 2004), and FX activation by the FVIIa/TF complex (Baugh *et al.*, 2000). During FIX activation by FXIa, the efficiency of the second cleavage after Arg^{180} is enhanced by conformational changes resulting from the first cleavage after Arg^{145}. The 7-fold greater catalytic efficiency of the second cleavage explains the absence of significant accumulation of the intermediate FIXα. A similar mechanism appears to explain the limited accumulation of the intermediate meizothrombin during prothrombin activation by FXa (Orcutt and Krishnaswamy, 2004). As presented in Chapters IV, V and VI, our data disagree with previous proposals for the mechanism by which FXIa activates FIX on several key points, which are listed in Table10-1.

Table 10-1. Features of models for FIX activation by FXIa.

Feature	Published	Our Results
General Mechanism	"Processive"	Release-Rebind
Initial Exosite Interaction	Catalytic Domain	A3 domain
Primary Heavy Chain FIX Binding Site	A2 Domain	A3 Domain
Catalytic Domain Exosite	Evidence For	No Evidence For
Binding to Catalytic Domain Required before Binding to Heavy Chain	Yes	No

The features listed in Table 10-1 for published models come primarily from one laboratory. The reason that our results are so discrepant with results from this group is not entirely clear; however, our experiments incorporated several features that we feel are better suited to the analysis of this reaction. First, we used densitometry of full time course experiments on SDS-polyacrylamide gels to establish progress curves for formation of both the intermediate FIXα and the protease FIXaβ. The published data relied primarily on a chromogenic assay in which FIXaβ generated in the first stage of an assay was used to generate FXa in the second stage. It is difficult to achieve reproducibility with this two-stage approach, and the assay does not yield information about non-enzymatic (FIXα) intermediate accumulation. Second, we used chimeras and site-directed mutants of FXI and PK to identify exosites, using loss-of-function and gain-of-function strategies. In comparison, the older published work relied on peptide inhibition approaches, which can be difficult to interpret, as peptides may not accurately mimic epitopes on the whole protein.

Mutagenesis analysis identified residues in the FXIa A3 domain that either constitute a FIX-binding exosite, or are required for proper conformation of the exosite. The inability of FIX to bind to zymogen FXI indicates the exosite is either not formed or unavailable. That the residues we identified as components of the exosite are buried in the zymogen structure are consistent with this hypothesis. Presumably a conformational change induced by subunit activation exposes this site, allowing binding to occur. Evidence for a significant conformational change in FXI upon activation to FXIa is indirect, coming from rotary shadowing electron microscopic images that appear to show a shape difference between FXI and FXIa. Strategies that resolve the three-dimensional structures of FXIa, such as crystallographic structures of the molecule alone or in complex with FIX are

needed to better define the structural elements involved in the FIX-FXIa interaction. FXIa is apparently a difficult molecule to crystalize, hampering efforts in this regard.

Most protease-substrate interactions required for thrombin generation during hemostasis occur on phosphatidylserine-rich membranes of activated platelets or damaged tissues, and require a protein cofactor. The K_ms for these reactions are heavily influenced by the protease and substrate binding to the phospholipid, while the presence of the cofactor enhances k_{cat}. FXIa activation of FXI appears to be the exception to this model, as phospholipid does not enhance the reactions and no cofactor appears to be required. For this reaction, K_m is largely determined by an interaction between the FIX Gla-domain with the FXIa A3 domain. The involvement of the Gla-domain suggests that FXIa should compete with phospholipid for FIX. Consistent with this, using surface plasmon resonance, we recently determined that FXIa, but not FXIa/PKA3, inhibits FIX binding to immobilized phosphatidylserine-rich surfaces (Gailani *et al.*, 2013; 2014).

While our data suggest that FXIa would activate FIX equally well in solution and on a surface, the environments in which the reaction occurs *in vivo* are not established. Despite the absence of a Gla-domain, FXI and FXIa do bind to platelet receptors such as glycoprotein 1bα (Baglia *et al.*, 2004) and ApoER2 (White-Adams *et al.*, 2009), suggesting FXIa-mediated FIX activation may occur on the platelet surface. FIXaβ would then be in a position to participate in FX activation on the platelet in the presence of the cofactor FVIIIa. While the FXI/XIa-platelet interaction does not appear to influence protease function in static clotting and thrombin generation assays, we predict that it may be necessary for maintaining the correct position of FXIa relative to a clot in flowing blood. We are developing flow systems in the laboratory to test FXI variants such as the

monomers described in Chapter VII and the heterodimer described in Chapter VIII, which function reasonably normally in static assays, but would be predicted to fail under flow if one subunit of the dimer was required solely for binding to a platelet.

The Factor XIa A3 Domain as an Antithrombotic Target

In humans, compelling epidemiologic data support a role for FXI in arterial and venous thrombotic disorders (Doggen *et al.*, 2006; Meijers *et al.*, 2000). These observations have spurred an interest in developing inhibitors of FXIa as antithrombotic drugs. Approaches that have been investigated include (1) inhibition of FXI activation or FXIa activity with monoclonal antibodies (Tucker *et al.*, 2009; Cheng *et al.*, 2010), (2) reduction of plasma FXI with anti-sense oligonucleotides (Crosby *et al.*, 2013), and inhibition of FXIa with (3) synthetic protease active site inhibitors (Quan *et al.*, 2014), (4) synthetic allosteric inhibitors (Karuturi *et al.*, 2013), or (5) naturally occurring active site inhibitors (Ma *et al.*, 2013). While the traditional pharmacologic approach is to target the active site of the protease form of a target, data with antibodies directed against FXI provide a compelling argument for targeting the FXI A3 domain as an antithrombotic approach.

As discussed, exosite interactions are largely responsible for affinity and specificity of enzyme-substrate interactions in coagulation. IgG O1A6 is an anti-human FXI/XIa antibody that binds to the A3 domain, blocking the interaction between FIX and the exosite on FXIa (Tucker *et al.*, 2009). The antibody was tested in baboons using implantable collagen-coated grafts to induce thrombosis within arteriovenous shunts (Tucker *et al.*, 2009). O1A6 markedly reduced platelet and fibrin accumulation within the grafts, preventing occlusion and reducing thrombin-antithrombin (TAT) complex levels

downstream from the graft by >90%. This is consistent with a potent effect on thrombin generation. While, O1A6 was more effective than high dose aspirin in this model, unlike aspirin, it did not increase the bleeding time (Tucker *et al.*, 2009). The impressive antithrombotic effect of O1A6 was superior to those of an anti-FXI antibody (14E11) that blocks FXI activation by FXIIa (but not FXIa activation of FIX), and an anti-FXII antibody that prevents FXII activation (15H8). Surprisingly, in plasma clotting assays and flow models, O1A6 was considerably more potent than antibodies that block the FXIa active site (data not shown). This counterintuitive observation has been confirmed by investigators at other institutions. While the reason for this is not certain, we speculate that the relative "weakness" of the antibodies that target the active site may stem from their inability to prevent FIX from engaging FXIa at the A3 domain exosite. There are data to suggest that engagement of the exosite by FIX changes the protease active site. Given this, an antibody that effectively blocks the active site of free FXIa, may not be a good inhibitor of the active site of the FXIa-FIX complex.

Another advantage of targeting the A3 domain exosite is the specificity of the interaction. The catalytic domain of FXIa shares structural features in common with other members of the family of trypsin-related proteases. Inhibitors designed to target the active site of FXIa often cross-react, at least to some extent, with the plasma proteases α-kallikrein (a homolog of FXIa), activated protein C, FXa or thrombin, as well as the digestive enzyme trypsin. Inhibition of an exosite offers a more specific strategy for anti-thrombotic therapy. By identifying the structural basis for exosite mediated FIX-FXIa interaction, our data could facilitate development of small peptide or other small molecule inhibitors that target the exosite of FXIa.

The Factor XIa Interaction with Polyphosphate

FXI is activated slowly in solution by FXIIa and thrombin, implying that a cofactor is required to generate sufficient FXIa *in vivo*. The positive effects of polyanions such as dextran sulfate, silica and celite on FXI activation have been recognized for decades, and suggested that a cofactor for FXI activation may have polyanionic properties. PolyP would seem to qualify as such a cofactor. The ability of polyP to enhance FXII and FXI activation provides a link between activated platelets, FXI activation by contact activation, and FXI activation by thrombin.

FXI/XIa has two anion binding sites per subunit that are required for normal cofactor activity of heparin during FXIa inhibition by antithrombin. This contrasts with other coagulation proteases, and FXIa's homolog α-kallikrein, which have only one anion (heparin) binding site. The novel anion binding site on the FXI A3 domain is conserved across mammalian species suggesting functional importance. Our data suggest the possibility that the A3 and catalytic domain anion binding sites may function as a single larger binding site required for polyP-dependent interactions. We speculated above that FXI and FXIa may bind to platelet surface proteins, but it is also possible that the interaction with the platelet count be indirect, through polyP. While the polyanion binding mutants described in Chapter IX function reasonably normally in static plasma clotting assays, it will be interesting to test their ability to support fibrin formation and platelet activation in flow models.

The role of orthophosphate polymers (polyP) in FXI activation may reflect a more general mechanism by which FXI interacts with other polyphosphates that contribute to thrombus formation. RNA and DNA are polymers with phosphate backbones that appear

to contribute to thrombosis in mouse models (Kannemeier *et al.*, 2007; Brill *et al.*, 2012). Recent work indicates that DNA in chromatin material extruded from activated neutrophils (neutrophil extracellular traps or NETs) may be prominent in human venous thrombi. The release of NETs during neutrophil activation is thought to contribute to the innate immune response to pathogens, with the sticky viscous chromatin material trapping invading organisms. This material appears to also be prothrombotic (Fuchs *et al.*, 2010; Brill *et al.*, 2012). Interestingly, a significant amount of the fibrous material in venous clots thought to be fibrin may actually be DNA released from neutrophils. Our FXI polyanion binding variants provide us with the tools to determine if FXI interacts with nucleic acid polymers in a manner similar or different to standard polyP.

Investigators at Virginia Commonwealth University are designing FXIa inhibitors that work through an allosteric mechanism. The drugs are meant to dock at the anion binding site on the catalytic domain through ionic interactions, followed by additional binding interactions (some hydrophobic) that cause allosteric changes to the protease active site. We have tested some of these compounds and verified that they inhibit FXIa cleavage of a chromogenic substrate in a non-competitive manner, and are inhibitors of FIX activation by FXIa. Our FXIa anion binding variants can be used to verify the importance of the anion binding sites to the mechanism of action of these drugs.

Thoughts on the Factor XI/XIa Homodimer

One of the most provocative features of FXI is its homodimeric structure. From an evolutionary perspective, a gene for a protease with four apple domains that probably represents PK first appears in amphibians. An analysis of the predicted sequence of the A4

domain in the gene from the frog *Xenopus* indicates the encoded protein is a monomer. The gene for FXI is the result of a duplication involving this PK gene. Originally, the duplication was thought to have occurred during mammalian evolution (Ponczek *et al.*, 2008), but recent analysis indicates that separate genes for PK and a dimeric FXI protein are present in a primitive mammal (the duck billed platypus, a monotreme), suggesting duplication may have occurred in a reptilian ancestor. The function of the dimer has remained elusive, although results from our mouse carotid artery thrombosis studies indicate it is required for protease function *in vivo* under at least some circumstances.

A homodimeric structure is required for substrate recognition in the case of granzyme A (Hink-Schauer *et al.*, 2003), and for catalysis in the case of cyclooxygenase-2 (Dong *et al.*, 2011). For granzyme A, the substrate binds to an exosite on one subunit and is catalyzed by the other. In essence, the non-catalytic subunit serves as an exosite. For cyclooxygenase-2, the homodimer functions as a conformational heterodimer, with the activity of a catalytic monomer regulated by the other (allosteric) monomer. The dimeric structure of FXIa does not appear to be required for substrate recognition or catalysis (Smith *et al.*, 2008; Wu *et al.*, 2008). The work presented in Chapter VII shows that monomeric FXI is activated poorly by FXIIa at high protease to substrate ratios. This may explain the poor performance of monomers in our *in vivo* thrombosis model, which requires FXI activation by FXIIa. The *in vitro* data suggest that there are high affinity FXIIa binding sites on the FXI dimer that mediate dimer-dependent activation, with lower affinity sites supporting dimer-independent activation. Presumably, for the high affinity sites, FXIIa binds to one subunit of a FXI dimer while activating the other. This suggests that dimerization is an adaptation for proper activation; however, the parent homolog of

FXI, PK, is a monomer that is activated efficiently by FXIIa. Furthermore, FXIIa activation is not thought to be important for hemostasis. Indeed, FXI monomers are activated normally by thrombin.

As outlined in Chapter VIII, we are currently investigating the possibility that the dimeric conformation of FXIa is an adaptation that allows the protease to bind to a surface (perhaps a receptor on activated platelets) through one subunit, while engaging the substrate FIX through the other. The observation that binding sites for GP1b and factor IX are both located on the A3 domain suggests that for a single subunit platelet binding and FIX binding would be mutually exclusive events. Previously, members of our laboratory published a study using a monomeric FXI/PK chimera (FXI/PKA4) that lent credence to this hypothesis (Gailani *et al.*, 2001), although not all subsequent work was in support of this notion (Sinha *et al.*, 2005). Future studies with FXI monomers and heterodimers using flow systems in which thrombin generation is platelet-dependent should allow us to confirm or disprove this model.

References

Baglia, F.A., Shrimpton, C.N., Emsley, J., Kitagawa, K., Ruggeri, Z.M., López, J.A., Walsh, P.N. (2004) Factor XI interacts with the leucine-rich repeats of glycoprotein Ibα on the activated platelet. J Biol Chem *279*, 49323-49329.

Baugh, R.J., Dickinson, C.D., Ruf, W., Krishnaswamy, S. (2000) Exosite interactions determine the affinity of factor X for the extrinsic Xase complex. J Biol Chem *275*, 28826–28833.

Bird, J.E., Smith, P.L., Wang, X., Schumacher, W.A., Barbera, F., Revelli, J.P., Seiffert, D. (2012) Effects of plasma kallikrein deficiency on haemostasis and thrombosis in mice: murine ortholog of the Fletcher trait. Thromb Haemost *107*, 1141-50.

Brill, A., Fuchs, T.A., Savchenko, A.S., Thomas, G.M., Martinod, K., De Meyer, S.F.,

Bhandari, A.A., Wagner, D.D. (2012) Neutrophil extracellular traps promote deep vein thrombosis in mice. J Thromb Haemost *10*, 136-44.

Cheng, Q., Tucker, E.I., Pine, M.S., Sisler, I., Matafonov, A., Sun, M.F. White-Adams, T.C., Smith, S.A., Hanson, S.R., McCarty, O.J., Renné, T., Gruber, A., Gailani, D. (2010) A role for factor XIIa-mediated factor XI activation in thrombus formation *in vivo*. Blood *116*, 3981-3989.

Crosby, J.R., Marzec, U., Rebenko, A.S., Zhao, C., Gao, D., Matafonov, A., Gailani, D., MacLeod, A.R., Tucker, E.I., Gruber, A., Hanson, S.R., Monia, B.P. (2013) Antithrombotic Effect of Antisense Factor XI Oligonucleotide Treatment in Primates. Arterioscler Thromb Vasc Biol *33*, 1670-8.

Doggen, C.J., Rosendaal, F.R., Meijers, J.C. (2006) Levels of intrinsic coagulation factors and the risk of myocardial infarction among men: Opposite and synergistic effects of factors XI and XII. Blood *108*, 4045-4051.

Dong, L., Vecchio, A.J., Sharma, N.P., Jurban, B.J., Malkowski, M.G., Smith, W.L. (2011) Human Cyclooxygenase-2 is a sequence homodimer that functions as a conformational heterodimer. J Biol Chem *286*, 19035-19046.

Gailani, D., Geng, Y., Verhamme, I.M., Sun, M.F., Bajaj, S.P., Emsley, J. (2013) A model for binding of factor IX to the factor XIa apple 3 domain. ISTH OC18.4.

Gailani, D., Geng, Y., Verhamme, I.M., Sun, M.F., Bajaj, S.P., Messer, A., Emsley, J. (2014) The mechanism underlying activation of factor IX by factor XIa. (in press - Thrombosis Research).

Gailani, D., Ho, D., Sun, M.F., Cheng, Q., Walsh, P.N. (2001) Model for a factor IX activation complex on blood platelets: dimeric conformation of factor XIa is essential. Blood *97*, 3117-22.

Geng, Y., Verhamme, I.M., Messer, A., Sun, M.F., Smith, S.B., Bajaj, S.P., Gailani, D. (2012) A sequential mechanism for exosite-mediated factor IX activation by factor XIa. J Biol Chem *287*, 38200-9.

Hink-Schauer, C., Estébanez-Perpiñá, E., Kurschus, F.C., Bode, W., Jenne, D.E. (2003) Crystal structure of the apoptosis-inducing human granzyme A dimer. Nat Struct Biol *10*, 535-40.

Kannemeier, C., Shibamiya, A., Nakazawa, F., Trusheim, H., Ruppert, C., Markart, P., Song, Y., Tzima, E., Kennerknecht, E., Niepmann, M., von Bruehl, M.L., Sedding, D., Massberg, S., Günther, A., Engelmann, B., Preissner, K.T. (2007) Extracellular RNA constitutes a natural procoagulant cofactor in blood coagulation. Proc Natl Acad Sci USA *104*, 6388-6393.

Karuturi, R., Al-Horani, R.A., Mehta, S.C., Gailani, D., Desai, U.R. (2013) Discovery of allosteric modulators of factor XIa by targeting hydrophobic domains adjacent to its heparin-binding site. J Med Chem *56*, 2415-28.

Kleinschnitz, C., Stoll, G., Bendszus, M., Schuh, K., Pauer, H.U., Burfeind, P., Renné, C., Gailani, D., Nieswandt, B., Renné, T. (2006) Targeting coagulation factor XII provides protection from pathological thrombosis in cerebral ischemia without interfering with hemostasis. J Exp Med *203*, 513-518.

Ma, D., Mizurini, D.M., Assumpção T.C., Li, Y., Qi, Y., Kotsyfakis, M., Ribeiro, J.M., Monteiro, R.Q., Francischetti, I.M. (2013) Desmolaris, a novel factor XIa anticoagulant from the salivary gland of the vampire bat (*Desmodus rotundus*) inhibits inflammation and thrombosis in vivo. Blood. *122*, 4094-4106.

Meijers, J.C., Tekelenburg, W.L., Bouma, B.N., Bertina, R.M., Rosendaal, F.R. (2000) High levels of coagulation factor XI as a risk factor for venous thrombosis. N Engl J Med *342*, 696-701.

Merkulov, S., Zhang, W.M., Komar, A.A., Schmaier, A.H., Barnes, E., Zhou, Y., Lu, X., Iwaki, T., Castellino, F.J., Luo, G., McCrae, K.R. (2008) Deletion of murine kininogen gene 1 (mKng1) causes loss of plasma kininogen and delays thrombosis. Blood *111*, 1274-1281.

Orcutt, S.J., and Krishnaswamy, S. (2004) Binding of substrate in two conformations to human prothrombinase drives consecutive cleavage at two sites in prothrombin. J Biol Chem *279*, 54927–54936.

Ponczek, M.B., Gailani, D., Doolittle, R.F. (2008) Evolution of the contact phase of vertebrate blood coagulation. J Thromb Haemost *6*, 1876-1883.

Quan, M.L., Wong, P.C., Wang, C., Woerner, F., Smallheer, J.M., Barbera., Bozarth, J.M., Brown, R.L., Harpel, M.R., Luettgen, J.M., Morin, P.E., Peterson, T., Ramamurthy, V., Rendina, A.R., Rossi, K.A., Watson, C.A., Wei, A., Zhang, G., Seiffert, D., Wexler, R.R. (2014) Tetrahydroquinoline Derivatives as Potent and Selective Factor XIa Inhibitors. J Med Chem *57*, 955-969.

Renné, T., Pozgajová, M., Grüner, S., Schuh, K., Pauer, H.U., Burfeind, P., Gailani, D., Nieswandt, B. (2005) Defective thrombus formation in mice lacking coagulation factor XII. J Exp Med *202*, 271-281.

Revenko, A.S., Gao, D., Crosby, J.R., Bhattacharjee, G., Zhao, C., May, C., Gailani, D., Monia, B.P., MacLeod, A.R. (2011) Selective depletion of plasma prekallikrein or coagulation factor XII inhibits thrombosis in mice without increased risk of bleeding. Blood *118*, 5302-5311.

Sinha, D., Marcinkiewicz, M., Lear, J.D., Walsh, P.N. (2005) Factor XIa dimer in the

activation of factor IX. *44*, 10416-22.

Smith, S.A., Choi, S.H., Collins, J.N., Travers, R.J., Cooley, B.C., Morrissey, J.H. (2012) Inhibition of polyphosphate as a novel strategy for preventing thrombosis and inflammation. Blood *120*, 5103-10.

Smith, S.B., Verhamme, I.M., Sun, M.F., Bock, P.E., Gailani, D. (2008) Characterization of novel forms of coagulation factor XIa: independence of factor XIa subunits in factor IX activation. J Biol Chem *283* 6696-6705.

Tucker, E.I., Marzec, U.M., White-Adams, T.C., Hurst, S., Rugonyi, S., McCarty, O.J., Gailani, D., Gruber, A., Hanson, S.R. (2009) Prevention of vascular graft occlusion and thrombus-associated thrombin generation by inhibition of factor XI. Blood *113*, 936-944.

White-Adams, T.C., Berny, M.A., Tucker, E.I., Gertz, J.M., Gailani, D., Urbanus, R.T., de Groot, P.G., Gruber, A., McCarty, O.J. (2009) Identification of coagulation factor XI as a ligand for platelet apolipoprotein E receptor 2 (ApoER2). Arterioscler Thromb Vasc Biol *29*, 1602-1607.

Wu, W., Sinha, D., Shikov, S., Yip, C.K., Walz, T., Billings, P.C., Lear, J.D., Walsh, P.N. (2008) Factor XI homodimer structure is essential for normal proteolytic activation by factor XIIa, thrombin, and factor XIa. J Biol Chem *283*, 18655-18664.